SWEPT FREQUENCY BIOIMPEDANCE ANALYSIS FOR THE DETERMINATION OF BODY WATER COMPARTMENTS

Bruce H. CORNISH

B.App.Sc. Grad.Dip.Bus.Admin.

M.App.Sc. (*Med. Phys.*)

QUEENSLAND UNIVERSITY OF TECHNOLOGY
DOCTOR OF PHILOSOPHY THESIS EXAMINATION

CANDIDATE NAME: Bruce Herbert Cornish

CENTRE/RESEARCH CONCENTRATION   Medical & Health Physics

PRINCIPAL SUPERVISOR: Associate Professor BJ Thomas

ASSOCIATE SUPERVISOR(S):   Dr L Ward

THESIS TITLE: Swept frequency bioimpedance
                                             analysis for the determination
                                             of body water compartments

Under the requirements of PhD regulation 9.2, the above candidate was examined orally by the Faculty. The members of the panel set up for this examination recommend that the thesis be accepted by the University and forwarded to the appointed Committee for examination.

Name. A/Prof B J Thomas   Signature. QUT Verified Signature
       Panel Chairperson (Principal Supervisor)

Name. Dr D J Allan   Signature QUT Verified Signature
       Panel Member

Name. Dr L Morawska   Signature. QUT Verified Signature
       Panel Member

****

Under the requirements of PhD regulation 9.15, it is hereby certified that the thesis of the above-named candidate has been examined. I recommend on behalf of the Examination Committee that the thesis be accepted in fulfilment of the conditions for the award of the degree of Doctor of Philosophy.

Name ASSOC PROF B. W. THOMAS   Signature. QUT Verified Signature
                                                       29/11/94
       Examination Committee Chairperson

ABSTRACT

Bioelectrical impedance analysis, (BIA), is a method of body composition analysis first investigated in 1962 which has recently received much attention by a number of research groups. The reasons for this recent interest are its advantages, (*viz:* inexpensive, non-invasive and portable) and also the increasing interest in the diagnostic value of body composition analysis. The concept utilised by BIA to predict body water volumes is the proportional relationship for a simple cylindrical conductor, (volume $\propto$ length^2/resistance), which allows the volume to be predicted from the measured resistance and length. Most of the research to date has measured the body's resistance to the passage of a 50 kHz AC current to predict total body water, (TBW). Several research groups have investigated the application of AC currents at lower frequencies, (*eg* 5 kHz), to predict extracellular water, (ECW). However all research to date using BIA to predict body water volumes has used the impedance measured at a discrete frequency or frequencies.

This thesis investigates the variation of impedance and phase of biological systems over a range of frequencies and describes the development of a swept frequency bioimpedance meter which measures impedance and phase at 496 frequencies ranging from 4 kHz to 1 MHz. The impedance of any biological system varies with the frequency of the applied current. The graph of reactance *vs* resistance yields a circular arc with the resistance decreasing with increasing frequency and reactance increasing from zero to a maximum then decreasing to zero. Computer programs were written to analyse the measured impedance spectrum and determine the impedance, Z_c, at the characteristic frequency, (the frequency at which the reactance is a maximum). The fitted locus of the measured data was extrapolated to determine the resistance, R_0, at zero frequency; a value that cannot be measured directly using surface electrodes. The explanation of the

theoretical basis for selecting these impedance values (Z_c and R_0), to predict TBW and ECW is presented.

Studies were conducted on a group of normal healthy animals, (n=42), in which TBW and ECW were determined by the gold standard of isotope dilution. The prediction quotients L^2/Z_c and L^2/R_0, (L=length), yielded standard errors of 4.2% and 3.2% respectively, and were found to be significantly better than previously reported, empirically determined prediction quotients derived from measurements at a single frequency. The prediction equations established in this group of normal healthy animals were applied to a group of animals with abnormally low fluid levels, (n=20), and also to a group with an abnormal balance of extra-cellular to intracellular fluids, (n=20). In both cases the equations using L^2/Z_c and L^2/R_0 accurately and precisely predicted TBW and ECW. This demonstrated that the technique developed using multiple frequency bioelectrical impedance analysis, (MFBIA), can accurately predict both TBW and ECW in both normal and abnormal animals, (with standard errors of the estimate of 6% and 3% for TBW and ECW respectively).

Isotope dilution techniques were used to determine TBW and ECW in a group of 60 healthy human subjects, (male and female, aged between 18 and 45). Whole body impedance measurements were recorded on each subject using the MFBIA technique and the correlations between body water volumes, (TBW and ECW), and height^2/impedance, (for all measured frequencies), were compared. The prediction quotients H^2/Z_c and H^2/R_0, (H=height), again yielded the highest correlation with TBW and ECW respectively with corresponding standard errors of 5.2% and 10%. The values of the correlation coefficients obtained in this study were very similar to those recently reported by others. It was also observed that in <u>healthy</u> human subjects the impedance measured at virtually any frequency yielded correlations not significantly different from those obtained from the MFBIA

quotients. This phenomenon has been reported by other research groups and emphasises the need to validate the technique by investigating its application in one or more groups with abnormalities in fluid levels.

The clinical application of MFBIA was trialled and its capability of detecting lymphoedema, (an excess of extracellular fluid), was investigated. The MFBIA technique was demonstrated to be significantly more sensitive, ($P<.05$), in detecting lymphoedema than the current technique of circumferential measurements. MFBIA was also shown to provide valuable information describing the changes in the quantity of muscle mass of the patient during the course of the treatment.

The determination of body composition, (*viz* TBW and ECW), by MFBIA has been shown to be a significant improvement on previous bioelectrical impedance techniques. The merit of the MFBIA technique is evidenced in its accurate, precise and valid application in animal groups with a wide variation in body fluid volumes and balances. The multiple frequency bioelectrical impedance analysis technique developed in this study provides accurate and precise estimates of body composition, (*viz* TBW and ECW), regardless of the individual's state of health.

TABLE OF CONTENTS

Section	Title	Page

Appendices.

References.   167

Statement of original authorship.

The work contained in this thesis has not been previously submitted for a degree or diploma at any other higher education institution. To the best of my knowledge and belief, the thesis contains no material previously published or written by another person except where due reference is made.

Signed: QUT Verified Signature
....

Date: 15 - 6 - 94

ACKNOWLEDGMENTS

Professor Brian J Thomas is a professional held in the highest regard. His approach of scientific problem solving and of open discussion was most beneficial and gratefully appreciated. Brian was always eager to discuss developments in the program and offer suggestions and advice for alternate strategies. The benefit gained from frequent discussions with Brian was significant in the success of the program.

To embark on a doctoral research program on a part-time basis while continuing with full-time employment in a completely unrelated area could have been an extremely intimidating experience. However the experience has been enlightening, encouraging and very rewarding. The attitude and input of both of my supervisors, (Prof. Brian J Thomas and Dr. Leigh Ward), have been an integral component leading to the success of the entire program. The experience gained from working with Brian and Leigh in the writing of scientific journal articles has been very valuable and I thank them sincerely for all of their efforts during the entire study.

None of this would have been possible without the encouragement of my dear wife Beverley. She has been the mainstay of support over the many years of my post-graduate study. I am eternally grateful for her unending support and patience.

LIST OF PUBLICATIONS

The following articles were written and published as a direct result of the work contained in this thesis.

1   Ward LC, Cornish BH. Use of a spreadsheet program for Deming's linear regression analysis. *Comp Biol Med.* 1991;37,101.

2   Thomas BJ, Cornish BH, and Ward LC. Bioelectrical impedance analysis for measurement of body fluid volumes: A review. *J Clin Eng.* 1992; 17: 505,510.

3   Cornish BH, Ward LC and Thomas BJ. Measurement of extracellular and total body water of rats using multiple frequency bioelectrical impedance analysis *Nutrition Research* 1992; 12: 657,666.

4   Ward LC, Bunce IH, Cornish BH, Mirolo B, Thomas BJ, Jones LC. Multi-frequency bioelectrical impedance augments the diagnosis and management of lymphoedema in post-mastectomy patients. *Eur J Clin Invest.* 1992; 22: 751.

5   Cornish BH, Thomas BJ and Ward LC. Improved prediction of extracellular and total body water using impedance loci generated by multiple frequency bioelectrical impedance analysis. *Phys Med Biol.* 1993; 38: 337,346.

6   Cornish BH, Ward LC, Thomas BJ. Alteration to the extra- to intra-cellular fluid balance measured by multiple frequency bioelectrical impedance analysis. *Nutrition Research* 1994; 14:717,727.

LIST OF FIGURES

Figure	**Caption**	**Page**

LIST OF TABLES

LIST OF ABBREVIATIONS

BIA   Bioelectrical impedance analysis.

ECW   Extracellular water.

FFM   Fat-free mass.

ICW   Intracellular water.

MFBIA Multiple frequency bioelectrical impedance analysis.

SEE   Standard error of the estimate.

SFBIM Swept-frequency bio-impedance meter.

TBW   Total body water.

SECTION 1

INTRODUCTION.

§ 1   INTRODUCTION

Assessment of human body composition is of significant clinical importance in investigating and monitoring the nutritional status and health of an individual. Various methods of body composition analysis are used in a diverse range of applications including:- nutritional assessment of the elderly and the very young; monitoring the fluid balance in post-operative and burns patients and critically ill neonates; investigations in exercise physiology; as well as monitoring individuals with conditions such as anorexia, obesity or oedema.

Research to establish indirect methods of determining the composition of the human body *in vivo* began in the 1940's. Behnke, (1941), used a two compartment model of the body; fat and fat-free mass (FFM) to describe body composition. Keys and Brozek, (1953), introduced a four compartment model which divided the mammalian body into four chemical groups; fat, water, protein and mineral, (figure 1.1). However only in recent years has technology enabled the determination of these four compositional variables *in vivo*. Pace and Rathburn, (1945), established that water is not present in stored triglyceride (fat) and that the proportion of water in fat-free mass (FFM) is 73.2%, (Beddoe *et al.*, 1985). This direct relationship between total body water (TBW) and fat-free mass (FFM) has resulted in the wide acceptance of TBW as an index of FFM in the human body.

Water, the largest of the four compartments in the model proposed by Keys and Brozek, can be subdivided into extracellular and intracellular components. Extracellular water (ECW) comprises mainly lymph, plasma and interstitial fluid, and carries the extracellular solids (ECS). Intracellular water (ICW), contained within the membranes of all cells, is the solvent for

intracellular solids (ICS). Heymsfield *et al.*, (1993), describe the 'metabolic fluid' model which divides the fat-free mass into fluid and solid constituents.

The cell membrane is not simply a container for cell constituents, but has an integral role in the control of substances into and out of the cell. There are complex mechanisms which actively and selectively pump particular ions between the intra- and extracellular fluids. However water molecules readily and freely diffuse across the cell membrane in both directions maintaining a dynamic equilibrium. The quantification of TBW and FFM has attracted a great deal of attention from research groups over recent years and a number of methods of determining TBW or FFM have been developed.
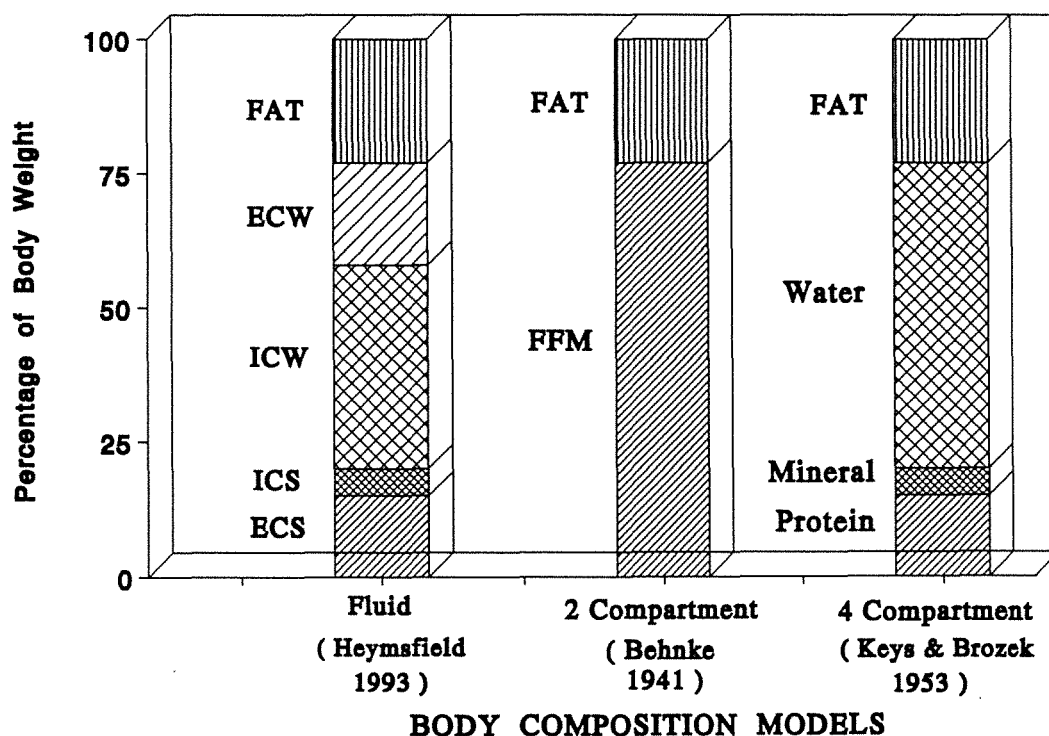
FIGURE 1.1

Components of body composition models.

§ 1.1 TECHNIQUES OF BODY COMPOSITION MEASUREMENT

Procedures for the measurement of body composition vary greatly in many respects including:- capital equipment costs, portability, subject discomfort, invasive/non-invasive, precision, accuracy and technical difficulty. In this section many of the various methods of body composition measurement are described briefly together with the major advantages and disadvantages of each. While the list of methods described is not totally comprehensive it represents the principal methods used in the determination of body composition in recent research.

ANTHROPOMETRY

Anthropometric data are the major facilitators of the estimation of body composition in studies conducted outside major clinical or research facilities. Values from the determination of skinfold thickness at various sites and measurements of bone dimensions and limb circumferences can be used in multiple regression equations to predict body density and to calculate body fat and fat-free mass, (body weight - body fat). Greatest emphasis has been placed on the use of skinfold thickness measurements to estimate body fat. This approach is based on two assumptions: the thickness of the subcutaneous adipose tissue reflects a constant proportion of the total body fat; and the sites selected for measurement represent the average thickness of the subcutaneous adipose tissue. Neither of these assumptions has been proven to be true: furthermore, because there is little information on the distribution of fat in the body of the general population, the validity of using skinfold equations to predict body composition is restricted to populations from whom these equations were derived.

The measurement of skinfold thickness is made by grasping the skin

and adjacent subcutaneous tissue between the arms of a constant pressure (0.1 N mm^{-2}) calliper set. Wilmore and Behnke, (1969 & 1970), developed separate prediction equations for lean body mass, (LBM), and body density, (BD), for males and females.

These equations for adult males are:

$$LBM \ (kg) = -6.481 + 1.1401 \ ht + 0.7453 \ Wt \\ -0.2423 \ M_2 - 0.2017 \ M_3 + 0.2100 \ M_4$$

$$BD \ (g \ cm^{-3}) = 1.06671 + 0.00098 \ ht - 0.00027 \ M_1 \\ - 0.00071 \ M_2 - 0.00040 \ M_3 + 0.00074 \ M_4$$

and for adult females:

$$LBM \ (kg) = 8.629 + 0.680 \ Wt - 0.163 \ F_1 - 0.100 \ F_2 - 0.054 \ F_3$$

$$BD \ (g \ cm^{-3}) = 1.06234 - 0.00068 \ F_1 - 0.00039 \ F_2 - 0.00025 \ F_3$$

Where   ht = height (m)   Wt = weight (kg)

M_1 = suprailiac skinfold (mm) F_1 = scapula skinfold (mm)

M_2 = abdominal skinfold (mm) F_2 = triceps skinfold (mm)

M_3 = thigh skinfold (mm) F_3 = thigh skinfold (mm)

M_4 = knee skinfold (mm)

Durnin and Womersley, (1974), and Jackson *et al.*, (1980), also derived regression equations to predict whole body density. However they used three or four skinfold measurements together with age and gender combined in a logarithmic expression. This type of mathematical function was suggested necessary as skinfold thickness is not linearly related to subcutaneous fat.

eg.   for males aged between 20 and 29:

$$BD \ (g \ cm^{-3}) \ = \ 1.1631 \ - \ 0.0632 \ \log \ (\ S_b + S_t + S_{sc} + S_{si} \ )$$

and for females aged between 20 and 29:

$$BD \ (g \ cm^{-3}) \ = \ 1.1599 \ - \ 0.0717 \ \log \ (\ S_b + S_t + S_{sc} + S_{si} \ )$$

(Durnin and Womersley, 1974)

where: S_b = biceps skinfold (mm) S_{sc} = subscapular skinfold (mm)

S_t = triceps skinfold (mm) S_{si} = supra-iliac skinfold (mm)

The precision of a measurement of skinfold thickness is dependent upon the skill of the anthropometrist and the site measured. Edwards *et al.*, (1955), report a precision of 5% by a properly trained anthropometrist, however they noted that this error can increase slightly if skinfold thicknesses get very large (> 15 mm) or small (< 5 mm). Lohman, (1981), reports that measurements on the same subjects can vary between operators by as much as 10 % and the best precision in body composition predicted by anthropometry determined by densitometry is approximately 5%, (depending on the prediction equation and sample of subjects). It should also be noted that almost all prediction equations include terms based on age, gender and sometimes weight; all of which increase the correlation between measured and accepted values for a given sample group.

The technique is ideal for use in field studies and with a total cost of the instrumentation as low as $ 100 it appears an attractive possibility to body composition analysis. However while the precision may be as low as 5% for a particular operator, the accuracy or validity of the measurement is highly dependent on the skill of the operator and also on the population, (age, ethnic origin, fitness level, state of health), being studied, (Lukaski, 1987).

DENSITOMETRY

This method is based on the two compartment model and the known densities of fat and fat-free mass (0.900 and 1.100 g cm^{-3}). These densities were confirmed by direct chemical analysis in mammals (Mendez and Keys, 1960). The apparent weight of the subject when fully submerged is determined and using Archimedes' principle, the whole body volume can be calculated.

$$Volume = \frac{(real\ Mass\ -\ apparent\ Mass)}{density\ of\ water}$$

This volume needs to be corrected for the residual lung volume during submersion which makes a considerable contribution (1-2 L) in the estimate of total body volume. A second volume, gastrointestinal gas, is considerably smaller ($\approx$100 mL) and is not considered. Using the corrected body volume and the subject's mass, the whole body density can be calculated. Several equations have been derived to estimate percent body fat from whole body density, (BD expressed in g cm^{-3}). For example:-

$$\%\ FAT\ =\ \{\ (4.570\ /\ BD)\ -\ 4.142\ \}\ *\ 100$$

Brozek *et al.*, (1963).

$$\%\ FAT\ =\ \{\ (4.950\ /\ BD)\ -\ 4.50\ \}\ *\ 100$$

Siri, (1956).

These equations assume a constant level of hydration and a constant proportion of bone mineral to muscle. These assumptions were investigated by Siri, (1956), who identified the normal variation of water content as the largest single source of variability in the density of the fat-free body.

Werdein and Kyle, (1960), found a variation of 1 to 3% in the water content of the fat-free mass in healthy humans. Siri, (1956), concluded that the variation in protein / mineral ratio could lead to a variation in percent body fat of 2.1%. Based on these estimates of variability in bone mineral density and hydration of the fat-free body Lohman, (1981), calculated the theoretical error of 4% for predicting body fat in a population using densitometry. The present limit of precision of body density measurements is 0.0020 g cm^{-3} or 1% body fat, (Mendez and Lukaski, 1981). This suggests that the overall error of prediction of fat and fat-free mass in healthy humans using densitometry is 5%.

The results of densitometry are highly reproducible but the technique is limited to subjects who are: (i) able to be fully submerged in water, and (ii) not apprehensive about submersion. These limitations render the technique inappropriate for the very young or old and many subjects in states of ill-health. The physical size of the equipment involved makes it inappropriate for field studies. The capital cost of the equipment is approximately $30 000 but with minimal operating costs.

ISOTOPE DILUTION

The isotopes of hydrogen and ogygen, (deuterium ^{2}H, tritium ^{3}H and ^{18}O), are commonly used to measure total body water using the technique of isotope dilution analysis. The typical procedure for using labelled water includes either the ingestion or the intravenous injection of a specified quantity of the tracer. After an appropriate equilibration period a sample of blood or urine is obtained. The calculation of TBW volume is based on the relationship: $C_1 V_1 = C_2 V_2$ where $C_1 V_1$ is the amount of tracer administered, C_2 is the final concentration of tracer in the biological fluid, and V_2 is the

volume of TBW. Losses of the tracer in urine during the procedure need to be accounted for.

The length of time required for tracer equilibration depends on the characteristics of the study sample. Lukaski and Johnson, (1985), reported that in healthy humans equilibration occurs in saliva, plasma and urine within 2 hours after ingestion of the tracer and remains at a constant concentration for the next 3 hours. Moore *et al.*, (1963) and Streat *et al.*, (1987), found that in individuals suffering from excess water accumulation equilibration may require 4-6 hours.

Liquid scintillation is a convenient and efficient method of detection for radioactive tritium. Deuterium has been measured using a variety of techniques including fixed filter infrared absorptiometry, gas chromatography, mass spectrometry, and Fourier transform infrared spectrometry, (Lukaski, 1987). The main advantage associated with deuterium is that it is not radioactive, hence it delivers no radiation dose to the subject; and is nontoxic at the dose rates used.

The quantity of tracer given depends on the type of tracer administered, the analytical system used, and the degree of precision required. In general the smallest dose that allows the required analytical precision and accuracy and provides the lowest risk to the subject should be given. Among researchers using tritium, a common adult dose is 2 MBq which results in an effective dose equivalent of 0.28 mSv, (Culebras and Moore, 1977). This radiation dose may be compared with the ICRP 60 (International Commission on Radiological Protection, 1991) recommended limit of 1.0 mSv per year for members of the public. Although these recommendations do not apply to medical applications they can be used for comparison. When deuterated water is used the dose required varies from

0.1 g to 1.0 g per kg body weight depending on the analytical system used (Nielsen *et al.*, 1971).

Total body water can be further subdivided into intracellular water (ICW) and extracellular water (ECW), and while water molecules pass freely between the two subcompartments there are some molecules or ions which do not, and remain in the ECW. When these substances are labelled with a radioactive marker they become effective dilution tracers of ECW. Typical examples of these substances are the inulin molecule and the bromide and sulphate ions.

The administering of an external substance constitutes an invasive procedure and when this substance is radioactive its use needs to be well considered in children and women of child bearing age, and is generally not appropriate for serial studies. While most isotopic tracers are only moderately expensive they all require sophisticated analytical systems. Although the analytical equipment is not portable, the technique is adaptable to field studies as it is not necessary to analyse the biological samples immediately after collection.

Determination of body water by isotope dilution is one of the few direct methods available for *in vivo* body composition analysis. The precision associated with the detection of deuterium in biological fluids is between 1.3% and 2.5% depending on the type of instrument and tracer concentration, (Lukaski, 1987). The corresponding precision associated with liquid scintillation counting of tritium can be less than 1%. However it has been shown that isotope dilution using deuterium or tritium overestimates TBW by 1-5% due to exchange of the label with nonaqueous hydrogen in the body, (Sheng and Huggins, 1979). The capital costs associated with liquid scintillation counting equipment are quite high while the cost of

consumables are usually low depending on the isotope used.

ELECTRICAL CONDUCTIVITY (TOBEC)

As with the impedance method, the subject of this thesis, this method takes advantage of the difference in electrical conductivity and dielectric properties of fat and fat-free tissues to estimate body composition. The instrument is a long uniform solenoid driven by 2.5 - 5.0 MHz oscillating current. The oscillating magnetic field produced will induce an electrical eddy current in any conductive material placed inside the coil. The resulting secondary currents create a back *emf* and increase the impedance to the primary current. The difference in impedance measured when a subject is placed in the solenoid is used to calculate the conductivity of the whole body. Segal *et al.*, (1985), found that height^2 x conductivity gave the best prediction of fat-free mass, and when compared with densitometry gave a standard error of prediction of 3.7%.

Van Loan and Mayclin, (1987,a), describe a second generation instrument (TOBEC II) which generates a magnetic field 79 cm in diameter and 185 cm long with an oscillating frequency of 2.5 MHz. The subject is passed through the magnetic field and the resulting resistive and inductive changes are represented by a phase curve. While the phase is determined by both the geometric shape and the distribution of fat-free tissue, the shape of the phase curve does not 'visually' represent either geometry or fat-free mass distribution. As the phase curve is a periodic function a Fourier technique is applied to analyse the complex waveform. Multiple regression using the Fourier coefficients yields a correlation with total body water determined by least squares regression of r = 0.98.

The capital cost of the TOBEC instrument is ~$100 000 while operating costs are minimal. The technique using large heavy equipment is not a feasible alternative for use in field studies.

ULTRASOUND

This method uses an instrument in which electrical energy is converted in a probe to high frequency ultrasonic energy, which is then transmitted into the body in the form of short pulses. As these ultrasonic waves impinge perpendicularly upon the interfaces between tissues which differ in acoustic properties, part of the ultrasonic energy is reflected to the receiver in the probe and is transformed to electrical energy. The time displacement of this echo from the original pulse is represented as a vertical deflection of the horizontal time baseline on an oscilloscope. Assessment of adipose tissue thickness is made in A-scan which is the depth reading mode of ultrasound.

Borkan *et al.*, (1982), evaluated ultrasound and skinfold methods to predict body fat determined by potassium, [40]K. Although measurements made with the two techniques at the same site typically produced different mean estimates of adipose tissue thickness, the values were highly correlated (r > 0.80) with each other, indicating similar relative ranking by each technique. Fanelli and Kuczmarski, (1984), suggested that ultrasound and the calliper methods were equally good predictors of body fat, with correlations with densitometry being r = 0.809 and r = 0.779 respectively.

Although these data suggest a reasonable validity of the ultrasound approach, certain limitations have restricted its general acceptance. The optimum signal frequency has not been well defined. The literature details a

range of 2.5-7.5 MHz with the best predictive accuracy associated with the highest frequency, (Fanelli and Kuczmarski, 1984). A further difficulty is inter-operator variation and in particular the need for uniform and constant pressure applied by the probe to the scan site. Changes in pressure by probe application can affect the distribution of adipose tissue and subsequently affect the ultrasonic determination of adipose thickness. The cost of an ultrasound unit, (>$40 000), dedicated to body composition studies is not beyond the limitations of many budgets but when the cost of appropriately qualified personnel is taken into consideration the method may be inappropriate in many situations.

POTASSIUM

Potassium is not present in stored triglyceride and is essentially an intracellular cation. It also has a naturally occurring, (0.00118%), radioactive isotope ^{40}K which emits a 1.46 Mev gamma ray. Detection of this γ-ray can therefore be used to measure the body content of ^{40}K and hence total body potassium. Measurement of total body potassium requires specially constructed facilities with a large shielded room, or shadow shielded detectors, to reduce background radiation from cosmic and terrestrial sources. The gamma ray detectors in current systems consist of large thallium activated sodium iodide crystals which are positioned around the subject. The NaI crystal system has adequate energy resolution to permit selective counting of the 1.46 Mev gamma emissions from ^{40}K.

The attenuation of the gamma radiation may be determined by using a uniformly distributed caesium 137 source positioned very briefly under the supine subject. These attenuation factors are used to correct for differences in body size and geometry for each subject. Lykken *et al.*, (1983), report an

accuracy and precision of within 3% provided subjects shower to remove any contamination from bismuth 214, (a daughter of airborne radioactive radon). Using a concentration of potassium in men and women of 2.46 and 2.28 g per kg of fat-free mass, (Lukaski *et al.*, 1985), the fat-free mass of the subject can be determined.

An accurately calibrated, well shielded whole body counting system together with standard procedures for correction of counts due to body geometry, self absorption and control of bismuth background can measure absolute total body potassium and subsequently fat-free mass. The cost of such installations, (in excess of $200 000 for a shadow shield system and $1M for a full steel room), together with technical support may prove inhibitive for many clinical institutions. Obviously the technique is generally not applicable to field studies of any type.

COMPUTED TOMOGRAPHY (CT)

Computed tomography (CT) can be used to determine regional body composition. The difference in X-ray attenuation of the body tissues is used to construct a two dimensional image of a thin cross sectional "slice" of the subject. Different methods have been used with the CT scan to analyse body composition. The structure of interest can be traced directly on the viewing console and the cross sectional area of adipose, bone, muscle or visceral organ determined. Using the slice thickness the volume can be calculated by summing over the required number of slices. This technique has been used to assess changes in muscle and adipose tissue in malnutrition (Heymsfield *et al.*, 1982), and to describe cross sectional differences in abdominal fat distribution during aging (Borkan *et al.*, 1985).

Kvist *et al.*, (1990) used CT measurements of adipose tissue from the Lumbar 4-5 vertebrae to predict total body fat. Compared to total body potassium the CT predictions had standard errors of 9% and 7% in men and women respectively, but an improvement of 2% was achieved in both groups when the weight/height ratio was included in the prediction equation.

Although the potential of CT scanners for body composition is promising, practical constraints limit their general use. Tothill, (1990), suggest that the effective dose equivalent for a CT scan is typically 0.2 mSv. This radiation dose may be compared with the ICRP 60 (International Commission on Radiological Protection 1991) recommended limit of 1.0 mSv per year for members of the public. Although these recommendations do not apply to medical applications they can be used for comparison. The exposure to ionising radiation prevents its application to whole body scans, multiple scans in the same individual, or scans of pregnant women or children. The cost and general availability of modern CT scanners prohibit the routine exclusive use for body composition studies.

MAGNETIC RESONANCE IMAGING (MRI)

This method uses the magnetic field associated with the hydrogen nucleus in the water molecule. An external magnetic field is applied across the body which aligns the magnetic moment of the hydrogen nuclei. A pulsed radio frequency wave is directed into body tissues. Hydrogen nuclei absorb the radio frequency energy *via* interaction with the magnetic moment, which causes the resultant nuclear magnetic moment to precess about the direction of the external magnetic field. When the radio signal is switched off the resultant magnetic moment returns to its original value and direction in a time characterised by a time constant T_1. The transverse magnetic

moment also decays to zero with a time constant T_2. These time constants, T_1 and T_2, are known as the longitudinal and transverse relaxation times. The excited nuclei emit the absorbed energy as radio frequency radiation and this emitted radiation is detected and subsequent computer analysis develops an image. Body tissues have characteristic relaxation times and by manipulating instrument parameters the image intensity and contrast can be adjusted. As the technique relies on hydrogen nuclei the image contrast between fat and muscle is high. Using optimum instrument parameters accurate estimation of fat and fat-free tissues is possible.

The application of MRI to body composition studies is only in the initial stages of development and hence it is difficult to present a fair evaluation of the technique. However preliminary studies are promising. Hayes *et al.*, (1982), quantified the water distribution of saline filled and normal rat lungs and obtained an error of less than 3% in phantoms. Lewis *et al.*, (1986), used MRI to determine total body water in baboons with an accuracy of 3% compared with gravimetric results.

The advantage of MRI over computed tomography is that it does not use ionising radiation. It has the capability to produce images in response to intrinsic tissue variables. As well as hydrogen, MRI has the potential to image phosphorus (^{31}P) and also carbon (^{13}C), (Allen, 1990). The optimism of possible future applications of MRI must be tempered with the practical limitations of restricted availability and very high cost.

NEUTRON ACTIVATION ANALYSIS

Neutron activation systems deliver a beam of fast neutrons to the subject. The energy of these neutrons are decreased by successive collisions,

and are eventually captured by atoms of the target elements in the body producing excited or radioactive nuclides, eg. ^{15}N, ^{49}Ca. The excited nuclei return to ground state energy by the emission of gamma photons with an energy characteristic of the nuclide; the emission of the γ photon is almost instantaneous, (a prompt γ). When the product nucleus is radioactive a delayed γ may be emitted. The type of gamma emission, (prompt or delayed), is dependent upon the nuclide: *eg* ^{15}N emits a prompt gamma while ^{49}Ca emits a delayed gamma with a half life of 8.9 minutes. By using sensitive gamma spectroscopy the detection of the characteristic gamma photons enables the identification of many elements. The neutron sources used vary from cyclotrons to plutonium-238/beryllium and californium-252 isotopic sources.

The dose equivalent delivered to the subject varies considerably from 3 mSv to 20 mSv, using a ^{238}Pu-Be neutron source, (Tothill, 1990). Although Krishnan *et al.*, (1990), quote a mean effective dose equivalent of 0.2 mSv for the measurement of total body nitrogen using a ^{252}Cf neutron source. These dose equivalents were calculated using a quality factor of 10; which may underestimate the real dose equivalent. This effective dose equivalent may be compared with the ICRP 60 (International Commission on Radiological Protection, 1991) recommended limit of 1.0 mSv per year for members of the public. The precision of *in vivo* neutron activation analysis is between 2% and 5% of body mineral, depending on the system and absorbed dose (Tothill, 1990; Krishnan *et al.*, 1990; Ryde *et al.*, 1990).

More information can be gained from neutron activation analysis than by any other available method. However, factors such as the high cost (in excess of $50 000), the need for skilled operators, lack of mobility, and the use of ionising radiation preclude its general use in the assessment of body composition. Neutron activation analysis is currently used to determine body

nitrogen, (an indicator of body protein), and chlorine by the prompt γ ray analysis technique, but only at relatively few centres.

DUAL ENERGY X-RAY ABSORPTIOMETRY (DEXA)

This technique makes use of the difference in x ray absorption between bone and soft tissue. The absorption of an X-ray beam passing through bone and soft tissue is given by:

$$I = I_0 \exp^{-(\mu_b x + \mu_{st} y)}$$

where:
I = transmitted intensity.

I_0 = incident intensity.

x = bone thickness.

y = soft tissue thickness.

μ_b = mass attenuation coefficient of bone.

μ_{st} = mass attenuation coefficient of soft tissue.

The mass attenuation coefficients μ_b and μ_{st} vary with x ray energy.

A tightly collimated x ray beam of two different energies is directed at the subject. The subject is scanned in a rectilinear pattern and the attenuation measured at each pixel for both energies. The x rays are detected by a cadmium tungstate scintillator coupled to a photomultiplier tube. The transmitted intensity at energies E_1 and E_2 are given by:

$$I_1 = I_{o_1} \exp^{-(\mu_{b_1} x + \mu_{st_1} y)}$$

$$I_2 = I_{o_2} \exp^{-(\mu_{b_2} x + \mu_{st_2} y)}$$

By combining and eliminating y from the above equations an expression for the bone thickness, x, in a given pixel can be obtained:

$$ x = \frac{\ln(I_1/I_{o_1}) - R \ln(I_2/I_{o_2})}{R\,\mu_{b_2} - \mu_{b_1}} \qquad where \quad R = \frac{\mu_{st_1}}{\mu_{st_2}} $$

Similarly by eliminating x an expression for the soft tissue thickness, y, could be obtained. By integrating over any region of interest the bone mineral mass and soft tissue mass can be determined. When used in regions not containing bone the technique can differentiate between fat and fat-free mass.

Optimum determination of thicknesses x and y requires a large difference between I_1/I_{o1} and I_2/I_{o2} and also between μ_{b1} and μ_{b2}. To achieve these differences x ray energies of approximately 40 keV and 100 keV are used. The dual energy beam can be generated by two different methods:

(i)   dual kV system where the x ray tube produces alternating pulses at 70 kV and 140 kV with effective beam energies of 43 keV and 110 keV;

(ii)   K edge filtered x ray system where the x ray tube is operated at a constant potential and a K edge filter provides the required dual energy, (*eg.* a cerium filter with a K edge of 40.4 keV).

Sorenson, (1991), reports that the exposure and dose delivered to the subject using a K edge filtered system is about one third that of a dual kV system, to achieve the same precision. Sorenson also reports that the precision of the bone mineral density measurement is dependent upon the thickness of the subject and the x ray exposure, with a maximum precision of 0.5% achieved with a K edge filtered system and subject skin exposure of

1 mR.

DEXA has been shown to be a reliable technique to predict bone mineral mass, (Wahner *et al.*, 1988). Despite the relatively small difference in the x ray mass attenuation coefficients of fat and fat-free mass, recent studies (*eg* Pritchard *et al.*, 1993) have used the technique to determine fat-free mass and body fat, (precision ±8% compared with isotope dilution or densitometry). While the DEXA technique provides bone mineral mass measurements with a high degree of precision and low subject radiation dose it is less precise when used to measure the ratio of fat to fat-free tissue. The x ray installation needs to be a dedicated system with a cost of approximately $ 100 000.

BIOELECTRICAL IMPEDANCE ANALYSIS (BIA)

The hypothesis that bioelectrical impedance measurements can be used to determine fat-free mass is based on the principle that the impedance of a conducting body is related to the conductor length, cross sectional area, and signal frequency. Using a constant signal frequency the impedance is given by:

$$Z = \rho L / A$$

where Z = impedance (Ω)

ρ = resistivity of the medium (Ω cm)

L = conductor length (cm)

A = cross sectional area (cm^2)

and V = volume (cm^3) = $A * L$

Eliminating A yields: $$V = \rho L^2 / Z$$

The human body contains intra- and extracellular fluids which behave as conductors, and cell membranes and tissue interfaces which behave as imperfect capacitors. These conductors and capacitors respectively provide the resistive (R) and reactive (X) components of the total body impedance, given by:

$$Z = \sqrt{(R^2 + X^2)}$$

The underlying principle of BIA assumes the body is an isotropic conductor with a uniform length and cross-sectional area. This assumption is in fact incorrect. The geometrical shape of the human body more closely approximates five cylinders (two arms, two legs and a trunk), excluding the head. As resistance is inversely proportional to cross-sectional area the arms have the greatest influence on whole body impedance but the smallest contribution to body volume. Secondly, isotropic conduction denotes that current density is uniformly distributed along axes in all directions. This does not occur throughout the human body. Due to organs such as the lungs, intramuscular fat and numerous tissue interfaces which all act as dielectric conductors, electrical conduction is anisotropic through certain body segments. However despite these limitations BIA has proven to be a reliable technique in body composition measurement.

Nyboer *et al.*, (1943), demonstrated experimentally that biological volumes were related inversely to impedance. Lukaski *et al.*, (1985), used a constant current of 800 μA at a frequency of 50 kHz to measure body impedance and concluded that, as the reactance (X) was small relative to the resistance (R), resistance was a better predictor and the volume could be expressed as:

$$V \propto L^2 / R$$

and   **TBW** $\propto$ **ht^2/R**

       where   TBW = total body water

                     ht = person's height

There has been a great deal of research conducted establishing and validating the technique of bioelectrical impedance analysis at 50 kHz, (for a review see Lukaski, 1987). However there are still conflicting opinions as to what parameters, (other than ht^2/R), should be included in the prediction equations and the degree of enhancement caused by their inclusion, (Diaz, 1989). A number of research groups have developed prediction equations based on impedance measurements at 50 kHz and some of these are listed below.

FFM = 0.734 ht^2/R + 0.116 Wt + 0.096 X + 0.878 S - 4.03

(Lukaski and Bolunchuk, 1987)

FFM = 0.00085 ht^2 + 0.3767 Wt - 0.02375 R - 0.1531 Age + 17.7868

(Van Loan and Mayclin, 1987,b)

FFM = 0.485 ht^2/R + 0.338 Wt + 5.32   for Males

FFM = 0.475 ht^2/R + 0.295 Wt + 5.49   for Females

(Lohman, 1988; cited in Graves *et al*, 1989)

FFM = 0.0006636 ht^2 - 0.02117 R + 0.62854 Wt - 0.12380 Age + 9.33285

for < 20% BF

FFM = 0.0008885 ht^2 - 0.02999 R + 0.42688 Wt - 0.07002 Age + 14.5243

for > 20% BF   (Segal *et al,* 1988)

FFM = 0.4936 ht^2/R + 0.3332 Wt + 6.493   for Males

FFM = 0.6483 ht^2/R + 0.1699 Wt + 5.091   for Females

(RJL Systems Inc, Detroit. see Fuller, 1993)

where   FFM = fat-free mass (kg)   ht = height (cm)

            R = resistance at 50 kHz (Ω)   Wt = total body weight (kg)

            X = reactance at 50 kHz (Ω)   S = sex (1=male 0=female)

The standard error of prediction of FFM stated by Lukaski, (1987), based on

densitometry was 4%.

At low frequencies the membrane capacitance increases considerably and the current passes predominantly through the extracellular fluid. Research has taken advantage of this phenomenon to estimate the extracellular subcompartment of total body water. Espejo *et al.*, (1989), investigated the correlation between the bioelectrical impedance at 1.0 kHz and the extracellular water volume (ECW) measured by isotope dilution using bromide ions. The correlation coefficient obtained, (r = 0.95 between L^2/Z_1 and ECW), suggests that impedance measurements at low frequencies may be able to predict ECW. While this result is promising it has only been validated in a small study on animals, (n=7), and with the use of needle electrodes.

The use of bioelectrical impedance analysis to predict body water and fat-free mass is becoming more widely accepted and popular. This is due to its precision and accuracy being comparable or better than other common techniques but also because of its other numerous advantages. The current capital cost is comparatively low (~$6 000) while operating costs are minimal. It is a noninvasive procedure with an absolute minimum of stress or discomfort to the subject, can be repeated as frequently as desired irrespective of state of health, and is suitable for application in field studies. A modification of this technique is the basis of this thesis and hence there is a detailed description of the principles involved in the next section, (§2).

§ 1.2 SUMMARY OF TECHNIQUES

Garrow, (1982), summarises the characteristics of the ideal method for assessing human body composition as: being relatively inexpensive at initial

purchase and for maintenance of operation, causing little inconvenience for the subject, able to be operated by unskilled technicians, and yielding highly reproducible and accurate results. Unfortunately no method is available that meets these stringent criteria. Table I shows a relative comparison of the major characteristics of the methods discussed.

TABLE 1.1

Limitations* of methods of determining human body composition (adapted from Lukaski, 1987).

Method	Cost	Technical difficulty	Precision
Anthropometry (Skinfolds)	1	2	2
Densitometry	3	4	5
Isotope Dilution (TBW):			
- Deuterium	2	3	3
- Tritium	3	3	3
Electrical Conductivity (TOBEC)	5	1	4
Ultrasound	3	3	3
Potassium	4	4	4
Computed Tomography (CT)	5	5	3
Magnetic Resonance Imaging (MRI)	5	5	3
Neutron Activation Analysis (NAA)	5	5	5
Dual Energy X-ray Absorption (DEXA)	4	4	4
Bioelectrical Impedance Analysis (BIA)	2	1	4

* Ranking system: ascending scale, 1 = least and 5 = greatest.

Bioelectrical impedance analysis, (BIA), is a method which is quick and simple in its application, non-invasive, offers virtually no inconvenience to the subject, can be operated by unskilled technicians and yields reproducible results. However the accuracy of body composition predictions using single frequency BIA instruments, in subjects of illhealth, has been questioned, (Battistini *et al.*, 1992; Jebb and Elia, 1993). Current BIA techniques use impedance measurements at a single fixed frequency to estimate total body water, (the sum of extra- and intracellular water). However the variation of impedance with frequency may provide valuable detail about the extra- to intracellular fluid balance and subsequently yield more accurate estimates of both total body water and extracellular water in subjects of normal as well as altered states of health. The ensuing sections detail investigations in the application of multiple frequency bioelectrical impedance analysis to estimate total body water and extracellular water in subjects of normal health as well as those of altered states of health.

SECTION 2

MULTIPLE FREQUENCY

BIOELECTRICAL

IMPEDANCE ANALYSIS

(MFBIA).

§ 2 MULTIPLE FREQUENCY BIOELECTRICAL IMPEDANCE ANALYSIS (MFBIA)

When an alternating electric current (AC) passes through the body it will pass through both the extracellular and intracellular fluid compartments in a ratio dependent upon the frequency and also the electrical characteristics of the body. The extracellular pathway is considered to be purely resistive whereas the intracellular pathway includes the capacitive effect of the cell membrane and consequently has a reactive component. To investigate the behaviour of AC current through the body it is therefore necessary to examine equivalent electrical circuit models of biological tissue.

§ 2.1 EQUIVALENT CIRCUITS FOR BIOLOGICAL TISSUE

A large number of equivalent circuits have been proposed (summarised by:- Cole, 1968; Schanne and Ceretti, 1978; Zhang and Willison, 1991). All equivalent circuits comprise a series/parallel network of resistors and capacitors and must have the following characteristics when an electric potential is applied:

► At zero frequency (DC), the current must pass entirely through the resistance representing the extracellular fluid because the impedance of the cell membrane capacitance will be infinite.

► As the frequency increases, the current will pass through both the extracellular and intracellular pathways. The proportion in each will be dependent upon frequency.

The simplest and most widely used model of electrical behaviour of biological tissue is shown in figure 2.1; R_e and R_i represent the resistance of the extra- and intracellular fluids respectively and C represents the capacitance of the cell membrane.

Rₑ

EXTRACELLULAR   BRANCH

· INTRACELLULAR   BRANCH

Rᵢ   **C**
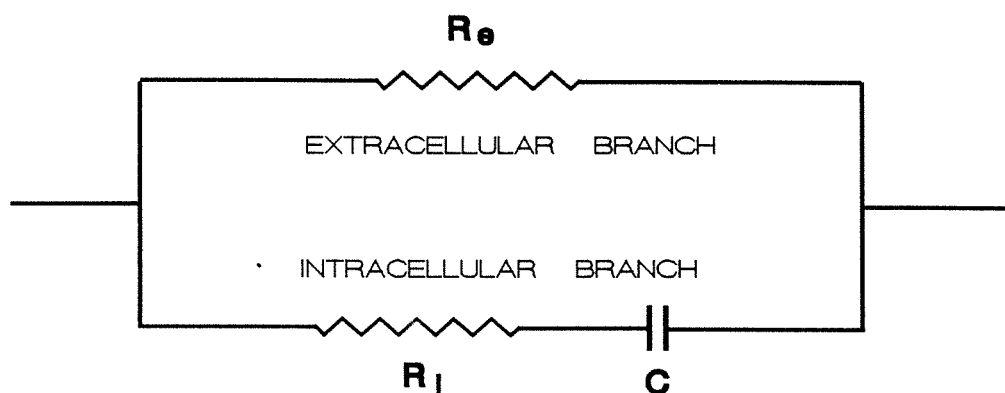
FIGURE 2.1

Simplified equivalent circuit for biological tissue

Asami *et al.*, (1989), and Zhang and Willison, (1991), proposed a "double shell model" for a cell suspension of lymphocytes (figure 2.2). In this model C_1 and C_2 represent the capacitance of the cell membrane and lysosome[1] membrane respectively; R_1, R_2 and R_3 are the resistances of the extracellular fluid, cytoplasm and lysosome interior. This "double shell" model enabled Zhang and Willison to quantify characteristics of a given cell type using impedance measurements of monocellular suspensions.

While the analysis of measurements based on the "double shell" model may provide greater detail about monocellular suspensions, it is the simple model represented in figure 2.1 that enables the relationship between the

---

[1] an intracellular cytoplasmic body bound by a single membrane.

volumes of the extra- and intra-cellular fluids and the measured impedance to be determined. Consequently the simplified equivalent circuit as shown in figure 2.1 is the most appropriate for discussion in this thesis.
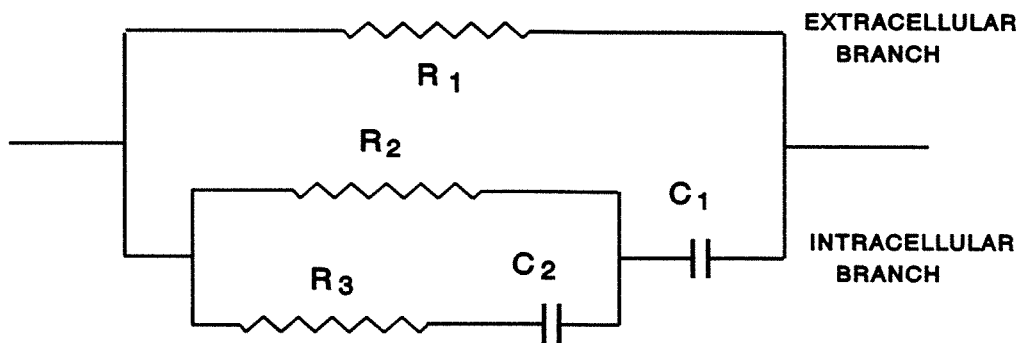
FIGURE 2.2

Equivalent electrical circuit for suspension of lymphocytes.

§ 2.2   FREQUENCY   RESPONSE   OF   THE   EQUIVALENT CIRCUITS

Almost all previous research using bioelectrical impedance to estimate body composition has been limited to single frequencies and not investigated the overall frequency response of biological impedance.

The relative magnitudes of the extracellular and intracellular components of impedance of an alternating current (AC) are frequency dependent. At zero frequency the capacitor acts as a perfect insulator and all of the current passes through the extracellular fluid, hence the resistance, R_0, at zero frequency equals R_e. At infinite frequency the capacitor acts as a perfect conductor and the current passes through the parallel resistive combination. The resistance at infinite frequency is given by $R_\infty = R_i R_e / (R_i + R_e)$. The measured values of R_0 and R_∞ would therefore directly provide

the values of R_e and R_i required for the estimation of ECW and ICW. However the practical constraints of skin-electrode impedance do not permit application of DC (direct current) or very high frequency AC currents using electrodes placed on the skin, hence the values of the frequencies commonly used can only approximate the ideal measurement frequencies.

The impedance of the equivalent circuit in figure 2.1 at an angular frequency ω, where $\omega = 2\pi$ * frequency, is given by:

$$Z = R_\infty + \frac{R_0 - R_\infty}{1 + (j\omega\tau)}$$

(eqn 2.1)

$$\text{where} \qquad R_\infty = \frac{R_i \, R_e}{R_i + R_e} \qquad \text{and} \qquad R_0 = R_e$$

Where τ, the time constant of a capacitive circuit, describes the rate at which charge accumulates and disperses from capacitive components, and subsequently affects the impedance to AC current. For the circuit shown in figure 2.1 the time constant is given by:

$$\tau = (R_e + R_i) \, C$$

(eqn 2.2)

However in biological tissues, C and hence τ are not constant but distributed about a mean value, (Pethig, 1979). Equation 2.1 describes the complex impedance of the circuit in figure 2.1. By separating the real and imaginary parts, expressions for the resistance (R) and reactance (X) can be obtained, (equations 2.3 and 2.4).

$$R = R_\infty + \frac{R_0 - R_\infty}{1 + \omega^2 \tau^2}$$

<div align="right">(eqn 2.3)</div>

$$X = - \frac{\omega \tau (R_0 - R_\infty)}{1 + \omega^2 \tau^2}$$

<div align="right">(eqn 2.4)</div>

Where the impedance, Z, is the vector sum of the resistance, R, and reactance, X. Eliminating the parameter $\omega\tau$ from equations 2.3 and 2.4 yields:

$$R^2 + X^2 - R(R_0 + R_\infty) + R_0 R_\infty = 0$$

<div align="right">(eqn 2.5)</div>

On a plot of reactance (X) vs resistance (R) equation 2.5 represents a circle with the centre on the R axis at $(R_0+R_\infty)/2$ and with a radius $(R_0-R_\infty)/2$ (for convenience the negative X axis is usually drawn upwards as shown in figure 2.3). This impedance locus is known as a Cole-Cole plot and represents the impedance of the circuit for frequencies from zero to infinity. With increasing ω the tip of the impedance vector (Z) moves anticlockwise around the locus. At any given frequency the magnitude of the impedance is represented by the length of the vector, the phase by the angle between the vector and the R axis, and the resistance and reactance by the coordinates of the point on the locus.
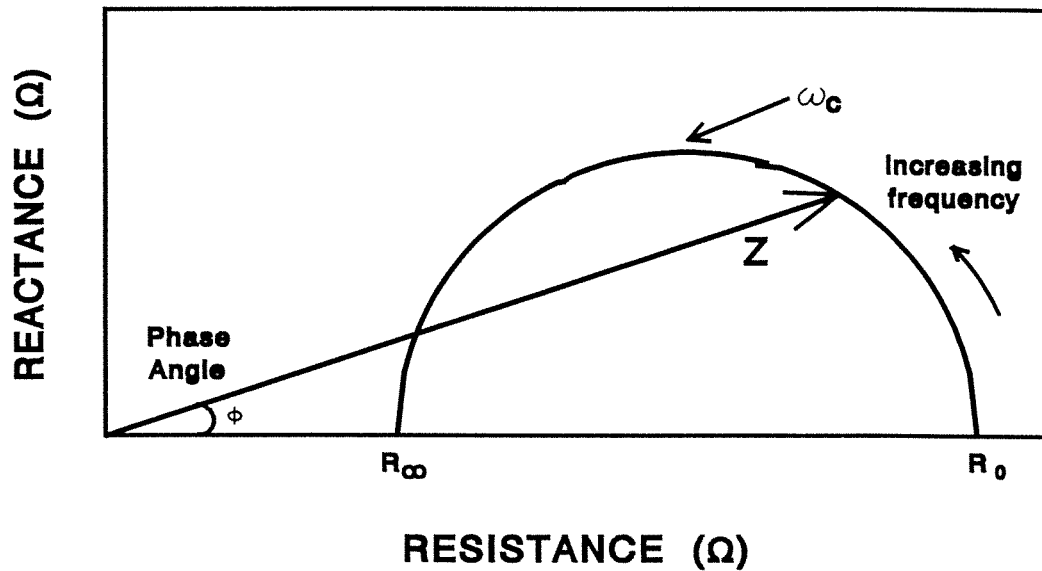
FIGURE 2.3

Impedance locus for the simplified equivalent circuit

for biological tissue, (figure 2.1).

If the value of the expression for the circuit reactance in equation 2.4 is maximised by differentiating with respect to ω and equating to zero, the result identifies the frequency at the peak of the locus. This is known as the characteristic frequency, ω_c, and is given by:

$$\omega_c = \frac{1}{\tau} \qquad \qquad where \qquad \omega_c = 2\pi f_c$$

(eqn 2.6)

Cole, (1928), reported that the locus resulting from impedance measurements of biological specimens remain circular in shape but with a centre depressed below the resistance axis as shown in figure 2.4. The

depressed centre results from the cell membrane being an imperfect capacitor and the large variation in cell type, structure and size in a biological organism causing a distribution of time constants, (Fricke, 1932; Cole, 1968; Schwan, 1957). Cole and Cole, (1941), showed that when there is a distribution of time constants the complex impedance can be represented by:

$$Z = R_\infty + \frac{R_0 - R_\infty}{1 + (j\omega\tau)^{(1-\alpha)}}$$

(eqn 2.7)

where α has a value between 0 and 1, and $\frac{1}{2}\pi\alpha$ is the angle to the depressed centre as illustrated in figure 2.4.

RESISTANCE (Ω)
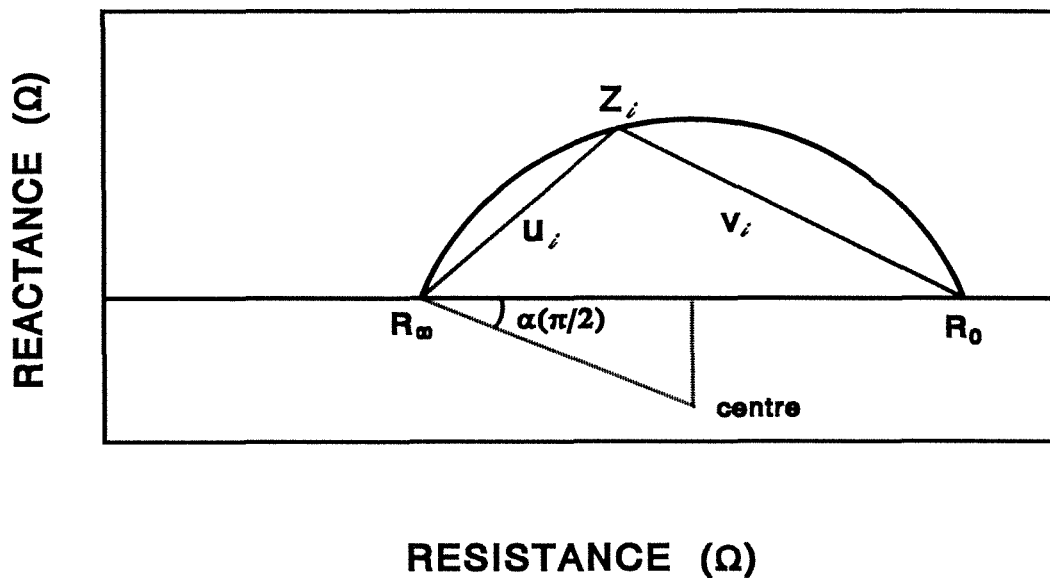
FIGURE 2.4

Measured impedance locus from a biological system.
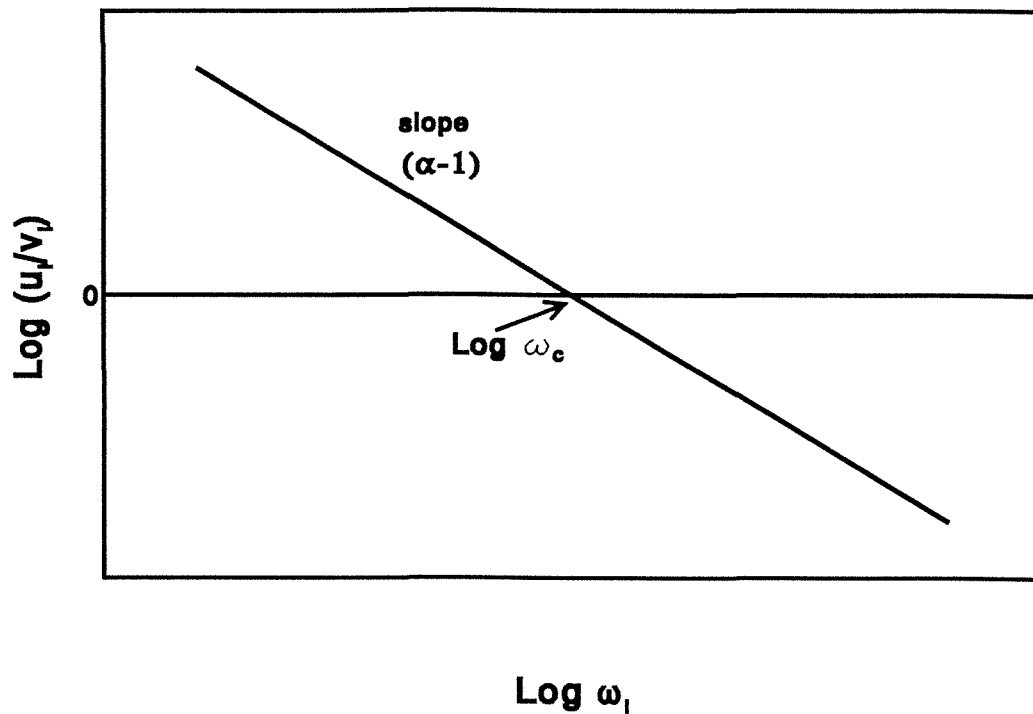
FIGURE 2.5

Graphical determination of ω_c.

The characteristic frequency can be determined by first calculating the lengths of chords u_i and v_i (figure 2.4), which join the infinite frequency, R_∞, and zero frequency, R_0, intercepts to the data points at frequency ω_i. A plot of $log(u_i/v_i)$ vs $log(\omega_i)$, figure 2.5, yields a straight line with a slope $(\alpha-1)$ and an x-axis intercept of ω_c, the characteristic frequency, (Cole and Cole, 1941).

Ohm's law confirms that currents in parallel branches are inversely proportional to the impedance of the branch. Using this and equation 2.6 an expression for the ratio of the current through the extracellular branch, (I_e), to the current in the intracellular branch, (I_i), at the characteristic frequency can be found.

$$\left(\frac{I_e}{I_i}\right)^2 = 2\left(\frac{R_i}{R_e}\right)^2 + 2\left(\frac{R_i}{R_e}\right) + 1 \qquad \textit{when} \quad \omega = \omega_c$$

(eqn 2.8)

The important feature demonstrated by equation 2.8 is that the ratio of the two currents is independent of the capacitance at the characteristic frequency, and determined solely as a function of the ratio of extra- to intracellular resistance. The prediction of total body water from impedance measurements is based on the measurement of the resistance to current flow in both the extra- and intracellular compartments. As the current at the characteristic frequency passes through both the extra- and intracellular fluids, and the ratio of the currents is dependent only on the resistances of the body fluids, and not the capacitance of cell membranes, the characteristic frequency should be a more appropriate frequency from which to predict TBW than the more commonly used frequency of 50 kHz at which the ratio I_e/I_i is also a function of the capacitance.

SECTION 3

DESIGN OF EQUIPMENT FOR THE MEASUREMENT OF BODY IMPEDANCE.

§ 3   DESIGN   OF   EQUIPMENT   FOR   THE MEASUREMENT OF BODY IMPEDANCE

This study investigated the relationship between body composition and the variation of body impedance with the frequency of the applied AC current.

§ 3.1   ELECTRODES AND ELECTRODE PLACEMENT

When the impedance of human subjects is measured surface electrodes are used in preference to needle electrodes thus overcoming problems associated with variations in insertion depth, possible tissue trauma and subject acceptance, (Hoffer *et al.*, 1969). The use of surface electrodes precludes the application of the bipolar technique, employed by Thomasset, (1962), due to skin-electrode impedance at the current drive electrode site, (Hoffer *et al.*, 1969; Lukaski and Bolunchuk, 1988). Consequently the tetrapolar surface electrode arrangement, consisting of two measurement electrodes and two distally positioned drive electrodes, was adopted. This electrode configuration has been used on humans by essentially all investigators since Hoffer *et al.*, (1969). The surface electrodes used throughout this study were Ag/AgCl electrocardiograph electrodes manufactured by 3M (Minnesota, USA). The skin electrode impedance also precludes the use of surface electrodes to measure DC resistance and establishes a lower frequency limit of 1-2 kHz, (Thomas *et al.*, 1992).

The placement of the electrodes is dependent upon the body segment being measured, however the drive electrodes need to be positioned sufficiently distal, (typically 5 cm), from the measurement electrodes to ensure an adequate distribution of the current throughout the tissues in the

measurement region. A typical electrode placement for the measurement of whole body impedance is shown in figure 3.1.
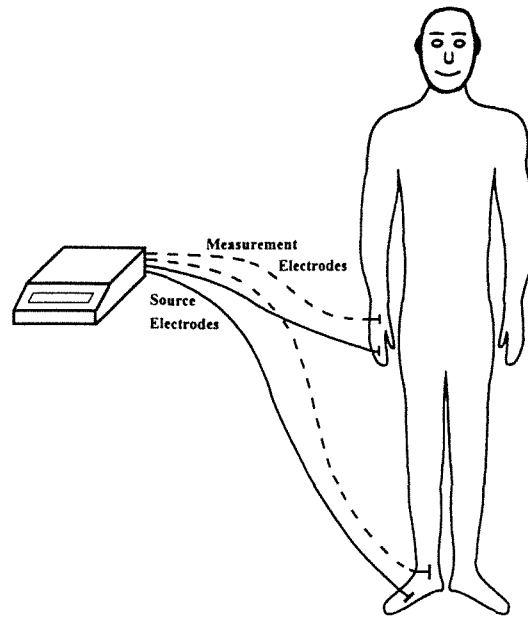
FIGURE   3.1

Typical electrode placement for the measurement

of whole body impedance in humans.

§ 3.2   MULTI-FREQUENCY BIO-IMPEDANCE METER

Some of the initial work, of this study, conducted on animals measured body impedance using a multi-frequency bio-impedance meter specifically manufactured for this study by SEAC (Brisbane, Australia). This instrument measured the impedance and phase at six individual frequencies using an AC current as listed in table 3.1. The frequency was set by a 1 MHz ceramic resonator with a 0.01% tolerance and the different frequencies obtained by digital division.

TABLE 3.1

Measurement frequencies and their drive currents for the

Multi-frequency bio-impedance meter

Frequency (kHz)	Current (µA)
100	800
50.0	800
32.5	800
10.0	400
3.25	200
1.00	100

The fine calibration of the instrument at each of the individual frequencies was established at the time of commissioning by the adjustment of designated *trim-pots* and was monitored on a daily basis using precision calibration resistors, (but required minimal further adjustment).

§ 3.3 SWEPT-FREQUENCY BIO-IMPEDANCE METER

From the results and success of the multi-frequency bio-impedance meter, (discussed in section §6), the specifications of the swept-frequency bio-impedance meter (SFBIM) were formulated. The SFBIM was constructed by SEAC (Brisbane, Australia) to specifications described, and sequentially measures the impedance and phase at up to 496 frequencies logarithmically spaced from 4 kHz to 1 MHz. The data, (comprising: the value of the frequency, the impedance index and phase index) are stored in the memory of the instrument before being uploaded to a computer.

The number of discrete frequency steps taken between measurements is referred to as the *delta* and can be varied from 1 to 16, (table 3.2), hence increasing the number of complete measurements (*logs*) able to be stored in

the instrument's memory. The leads which connect the electrodes to the instrument have active electrical screening to minimise any electrical noise which may be present, particularly at the higher frequencies.

TABLE 3.2

Variation in measurement log size with the number of frequencies sampled.

Delta value	Frequency points	Memory size (no. of logs)	Measurement time (s)
1	496	16	20
2	248	32	15
4	124	64	11
8	62	127	10
16	31	246	9

The impedance and phase data recorded are referred to as indices as they need to be rescaled using calibration files before being expressed in units of ohms and degrees respectively. This procedure was performed on a computer after uploading and is discussed in the next section (§3.4). The instrument is powered by a rechargeable battery and supplies a drive current of 350 μA (RMS) held constant over all frequencies. This is below that stated by the Australian standard (AS 3200.1, Standards association of Australia, 1990) which recommends a maximum AC current of 400 μA (RMS) at 4 kHz increasing to 10 mA at 100 kHz and higher.

§ 3.4 CALIBRATION OF THE SFBIM AND ANALYSIS OF IMPEDANCE MEASUREMENTS

The calibration procedure involves recording measurement logs on 11 standard resistors from 10 Ω to 1940 Ω and also an RC series combination

yielding an impedance of 470 Ω, 10° at 50 kHz. From these 12 calibration logs the offset of the phase and scaling of the impedance and phase indices are determined. The 11 measurement logs from the pure resistive circuits constitute a three dimensional matrix (figure 3.2).
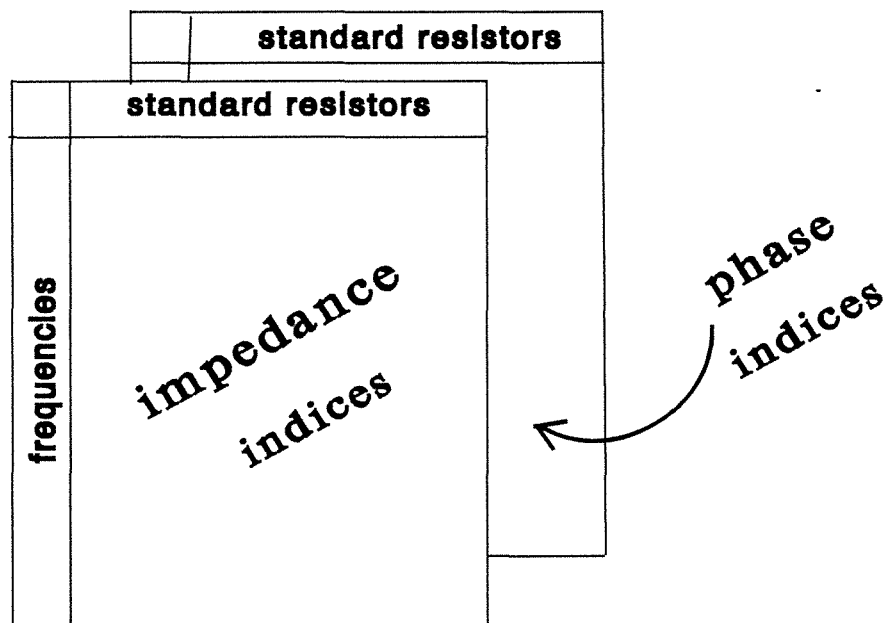
FIGURE 3.2

Calibration matrix to determine impedance and phase offset.

The measurement logs once recorded and stored in the SFBIM are then uploaded to a computer *via* the serial port incorporating an optical isolator to ensure that the subject, (should the electrodes still be connected), is completely isolated from any device connected to 240 v mains power. The impedance index at each frequency of a measurement log is converted to an impedance value (in ohms) by interpolation through the appropriate row of the first page of the calibration matrix. The interpolation ratio used to determine the impedance value is also applied to the same frequency row of the second page of the calibration matrix to ascertain the zero or offset to be applied to the phase index. The phase angle (in degrees) is determined by subtracting the offset and then rescaling knowing the phase index recorded at

470 Ω 50 kHz (from the RC calibration circuit) corresponds to 10°. Appendix A details the code of the computer program written to perform these operations.

An analysis software program was written to transform the impedance and phase indices into values measured in ohms and degrees respectively and then determines the best fitting circular locus, (Cole-Cole plot), described by equation 2.7. The equation of a circle is given by:

$$R^2 + X^2 - a*R - b*X + c = 0$$

(eqn 3.1)

$$centre = (\frac{a}{2}, \frac{b}{2}) \qquad radius = \sqrt{\frac{a^2}{2} + \frac{b^2}{2} - c}$$

Substituting Z^2 for $R^2 + X^2$ equation 3.1 can be rewritten as equation 3.2.

$$Z^2 = a*R + b*X - c$$

(eqn 3.2)

By substituting Z^2 the relationship is linearized and multiple linear regression can be used to find the values of a,b and c which describe the best fitting circle to the experimental data points. The standard error of the estimate of the radius of the circle is calculated as a statistical measure of the "goodness of fit". Although the measurements are recorded using the swept frequency bioimpedance meter the above analytical procedure is the same as that used for data from the multiple frequency bioimpedance meter; hence the analysis will continue to be referred to as MFBIA.

Quite often with human subjects the experimental data points at low frequencies, (< 7 kHz, figure 3.3), may deviate from the circular impedance

locus due to skin-electrode contact problems. Similar deviations may occur at the very high frequencies, (> 350 kHz), due to electrical noise in the leads. To prevent these slight deviations from adversely affecting the accuracy of the regression three options were introduced into the analysis program.

(1)   An optional lower frequency limit is available which allows the operator to exclude these data points from the regression analysis.

(2)   An optional upper frequency limit is available which similarly allows the exclusion of high frequency data from the regression analysis.

(3)   An optional rejection factor which allows the operator to automatically exclude, (from the regression analysis), any data point which is further from the fitted locus than a given percentage of the radius, (*eg.* exclude any point not within ± 5% of the distance from the centre).
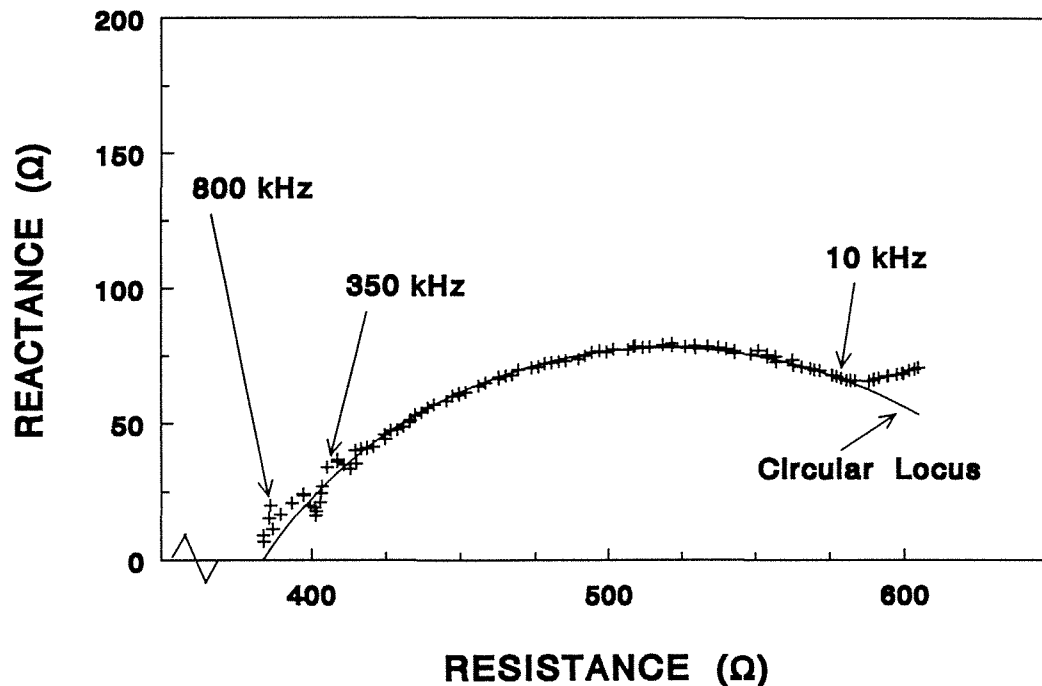
FIGURE 3.3

Cole-Cole plot obtained from MFBIM measurements of

a human volunteer using skin electrodes.

From the equation to the fitted curve the resistance at zero frequency, R_0, the characteristic frequency, f_c, the impedance at the characteristic frequency, Z_c, and the resistance at infinite frequency, R_∞, can be easily determined. The impedance, (or resistance and reactance), at any frequency between 4 kHz and 1 MHz can also be extracted from the experimental data points. The analysis program displays graphically the variation of both resistance and reactance with frequency and also the resistance vs reactance plot known as the Cole-Cole plot, (figure 3.3). The program also writes all of the relevant calculated data to an ASCII file for storage and future reference; an example of a typical output file and the associated graphics are given in appendix B.

Regular assessments of the accuracy and reproducibility of measurements were conducted over both short, (within 2 hours), and long term, (several months), periods of time. Components of known resistance and capacitance were used to construct several test circuits as described by figure 2.1. Regular monitoring of the SFBIM instrument was conducted using these test circuits with impedance ranging from 10 to 1000 Ω, and phase up to 40°. The accuracy of impedance measurements above 20 Ω was always less than ± 1%, and typically less than ± 0.5%. The accuracy of phase measurements was always less than ± 5%, and typically less than ± 2%. The reproducibility of both impedance and phase measurements was ± 0.5%.

SECTION 4

STATISTICAL METHODS.

§ 4   STATISTICAL METHODS

Several statistical methods were employed in the analysis of the data and the evaluation of the results. Some of the methods used include standard procedures such as: simple linear regression, multiple linear regression and the *student t* test of significance; these were performed using commercially available computer programs. The correlation coefficient (r) and standard error of the estimate (SEE) were used to evaluate the "goodness of fit" of the regression analysis. All statistical procedures employed throughout the study are established and accepted methods, however several techniques warrant explanation herein and are detailed in the following sections.

§ 4.1   DEMINGS REGRESSION

The least squares method of linear regression is the most commonly used statistical technique to estimate the slope and intercept. However, if the basic assumptions underlying the least squares model are not met the estimated line may be incorrect. The line obtained by least squares regression minimises the sum of squares of the distances between the observed data points and the regression line in a vertical direction (*ie* perpendicular to the independent variable axis). This assumes that the imprecision associated with the independent variable is insignificant compared to that of the dependent variable.

Deming, (1943), proposed that when there is an error variance associated with both variables the optimum regression line is obtained by minimising the sum of the square of the residuals in both the x and y directions simultaneously. To compute the slope by Deming's formula one must assume gaussian error measurements of x and y with constant

imprecision throughout the range of x and y values. If the ratio of the measurement errors of x and y can be estimated, the following formulae can be used when x is plotted along the abscissa, (Mandel, 1964). Given the equation to the line of regression is $y = bx + a$ then:

$$\textit{Deming's} \quad \textit{slope}: \qquad b = U + \sqrt{U^2 + (\tfrac{1}{\lambda})}$$

(eqn 4.1)

where:

$$U = \frac{\sum_{i=1}^{n} (y_i - \bar{y})^2 - (\tfrac{1}{\lambda}) \sum_{i=1}^{n} (x_i - \bar{x})^2}{2 \sum (y_i - \bar{y})(x_i - \bar{x})} = \frac{S_y^2 - (\tfrac{1}{\lambda}) S_x^2}{2 r S_x S_y}$$

(eqn 4.2)

and

$$\lambda = \frac{SE_x^2}{SE_y^2} = \frac{\textit{error variance of a single x value}}{\textit{error variance of a single y value}}$$

$$SEE = \sqrt{(\tfrac{n-1}{n-2})} * \sqrt{(S_y^2 - brS_xS_y)}$$

(eqn 4.3)

Cornbleet and Gochman, (1979), suggest that if the ratio (SE_x^2/SE_y^2) is not known then a reasonable first approximation is the ratio of the sample standard deviations, (SD_x^2/SD_y^2). As in the least squares method the y-intercept, a, is calculated from the slope:

$$a = \bar{y} - b\bar{x}$$

When measurements of two related variables are both subject to error, as they are in the clinical laboratory, the method of least squares regression may give two very different lines depending on which variable is chosen as the independent variable. Neither line expresses the functional relationship between the true values of the variables as both are altered by errors in the measurement of the 'independent variant', (Cornbleet and Gochman, 1979). Deming's regression analysis described here yields **one** regression line irrespective of which variable is chosen as the 'independent variant' and takes into account the errors of measurement of both variables. Deming's regression analysis was performed using a purpose-written spreadsheet program, (Ward and Cornish, 1991).

§ 4.2   BIAS AND LIMITS OF AGREEMENT

When two indirect methods of measuring a quantity need to be compared, a statistical approach which will assess the degree of agreement is needed. Bland and Altman, (1986), state that this is very different from calibration, where a known quantity is measured by a new method and the result compared with the true value or with measurements made by a highly accurate method. For the purposes of calibration the product-moment correlation coefficient (r) is an appropriate measure of the strength of the relationship. The analysis presented by Bland and Altman, (1986), for the agreement between two indirect measures of a quantity, examines and quantifies the difference between the measurements of the two methods and is described below.

The agreement between the two methods can be summarised by calculating the bias, estimated by the mean difference $(\bar{d})$ and the standard deviation of the differences. Although the measurements themselves may not

follow a gaussian distribution, the differences usually do. The distribution of the differences can be easily checked for 'normality' by inspection of the histogram for skew or very long tails. Having calculated the bias a judgement can be made as to whether a given method over- or under-estimates the accepted estimate, and this bias can be subsequently accounted for. However it is not only the value of the bias that is of interest in a clinical situation but more importantly the confidence interval of the bias. This confidence interval is commonly referred to as the *limits of agreement*.

The most commonly used limits of agreement is the 95% confidence interval (of the mean difference) calculated by finding the appropriate point on the *t* distribution with (n-1) degrees of freedom. The value of the bias indicates the amount of adjustment or offset needed for each measurement, but it is the width of the confidence interval which is an accurate measure of the closeness of the relationship; the smaller the interval the greater the accordance.

§ 4.3   DOUBLE CROSS-VALIDATION

Cross-validation is a statistical procedure designed to investigate the relationship between an indirect measurement of a given quantity and its known or true value. Subjects are randomly assigned to either the model or validation group and the appropriate measurements recorded. Regression analysis is then applied to the data from the validation group to determine the relationship between the indirect measurement and the known value of the quantity. This relationship known as the prediction equation is then applied to the measurements from the model group to determine the corresponding predicted values of the quantity, these predicted values are subsequently compared to the known values and the product-moment

correlation coefficient (r_m) calculated.

Kerlinger and Pedhazur, (1973), describe a double cross-validation procedure in which the converse actions are also performed *ie.* a prediction equation is determined using data from the model group and used to arrive at predicted values in the validation group which are subsequently compared with the known values and the corresponding correlation coefficient (r_v) calculated. It is then possible to study the differences between the correlation coefficients, (r_m and r_v), and the regression equations. If the results are close the two sample groups may be combined and the resulting regression equation used as the prediction equation. Kerlinger and Pedhazur, (1973, p284), state *"Double cross-validation is strongly recommended as the most rigorous approach to the validation of results from regression analysis in a predictive framework "*.

SECTION 5

ISOTOPE DILUTION

TECHNIQUES.

§ 5 ISOTOPE DILUTION TECHNIQUES

In order to investigate the relationship between impedance measurements and body fluid volumes independent and simultaneous measures of both TBW and ECW were ascertained by established methods of isotope dilution, (Lukaski, 1987). Determination of body water volumes by isotope dilution is one of the few direct methods available for *in vivo* body composition analysis and is often referred to as the gold standard. Sections §5.1 to §5.3 describe the general procedures employed and the instrumentation used; particulars of the various protocols applied are discussed in detail in relevant later sections.

§ 5.1 DETERMINATION OF TBW BY D_2O DILUTION

Water labelled with deuterium (^2H) or tritium (^3H) has been used extensively for the determination of TBW because the labelled water has the same distribution volume as body water, is exchanged by the body in a manner similar to unlabelled water, is nontoxic in tracer amounts and is measurable with accuracy (Pinson, 1952). However tritium is radioactive and its use needs to be well considered in children and women of child bearing age, and is generally not appropriate for serial studies. In this study deuterium oxide (D_2O) being non-radioactive was used at dosage rates of 1 g per kg of body weight, (Nielsen *et al.*, 1971), for animals and 0.5 g/kg for humans.

The dose was injected intraperitoneally (animals) or taken orally (humans) and after an appropriate equilibration time samples of blood were taken. The minimum time needed for equilibration varies between individuals but research has shown it to be: less than 2 hours in rats,

(Tisavipat *et al.*, 1974; Culebras and Moore, 1977; Rothwell and Stock, 1979); and less than 3 hours in healthy humans, (Lukaski, 1987; Blagojevic *et al.*, 1990; Kushner *et al.*, 1990). Plasma from the blood sample was separated by centrifuge at 1500 x g for 6 minutes at 10°C and the D_2O concentration determined by Fourier transform infrared spectroscopy (FTIR).

The deuterium-oxygen bond in D_2O absorbs infrared radiation strongly at a frequency 7.545 x 10^{13} Hz (wavenumber 2515 cm⁻¹) and its absorption band appears as a shoulder on the larger absorption band of the hydrogen-oxygen bond. When the absorption spectrum of a water background is subtracted the deuterium-oxygen peak is clearly visible in the absorbance spectrum, (figure 5.1). The area under the peak was calculated using an oblique baseline drawn between wavenumbers 2300 and 2700 cm⁻¹; this is similar to the approach of Blagojevic *et al.*, (1990), who used the absorbance at 2300 and 2650 cm⁻¹ to estimate the background of the D-O peak.
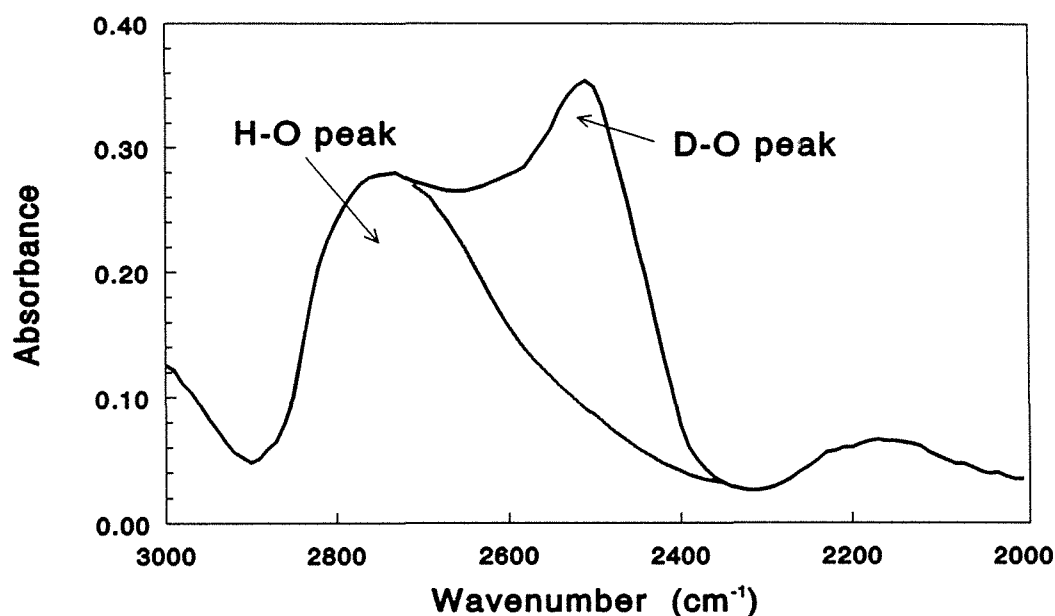
FIGURE 5.1

FTIR spectrum showing the Deuterium-Oxygen peak.

The spectra were recorded on a Perkin & Elmer FTIR single beam spectrometer model FTIR2000 using a resolution of 16 cm^{-1} and 128 scans. The cell used had a CaF_2 window with a path length of 0.1 mm and all spectra were measured at a constant ambient temperature of 20°C. A set of standards was produced by adding an accurately measured mass of D_2O to a known volume of plasma and then by serial dilution with further plasma. The area of the D-O peak was measured for each of the ten standards before and after each batch of 6 to 8 samples to ensure the stability of the instrument conditions. The reproducibility of the peak areas of the standards was shown to be less than ±1%. The calibration plot produced a linear relationship each and every time with a typical example shown in figure 5.2.
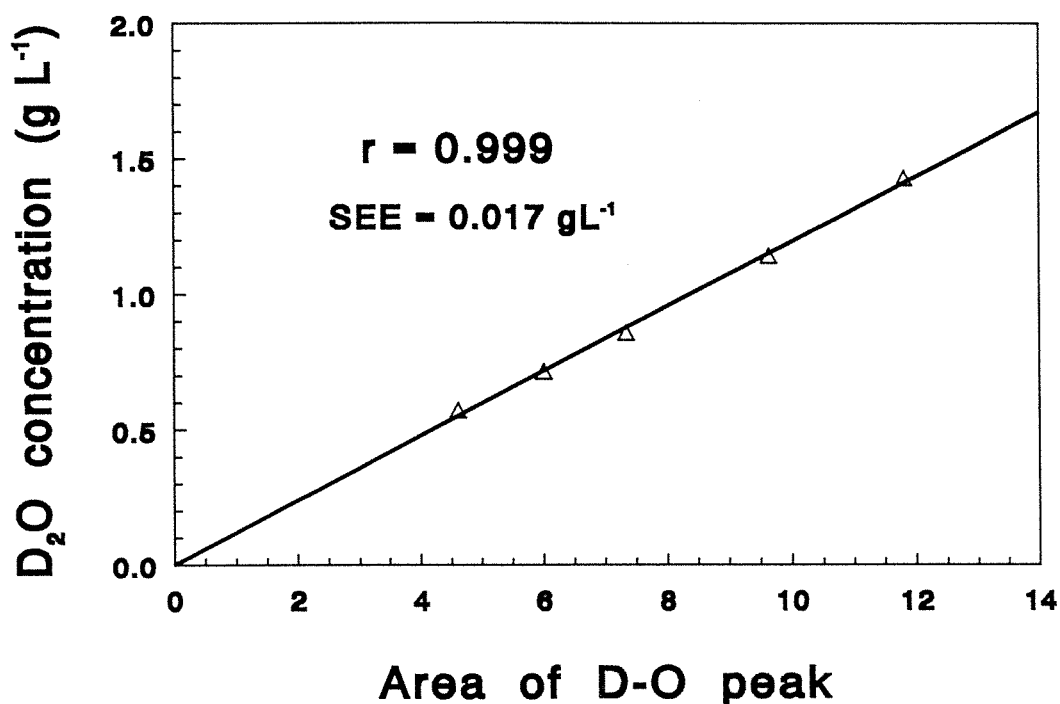
FIGURE 5.2

Calibration plot of the D_2O standards.

For a given plasma sample the area of the D-O peak was used to determine the D_2O concentration using the calibration graph (eg figure 5.2).

Knowing the water content of plasma to be 93.7% by volume, (Rothwell and Stock, 1979; Lukaski and Bolunchuk, 1988; Espejo *et al.*, 1989), the corresponding D_2O concentration in water was calculated and hence the TBW estimated using equation 5.1.

$$volume \; of \; TBW \; (L) \; = \; \frac{(\; mass \;\; of \;\; D_2O \;\; administered \;)}{[\; D_2O \;]_{plasma}} \; * \; 0.937$$

(eqn 5.1)

§ 5.2 DETERMINATION OF ECW IN ANIMALS BY [³H] INULIN DILUTION

Inulin is a polysaccharide with a molecular mass of 5200 and does not traverse the cell membrane. Hence its distribution space very closely approximates the ECW volume, and when labelled with tritium its concentration in very small samples can be easily and accurately measured by liquid scintillation counting.

The liquid scintillation process may be considered as a series of energy transfer steps mediated by an aromatic solvent and a fluorescent substance. The passage of ionising radiation through this solution causes ionisation and excitation of the solvent molecules. The ionised molecules quickly recombine with electrons to form excited molecules. An energy transfer occurs from the excited solvent molecules to fluorescent solute molecules which de-excite by emitting a photon. This photon emission is detected by photomultiplier tubes and the amplified electronic signals are measured and counted. The energy transfer process can be interfered with by the inclusion of impurities which subsequently reduce the photon yield. This phenomenon is known as quenching and decreases the overall counting

efficiency. Small variations in the amount of impurities can cause marked variations in the counting efficiency.

Using a Beckman liquid scintillation counter model 5801, the unquenched β spectrum of tritium was recorded in channel numbers 1 to 400. As the amount of quenching increases the pulse energy decreases, characterised by a shift in the spectrum to the left, (to lower energies). The channels ratio method of quench correction described by Dyer, (1980), was used and the number of counts in two adjacent windows of the spectrum recorded. The measured spectrum of a set of standards of known activity was recorded and the efficiency (measured count rate / activity) calculated.

The β spectrum for each tritium sample was recorded and the optimum channels ratio for tritium as described by Dyer, (1980), (counts in ch 201-400 / counts in ch 1-200) was calculated. From the quench curve and the calculated channels ratio the efficiency of each sample was determined and used to transform the total measured count rate into the sample activity.

Tritium labelled inulin was injected intravenously *via* a lateral tail vein in the rats at a dose rate of 1.67 MBq (45 µCi) kg^{-1} body weight. The equilibration time for inulin injected intravenously in rats is approximately 20 minutes, (Radin *et al.*, 1986). However, inulin is effectively cleared by the kidney and is often used to determine the glomerular filtration rate, (Guyton, 1981), hence after equilibrium is established the blood inulin concentration will decrease at an exponential rate (Lesser *et al.*, 1980). By measuring the radioactivity of blood samples over a period of time after equilibration, the exponential function can be determined and the 'equilibrated' activity at the time of injection (before clearance by the kidney) evaluated. Figure 5.3 shows the semi-logarithmic plot of activity *vs* time for a typical animal.
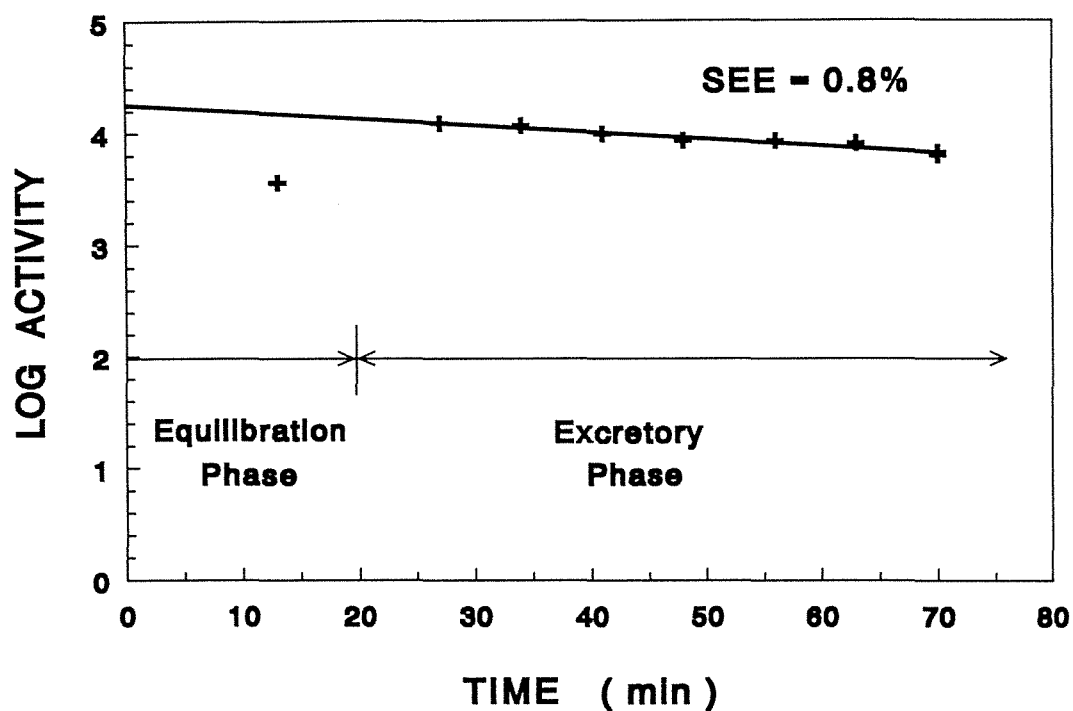
FIGURE 5.3

Decrease in blood inulin concentration with time after administration,

for a representative rat.

From the total activity injected and the specific activity after equilibration and knowing the water content of plasma, 93.7%, (Espejo *et al.*, 1989; Rothwell and Stock, 1979; Lukaski and Bolunchuk, 1988), the ECW volume was calculated using equation 5.2.

$$volume \ of \ ECW \ (L) \ = \ \frac{Total \ activity \ injected}{Specific \ activity \ of \ plasma} \ * \ 0.937$$

(eqn 5.2)

Where the activity and specific activity are expressed in MBq and MBq mL^{-1} respectively.

§ 5.3 DETERMINATION OF ECW IN HUMANS BY BROMIDE DILUTION

For the determination of ECW in humans, bromide was selected as the tracer to obviate any concerns associated with a radioactive tracer such as [³H] inulin. Bromide which has almost the same distribution as chloride (Cheek, 1954), has the advantage of good absorption following an oral dose, slow excretion, and only moderate penetration into cells, (Sharpless, 1970). In the first few hours it appears to penetrate the red blood cells primarily, (Pierson et al., 1978), and correction can be made for the loss of tracer, (see equation 5.3).

A bromide solution of 0.75 mol L^{-1} was administered orally at the rate of 1.0 mL per kg of body weight. The equilibration time for bromide, administered orally in humans, is accepted as less than 3 hours, (Segal et al., 1991). In a study designed to compare the equilibration of oral and intravenous administration of bromide, Vaisman et al., (1987), concluded that there was no statistical difference in blood bromide concentrations between 2 and 4 hours post-administration, hence equilibration time may be as low as two hours. The equilibration time allowed in this study was 3 to 3.5 hours. Blood samples were collected before dosing and again after equilibration.

The bromide assay procedure described here was established by Trapp and Bell, (1989), who validated the technique using neutron activation analysis. Forty microlitres of the sample plasma was precipitated by the addition of 40 μL of a 500 mmol L^{-1} solution of perchloric acid at 5°C. The samples were vortexed and centrifuged at 15600 x g for 5 minutes at 5°C. Forty microlitres of the supernatant was transferred to a new tube, and 400 μL of 176 mmol L^{-1} sodium acetate buffer (adjusted to pH 5.55 with concentrated acetic acid) and 400 μL of 0.625 mmol L^{-1} sodium fluorescein

were added. The reaction was started by the addition of 400 μL of 8.0 mmol L^{-1} chloramine-T. The resulting solution was vortexed and the reaction stopped after 10 minutes by the addition of 400 μL of a solution containing 40 mmol L^{-1} sodium thiosulfate and 40 mmol L^{-1} sodium carbonate. The reaction time of 10 minutes is the time of maximum absorbance of the coloured reaction product, (Oosting and Reijnders, 1980). The absorbance of the samples at a wavelength of 520 nm was measured using a Shimazu spectrophotometer model number UV265FW.
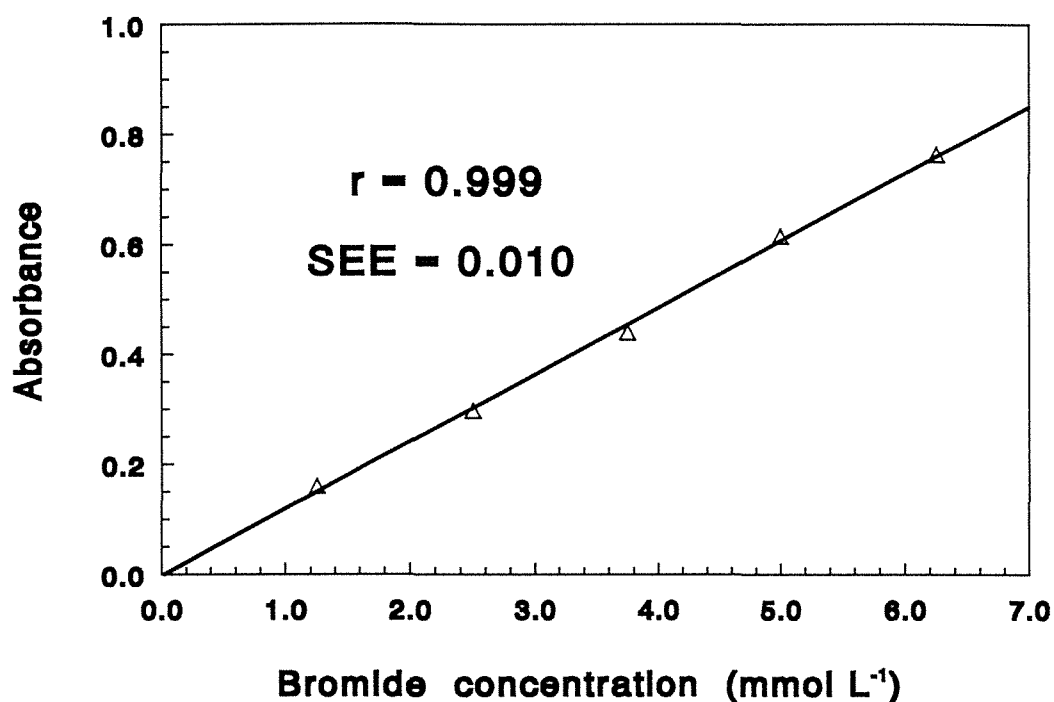
FIGURE 5.4

Absorbance *vs* Bromide concentration for the known standards.

The above procedure was also used to measure the absorbance of a set of standard plasma solutions of known bromide concentrations, (0, 1.25, 2.50, 3.75, 5.00 and 6.25 mmol L^{-1}), and the calibration plot of concentration *vs* absorbance determined (figure 5.4). Using the relationship derived from this graph the sample bromide concentrations were calculated from the

corresponding absorbance measurements. The calibration plot was determined immediately before each group of 12 to 15 samples and the standards re-measured immediately after to ensure the stability of the instrument conditions.

From the quantity of dose administered and the calculated increase in bromide concentration at equilibration the dilution volume of bromide can be calculated. However, as noted above bromide does suffer moderate penetration into the tissues but this can be accurately accounted for. The dilution volume after all necessary corrections is often known as the corrected bromide space (CBS), and as it is an accepted measure of extracellular fluid volume, for the purpose of discussion it will be referred to simply as ECW. The ECW volume was calculated using equation 5.3, (Trapp and Bell, 1989).

$$ECW \ (L) \ = \ \frac{Br_{dose} \ (mmol)}{[Br]_{plasma} \ (mmol \ L^{-1})} \ * \ 0.90 \ * \ 0.95 \ * \ 0.937$$

(eqn 5.3)

where: 0.90   is the fraction of the retained bromide dose that is assumed to remain extracellular[*];

0.95   is the Donnan equilibrium factor for bromide[*];

0.937   is the fraction of water in plasma[*].

[*](Espejo *et al.*, 1989; Lukaski and Bolunchuk, 1988).

SECTION 6

VALIDATION OF MFBIA

IN NORMAL ANIMALS.

§ 6 VALIDATION OF MFBIA IN NORMAL ANIMALS

To establish a relationship between body impedance measured by MFBIA and body composition, the extracellular and total body water volumes were measured in a sample population of Wistar rats. Forty two healthy adult Wistar rats, (22 males and 20 females), weights ranging from 200g to 650g, were used in the study. The animals had access to food and water *ad libitum* prior to the procedure and were housed in an animal house maintained at 22°C on a 12 hour light 12 hour dark cycle. The animals were anaesthetised throughout the experimental procedure with sodium phenobarbitone (Fawns & McAllan Pty. Ltd. Victoria) with a dose of 100 mg kg^{-1} body weight. Weight of the anaesthetised animal was recorded to the nearest 0.1 g. Ethical clearance for all procedures was obtained from both the Queensland University of Technology's Ethics Committee and the University of Queensland's Animal Ethics Committee, (refer appendix C).

§ 6.1 MFBIA MEASUREMENTS

The anaesthetised animal was positioned on a non-conducting surface with its dorsal surface upwards and limbs extended perpendicular to the longitudinal body axis. The MFBIA instrument described in section §3.2 using a tetrapolar electrode arrangement was used to measure the body impedance. The electrodes were fabricated from 5 cm 20 gauge stainless steel hypodermic needles by bending the shaft perpendicularly 6 mm from the tip. The electrodes were inserted subcutaneously into the subdermal tissue avoiding penetrating the muscle, with the tip directed distally along the dorsal midline of the body a distance of approximately 3 mm. One source

electrode was positioned in line with the superior edge of the orbit, and the other 4 cm from the base of the tail. Measurement electrodes were positioned; one in line with the posterior opening of the pinna, and the other in line with the iliac spines, (Hall *et al.*, 1989). The distance between the points of insertion of the measurement electrodes was measured to the nearest 0.1 cm.

An AC current was applied to the source electrodes, and the corresponding impedance and phase angle detected by the measurement electrodes were recorded at six discrete frequencies (1.0, 3.25, 10.0, 32.5, 50.0, 100 kHz). The coefficient of variation for repeated measures on the same animal was <1.0%. The procedures described in §2.2 were used to determine the resistance at zero frequency, R_0, and the impedance at the characteristic frequency, Z_c. An impedance plot of typical measurements obtained for one of the animals is shown in figure 6.1 and the salient features listed.

Many previous prediction equations for TBW do not include the reactive component of the impedance; Kushner and Schoeller, (1986), base their prediction of TBW on the resistance at 50 kHz *"because reactance had a negligible effect"*. Table 6.1 summaries the variation, between individual animals, of the frequency response and highlights the range of measured phase angles and body reactances at 50 kHz in this sample of 42 rats.
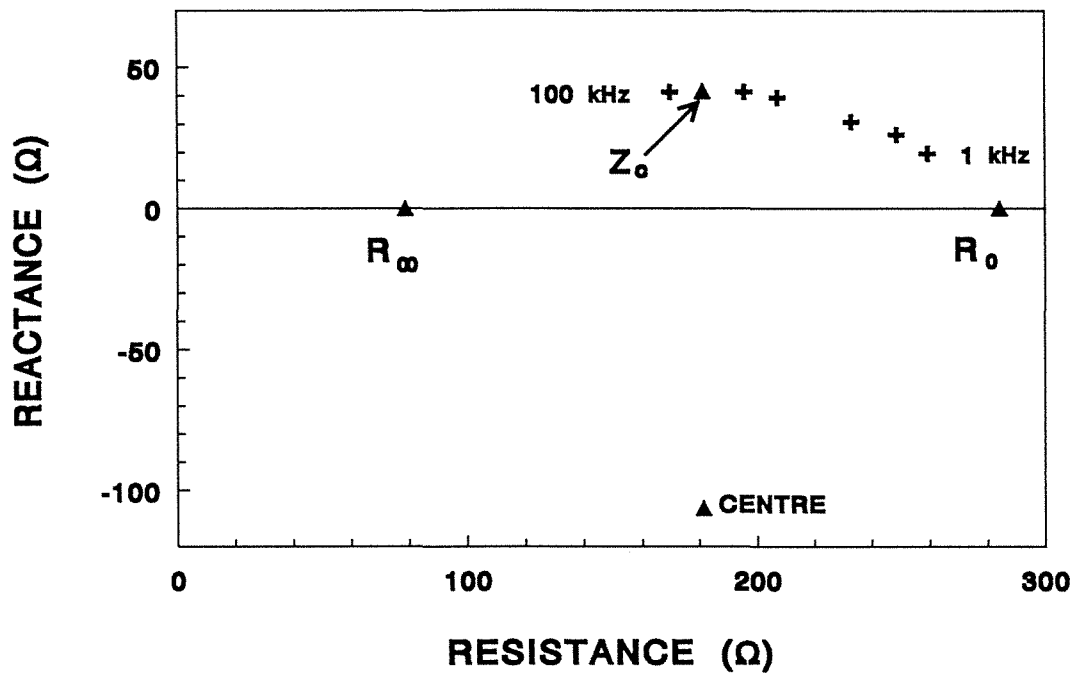
FIGURE 6.1

A typical impedance plot, from a rat, using MFBIA

measurements at 6 frequencies.

R_0 = 284 Ω f_c = 88 kHz

                         (ω_c = 553 kHz)

R_∞ = 79 Ω Z_c = 186 Ω

Centre = 181 Ω, -106 Ω α = 0.51

As seen in table 6.1 the measured reactance at 50 kHz is not negligible and shows a considerable variation, (coefficient of variation 20%), between rats which is larger than that of the resistance at 50 kHz, (coefficient of variation 13%). For this reason the utility of the measured impedance, (the vector sum of resistance and reactance), in predicting TBW was investigated.

TABLE 6.1

Variation of frequency response and BIA measurements at 50 kHz.

	f_c (kHz)[a]	ϕ (degrees)[b]	R_{50} (Ω)[c]	X_{50} (Ω)[d]
Range	53-334	6.3-18.1	189-304	24-81
Mean	156	12.5	238	53
SD	62	2.0	30.9	10.7
CV	40%	16%	13%	20%

[a] f_c - characteristic frequency (kHz)

[b] ϕ - phase angle at frequency 50 kHz (degrees)

[c] R_{50} - resistance at frequency 50 kHz (Ω)

[d] X_{50} - reactance at frequency 50 kHz (Ω)

The quotients L^2/Z_c and L^2/R_0, (where L is the distance between the measurement electrodes), were calculated and used in the correlation with TBW and ECW respectively. Impedance measurements also enabled the calculation of the prediction quotients for the previously reported bioelectrical impedance analysis (BIA) techniques, as described by others (Lukaski *et al.*, 1985; Jenin *et al.*, 1975; Espejo *et al.*, 1989).

§ 6.2 MEASUREMENT OF TBW AND ECW

Total Body Water by D₂O Dilution

The time required for deuterium oxide (D_2O) to equilibrate between all body compartments and tissues is approximately 2 hours in the rat (Hoffer *et al.*, 1969). Each rat was injected intraperitoneally with an accurately weighed amount of D_2O (Cambridge Isotope Laboratories, Massachusetts), 1.1 g kg^{-1} body weight, 150 minutes prior to killing by anaesthetic overdose. At the time of killing a 2 mL sample of blood was taken by cardiac

puncture. Plasma from this sample was separated by centrifuge at 1500 x g for 6 minutes at 10°C.

The plasma concentration of D_2O was determined by Fourier transform infrared spectroscopy (FTIR) as explained in section §5.1. During the procedure animals were constantly monitored and urination did not occur in any animal and therefore no correction for urinary loss of D_2O was necessary. Using a water content of plasma of 93.7% by volume, (Espejo et al., 1989; Rothwell and Stock, 1979; Lukaski and Bolunchuk, 1988), the corresponding D_2O concentration in water was calculated and hence the TBW estimated.

Extracellular Water by [³H] Inulin Dilution

The following procedure was conducted simultaneously with the previously described D_2O method such that both procedures concluded at the time the animal was killed.

Tritium labelled inulin (Amersham, England) was injected intravenously, *via* a lateral tail vein, providing a dose of 1.67 MBq (45 μCi) kg^{-1} body weight, (in a volume 180 μL kg^{-1}). The catheter was flushed through with 50 μL of normal saline to ensure the complete dose was administered to the vein. The tip of the tail was clipped and 20 μL blood samples taken at timed intervals up to 75 minutes postinjection. From the final blood sample, taken *via* cardiac puncture, four 20 μL samples of plasma were obtained. The blood samples were treated with 1 mL hydrogen peroxide to bleach the colour and 0.1 mL 5% hydrochloric acid to neutralise the hydrogen peroxide (Holleman and Dieterich, 1973). Scintillation fluid, volume 10 mL (ACS; Amersham, Illinois), was added and the activity determined by liquid scintillation spectrometry using the channels ratio method, (see §5.2), to correct for quenching.

After equilibration the fall in blood inulin concentration due to clearance by the kidneys approximates to a single exponential function (Lesser *et al.*, 1980), represented by a straight line on a semi-logarithmic plot, (figure 6.2). Using the slope of this line, fitted to the experimental data by least squares regression, and the mean activity of the final four plasma samples, the specific activity of the plasma at time zero was determined by extrapolation. This is the value of the specific activity of the plasma after equilibration but without the effect of clearance by the kidneys. From the total activity injected and the specific activity after equilibration the dilution factor was determined and using the water content of plasma, 93.7%, (Espejo *et al.*, 1989; Rothwell and Stock, 1979; Lukaski and Bolunchuk, 1988), the ECW volume was calculated.
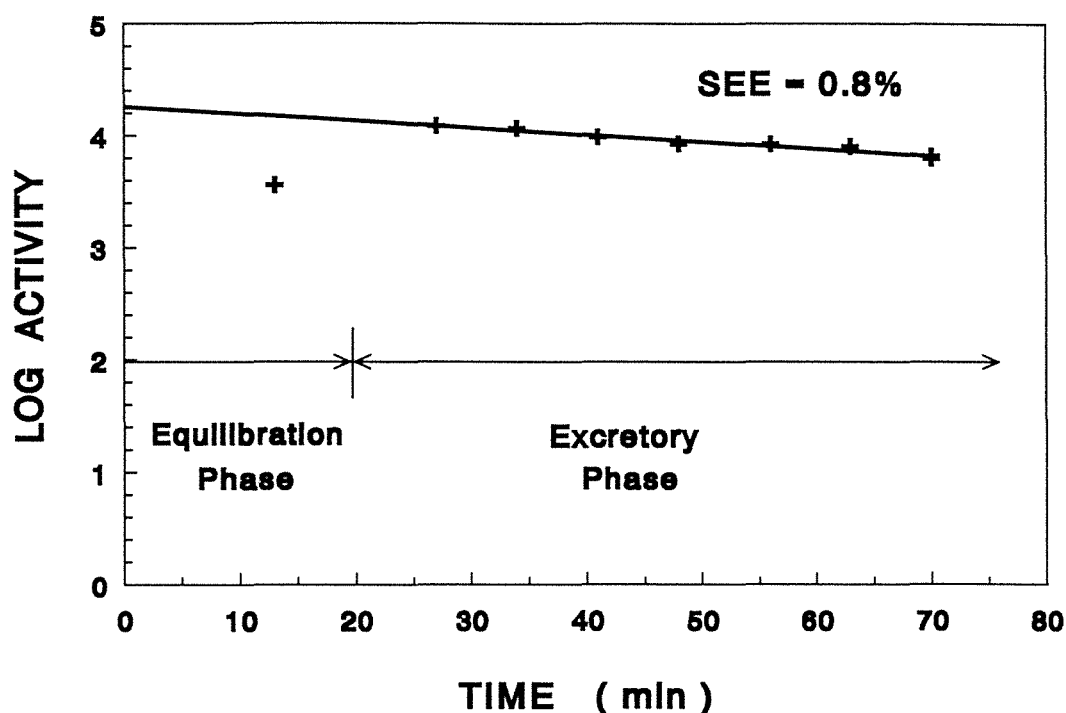
FIGURE 6.2

Decrease in blood inulin concentration with time after administration, for a representative rat. (Note: this is the same as figure 5.3)

Total Body Water by Desiccation

After the completion of the D_2O and inulin procedures the carcasses of the first seventeen animals were sealed in polythene bags and stored at -70°C. The frozen carcasses were cut into smaller segments and homogenised using a Waring commercial blender. The complete homogenised remains of each animal were then quantitatively transferred to a metal dish and dried in an oven maintained at 60 to 65°C until a constant weight was recorded over 24 hours. Desiccation time was dependent upon the size of the animal and varied from 3 to 5 days. TBW was determined by subtraction of the desiccated weight from the live body weight.

§ 6.3   CORRELATION   OF   MFBIA   WITH   ISOTOPE DILUTION

Regression analyses of the impedance data with TBW and ECW, (as measured by isotope dilution), were performed using published single frequency BIA prediction quotients and also MFBIA prediction quotients. The mean, standard deviation and range of all data collected for male, female and the total group of animals are listed in table 6.2 and the corresponding correlation coefficients and standard errors of prediction (SEE) are presented in table 6.3.

The standard error of prediction SEE = 10.1%, using the resistance at 50 kHz, R_{50}, is significantly greater (P<0.01) than that using the impedance at the characteristic frequency, Z_c, where SEE = 5.9%. The improvement (P<0.01) in the standard error of prediction , (SEE = 8.5% to 5.9%), by using the impedance instead of the resistance at the characteristic frequency indicates that the reactive component does have predictive value and that the impedance quotient L^2/Z_c was the best predictor of TBW in this group of animals. Figure 6.3a shows the plot of L^2/Z_c *vs* TBW for this group of rats.

TABLE 6.2

Summary of impedance and isotope dilution data for a group of normal rats.

QUANTITY	MALES (n=22) mean ± sd range	FEMALES (n=20) mean ± sd range	TOTAL (n=42) mean ± sd range
weight (g)	391 ± 137 191 - 661	276 ± 27 229 - 353	336 ± 116 191 - 661
length (cm) (between electrodes)	13.9 ± 2.0 10.3 - 17.6	12.6 ± 0.7 11.2 - 13.8	13.3 ± 1.6 10.3 - 17.6
R_{50} (Ω)	223 ± 27 189 - 292	256 ± 25 212 - 304	238 ± 31 189 - 304
Z_5 (Ω)	275 ± 30 235 - 353	320 ± 30 263 - 376	296 ± 38 235 - 376
Z_1 (Ω)	283 ± 31 239 - 362	330 ± 32 269 - 388	305 ± 39 239 - 388
R_c (Ω)	196 ± 23 156 - 231	215 ± 27 178 - 268	205 ± 27 156 - 268
Z_c (Ω)	205 ± 23 165 - 242	224 ± 25 189 - 275	213.9 ± 26 165 - 275
R_0 (Ω)	295 ± 33 245 - 376	346 ± 36 276 - 409	319 ± 43 245 - 409
L^2/R_{50} (cm$^2\Omega^{-1}$)	0.904 ± .289 0.430 - 1.356	0.626 ± .080 0.501 - 0.794	0.772 ± .257 0.430 - 1.356
L^2/Z_5 (cm$^2\Omega^{-1}$)	0.728 ± .221 0.362 - 1.054	0.500 ± .060 0.401 - 0.610	0.620 ± .201 0.362 - 1.054
L^2/Z_1 (cm$^2\Omega^{-1}$)	0.708 ± .214 0.356 - 1.022	0.485 ± .059 0.389 - 0.600	0.602 ± .195 0.356 - 1.022
L^2/R_c (cm$^2\Omega^{-1}$)	1.017 ± .288 0.559 - 1.614	0.746 ± .084 0.609 - 0.991	0.888 ± .255 0.559 - 1.614
L^2/Z_c (cm$^2\Omega^{-1}$)	0.972 ± .276 0.528 - 1.545	0.713 ± .078 0.594 - 0.929	0.849 ± .244 0.528 - 1.545
L^2/R_0 (cm$^2\Omega^{-1}$)	0.677 ± .199 0.347 - 0.999	0.464 ± .064 0.364 - 0.608	0.576 ± .185 0.347 - 0.999
TBW (mL) (D_2O space)	271 ± 87 130 - 463	192 ± 23 149 - 265	233 ± 76 130 - 463
ECW (mL) (Inulin space)	85.2 ± 22.4 50.4 - 119.2	63.4 ± 7.6 51.6 - 79.0	74.8 ± 20.2 50.4 - 119.2

TABLE 6.3

Comparison of correlation coefficients (r) and the standard errors of prediction (SEE, as a % of the mean) with TBW and ECW using established single frequency BIA methods and MFBIA for the same animals (n=42).

Referenced author(s)	Prediction quotient [a]	TBW	ECW
Single frequency prediction			
Lukaski *et al.*, (1985)	L^2/R_{50}	r = 0.950 SEE = 10.1%	————
Jenin *et al.*, (1975) and Segal *et al.*, (1991)	L^2/Z_5	————	r = 0.984 SEE = 4.8%
Espejo *et al.*, (1989) and Pullicino *et al.*, (1992)	L^2/Z_1	————	r = 0.988 SEE = 4.2%
Multiple frequency prediction			
Present study	L^2/R_c	r = 0.965 SEE = 8.5%	————
Present study	L^2/Z_c	r = 0.983 SEE = 5.9%	————
Present study	L^2/R_0	————	r = 0.993 SEE = 3.2%

[a] at the frequency (in kHz) indicated by the subscript.

As discussed earlier the current at zero frequency passes through the extracellular fluids only and hence the impedance R_0 is due to the ECW. The standard errors associated with the prediction of ECW using BIA, listed in table 6.3, show a significant progressive improvement (P<0.025) from SEE = 4.8% to 4.2% to 3.2% as the prediction frequency is decreased from 5 kHz to 1 kHz to zero. These results indicate that the impedance quotient L^2/R_0 is the best predictor of ECW in this group of animals. Figure 6.3b shows the plot of L^2/R_0 vs ECW for this group of rats.
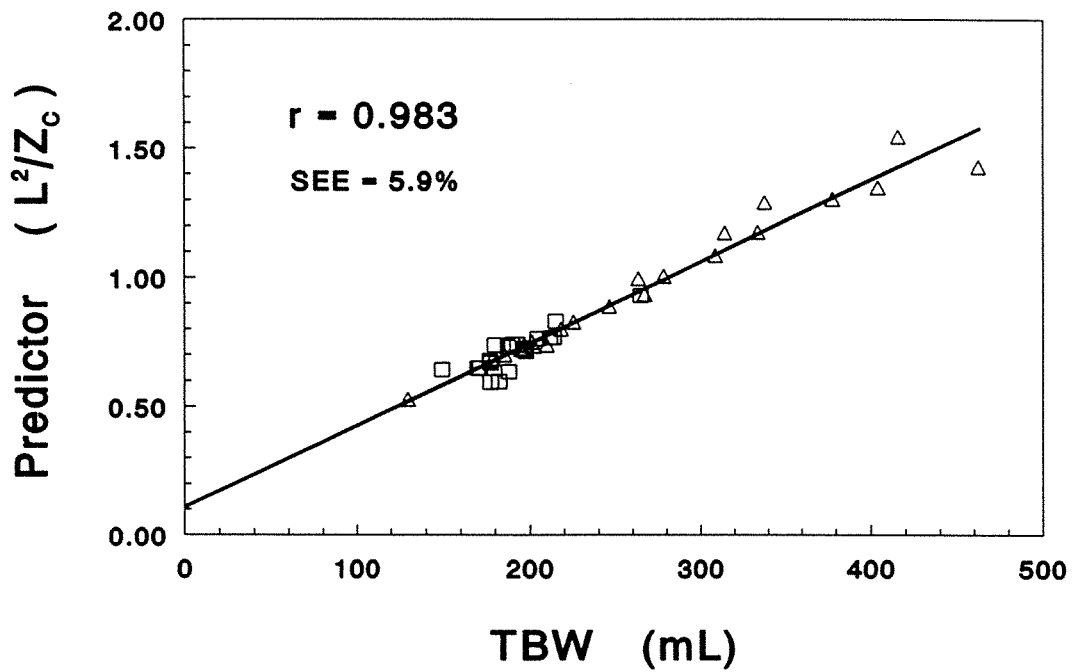
FIGURE 6.3a

Plot of L^2/Z_c *vs* TBW by D_2O dilution (n=42) ($\square$ females, $\triangle$ males).
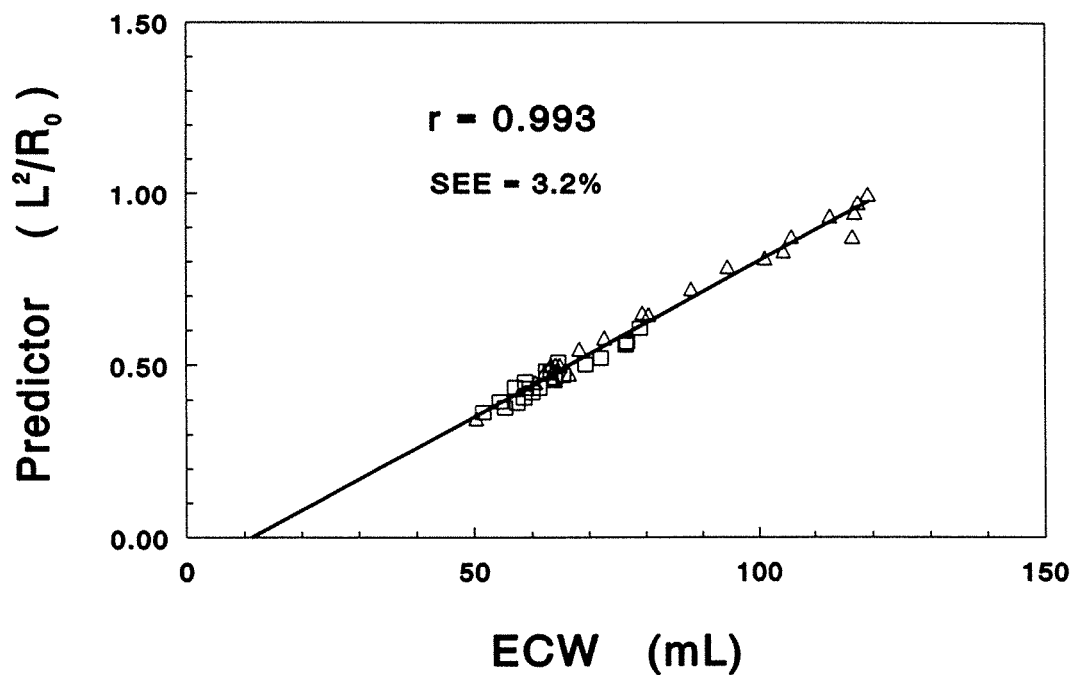
FIGURE 6.3b

Plot of L^2/R_0 *vs* ECW by [^{3}H]-Inulin dilution (n=42) ($\square$ females, $\triangle$ males).

The prediction equations for TBW and ECW based on these data are:

$$TBW \ (mL) \ = \ 304 \ \frac{L^2}{Z_c} \ - \ 25 \qquad SEE \ = \ 14 \ mL \ = \ 5.9\%$$

eqn (6.1)

$$ECW \ (mL) \ = \ 109 \ \frac{L^2}{R_0} \ + \ 12 \qquad SEE \ = \ 2.4 \ mL \ = \ 3.2\%$$

eqn (6.2)

The TBW measured by D_2O dilution had a very high correlation, (r=0.996), when compared with that measured by desiccation in the sample of 17 rats. The plot of TBW by D_2O vs TBW by desiccation is shown in figure 6.4.
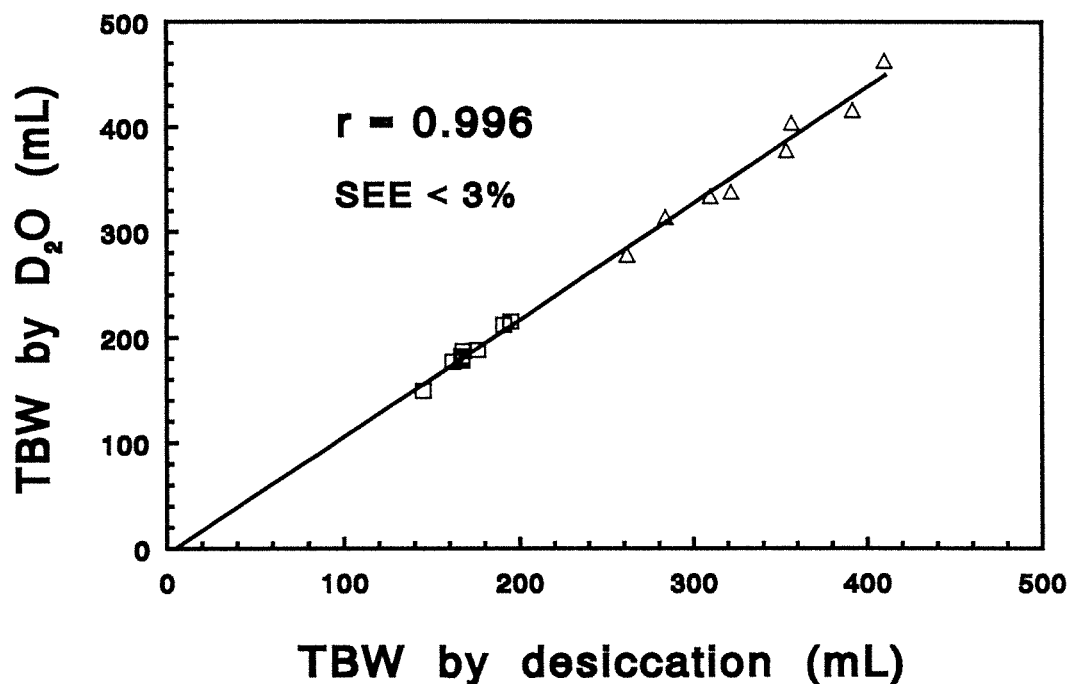
FIGURE 6.4

Plot of TBW by D_2O dilution vs TBW by desiccation.

(n=17) (☐ females, ▵ males).

§ 6.4   SUMMARY

The purpose of the desiccation procedure described in section §6.2, performed on a subset of the sample of rats, was to validate the results of the D_2O dilution technique of measuring TBW. Although the correlation between TBW measures by desiccation and by D_2O dilution was very high, (r = 0.996, SEE < 3%, n = 17), the mean value for TBW estimated by D_2O dilution was approximately 4% greater than that estimated by desiccation. Previous research (Schloerb *et al.*, 1950; Culebras and Moore, 1977; Sheng and Huggins, 1979) has shown this overestimation to be a consistent systematic error due to hydrogen ion exchange with body tissues in the dilution method. The volume measured by D_2O dilution is correctly termed the D_2O space. However, due to the very high correlation between these two direct methods, D_2O dilution is regarded as the 'gold standard' for *in vivo body composition* analysis, (Lukaski, 1987). For the purpose of discussion it will be referred to simply as TBW.

The use of Cole-Cole plots, in this study, to analyse the MFBIA data is the first application of this approach to estimate body fluid compartments. Others, (for example Kanai *et al.*, 1987), have used Cole-Cole plots in bioelectrical impedance analysis but without any attempt to predict fluid volumes. Recent research, (van Loan and Mayclin, 1992), has used measurements of bioimpedance at 25 frequencies to predict ECW and TBW. However van Loan and Mayclin did not combine the impedance measurements at different frequencies to arrive at a single prediction of ECW and TBW, but instead tested each frequency independently as a predictor of body water.

The MFBIA technique described enables the determination of the impedance at the characteristic and zero frequencies with the consequent

significantly improved prediction of TBW and ECW. This analysis can be done using measurements obtained at frequencies above 4 kHz, obviating the necessity of needle electrodes required to overcome the high electrode-skin impedance of contact electrodes at low frequencies; but still being able to extrapolate accurately to find the impedance at zero frequency.

SECTION 7

APPLICATION OF MFBIA

IN ABNORMAL ANIMALS.

§ 7 APPLICATION OF MFBIA IN ABNORMAL ANIMALS

Battistini *et al.*, (1992), have shown that, using BIA at a single fixed frequency, prediction equations established in normal populations underestimate TBW in adolescent obese subjects. Gray *et al.*, (1989), has similarly commented on the inappropriateness of BIA prediction equations, established for normal adults at a single fixed frequency to estimate body water in obese adults. Spence *et al.*, (1979), and Jebb and Elia, (1993), have also shown that acute changes in fluid status during haemodialysis alter body impedance, although quantification of the lost fluid cannot be reliably predicted by BIA measurements at a single frequency. These errors may be due to: (a) inappropriate use of equations derived from normal populations; (b) the assumption of a constant cylindrical configuration (Thomas *et al.*, 1992), a condition not met in a grossly obese subject; (c) limitations of *single* frequency BIA. This section investigates the validity of *multiple frequency* bioelectrical impedance analysis (MFBIA) to predict ECW and TBW in an animal model of an induced abnormal balance of extra- to intra-cellular water. Ethical clearance for all procedures described in sections §7.1 and §7.2 was obtained from both the Queensland University of Technology's Ethics Committee and the University of Queensland's Animal Experimentation Ethics Committee.

§ 7.1 DEHYDRATED ANIMALS

Twenty adult female Wistar rats had access to food *ad libitum* but were denied water for a period of forty hours immediately prior to the procedure. The rats were anaesthetised throughout the entire process during which their: ECW by [^{3}H] inulin, TBW by D_2O, and bioimpedance by

MFBIA were measured as described in sections (§5.2 & §6.2), (§5.1 & §6.2) and (§2.2 & §6.1) respectively. Table 7.1 details the experimental results for each rat.

TABLE 7.1

Bioimpedance results and body water volumes for twenty dehydrated rats.

Rat	Weight g	L^2/Z_c cm^2 Ω^{-1}	TBW mL	TBW % of Wt.	L^2/R_0 cm^2 Ω^{-1}	ECW mL	ECW % of Wt.
1	195	0.436	111.2	57.0 %	0.268	43.1	22.1 %
2	200	0.442	114.2	57.1 %	0.254	42.6	21.3 %
3	203	0.463	110.2	54.3 %	0.241	40.8	20.1 %
4	204	0.452	112.7	55.2 %	0.251	40.0	19.6 %
5	210	0.490	117.9	56.1 %	0.276	43.4	20.7 %
6	210	0.448	114.1	54.3 %	0.246	41.2	19.6 %
7	212	0.454	116.2	54.8 %	0.251	41.4	19.5 %
8	217	0.474	123.5	56.9 %	0.280	41.7	19.2 %
9	220	0.496	119.5	54.3 %	0.283	44.1	20.0 %
10	227	0.515	123.3	54.3 %	0.290	44.6	19.6 %
11	235	0.503	128.2	54.6 %	0.258	41.0	17.4 %
12	241	0.520	137.6	57.1 %	0.270	42.6	17.7 %
13	242	0.519	131.6	54.4 %	0.299	44.1	18.2 %
14	245	0.559	138.6	56.6 %	0.304	44.0	18.0 %
15	245	0.557	151.0	61.6 %	0.313	47.1	19.2 %
16	250	0.518	136.0	54.4 %	0.302	44.5	17.8 %
17	265	0.584	150.1	56.6 %	0.350	48.4	18.3 %
18	287	0.602	165.2	57.6 %	0.332	50.2	17.5 %
19	302	0.623	172.9	57.3 %	0.397	56.3	18.6 %
20	340	0.717	186.7	54.9 %	0.451	63.2	18.6 %
Mean	237.5	0.5186	133.0	56.0 %	0.2958	45.2	19.2 %
S.D.	36.5	0.0699	21.5	1.77 %	0.0519	5.6	1.25%

The dehydration resulting from the denial of water is evident when the measured body water volumes, (expressed as a percentage of body weight), are compared with that of the twenty normal female rats described in section §6, (table 6.2), and summarised in table 7.2. The percentages of TBW and ECW measured, (by isotope dilution), in the dehydrated rats were significantly less (P<.001) than those of normal healthy rats with ready access to water.

TABLE 7.2

Weight and body water volumes in normal and dehydrated female rats.

(mean ± S.D.)

	Weight g	TBW % of Wt.	ECW % of Wt.
Normal ♀ (n=20)	276 ± 27	69.6 ± 3.32 %	23.0 ± 1.71 %
Dehydrated ♀ (n=20)	238 ± 37	56.0 ± 1.77 %	19.2 ± 1.25 %

Regression analyses of the MFBIA prediction quotients with TBW and ECW, (as measured by isotope dilution), were performed and the results shown in figure 7.1. From these analyses prediction equations, (7.1 and 7.2), were derived for both TBW and ECW in this group of dehydrated animals.

The correlation between TBW and the single frequency prediction quotient, (L^2/R_{50}), was r = 0.74; considerably lower than the correlation obtained using the MFBIA prediction quotient, (L^2/Z_c), where r = 0.98. Similarly the correlation between ECW and the single frequency prediction quotient, (L^2/Z_5), was r = 0.91; significantly lower, (P < 0.05) than the correlation obtained using the MFBIA prediction quotient, (L^2/R_0), where r = 0.98.
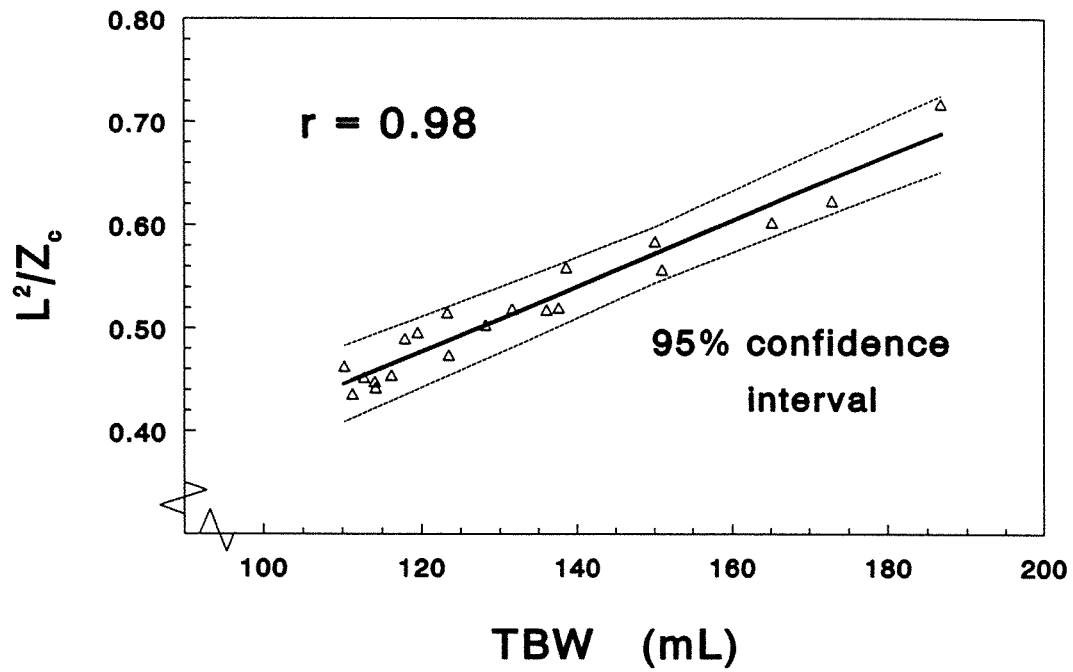
FIGURE 7.1a

L^2/Z_c *vs* TBW by D_2O dilution for a sample of dehydrated rats (n=20).
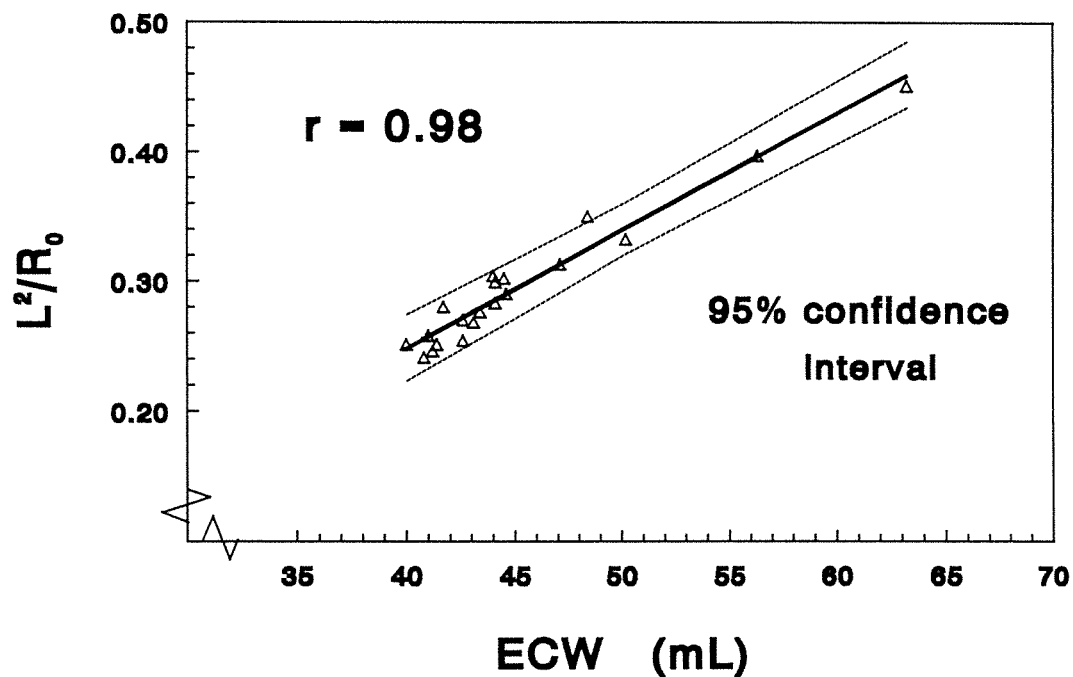
FIGURE 7.1b

L^2/R_0 *vs* ECW by [^{3}H]-Inulin dilution for a sample of dehydrated rats (n=20).

$$TBW \ (mL) \ = \ 298 \ \frac{L^2}{Z_c} \ - \ 22 \qquad SEE = 5.4 \ mL = 4.1\%$$

<div align="right">eqn (7.1)</div>

$$ECW \ (mL) \ = \ 104 \ \frac{L^2}{R_0} \ + \ 12 \qquad SEE = 1.3 \ mL = 2.9\%$$

<div align="right">eqn (7.2)</div>

Two separate procedures were performed to determine if there was any significant difference between these prediction equations, (equations 7.1 and 7.2), and the prediction equations derived from a sample of normal healthy rats, (equations 6.1 and 6.2).

(i)   Using the t distribution, statistical tests of significance were conducted on the regression parameters for normal and dehydrated rats to determine if there was any difference between the two sets of prediction equations. For both TBW and ECW no statistical difference ($P>0.05$) was found between the <u>regression coefficients</u> from both samples. Similarly no statistical difference ($P>0.05$) was detected between the <u>regression constants</u> from both samples.

(ii)   Predicted values of TBW and ECW were calculated using the equations established in the sample of normal healthy rats, and also using the equations (7.1 and 7.2) derived from the sample of dehydrated rats. The bias and limits of agreement between the two sets of predicted values were determined using the approach of Bland and Altman, (1986), described in section §4.2. The bias introduced in the measurement of TBW was -0.03 mL and the limits of agreement between -1 and +1 mL. When compared with the standard error of

the estimate (SEE = 5.4 mL, equation 7.1) associated with the prediction equation, the bias and limits of agreement suggest that the two equations are not significantly different. Similarly the bias introduced in the measurement of ECW was -0.8 mL and the limits of agreement between -1.2 and -0.3 mL. The standard error of the estimate of ECW was 1.3 mL, (equation 7.2), which also suggests that there is little if any difference between the two prediction equations.

Both of these statistical procedures demonstrate that the prediction equations, (6.1 and 6.2), established using MFBIA in normal healthy animals are equally valid when applied to a sample of animals which have a significantly lower than normal body water content.

§ 7.2　ANIMALS WITH A CONTROLLED ARTIFICIAL INCREASE IN ECW

Twenty healthy adult female Wistar rats, weights ranging from 300 g to 400 g, were used in the investigation. The animals had *ad libitum* access to food and water prior to the procedure and were anaesthetised throughout the experimental procedure with sodium phenobarbitone (Fawns & McAllan Pty. Ltd. Victoria) using a dose of 100 mg kg^{-1} body weight. Weight of the anaesthetised animal was recorded to the nearest 0.1 g. A volume of 25 mL of isotonic saline solution was progressively injected using an accurately known volume of between 4 and 5 mL into the upper peritoneal cavity *via* a 17 gauge polyethylene catheter inserted through the body wall. Impedance measurements were recorded initially and then 20 seconds after each injection. The entire process was conducted within a time period of 4 minutes. At the conclusion of the process the animal was killed with an overdose of anaesthetic.

The impedance measurements were analysed for each animal to determine R_0 and Z_c using the technique described in sections §2.2 and §6.1. The analysis of the relationship between the measured impedance values and the fluid volume injected is presented in the following two formats: (i) using the previously established MFBIA prediction equations, (6.1 and 6.2); and (ii) using the cross-validation technique described in section §4.3.

(i)   Established prediction equations

Using the prediction equations (6.1 and 6.2) the initial and subsequent body water volumes were calculated for each animal and hence the measured volume increases. These measured volume changes (ΔECW and ΔTBW) were plotted against the known volume changes (*ie* volume injected) for the pooled data of all 20 animals, (figure 7.2). The line of regression through the origin should have a gradient ideally equal to one. Table 7.3 summarises the regression results for both ECW and TBW.

TABLE 7.3

Gradients and correlation coefficients obtained from the regression
of measured values against known injected volumes for ECW and TBW
using injected volume ranges up to 20 mL and 25 mL.

Range of volume injected		0 to 20 mL	0 to 25 mL
Δ E C W	Slope	0.940	0.899
	Correlation Coeff.	0.990	0.981
	SEE (mL)	0.74	1.16
Δ T B W	Slope	1.076	1.021
	Correlation Coeff.	0.981	0.971
	SEE (mL)	1.10	1.56
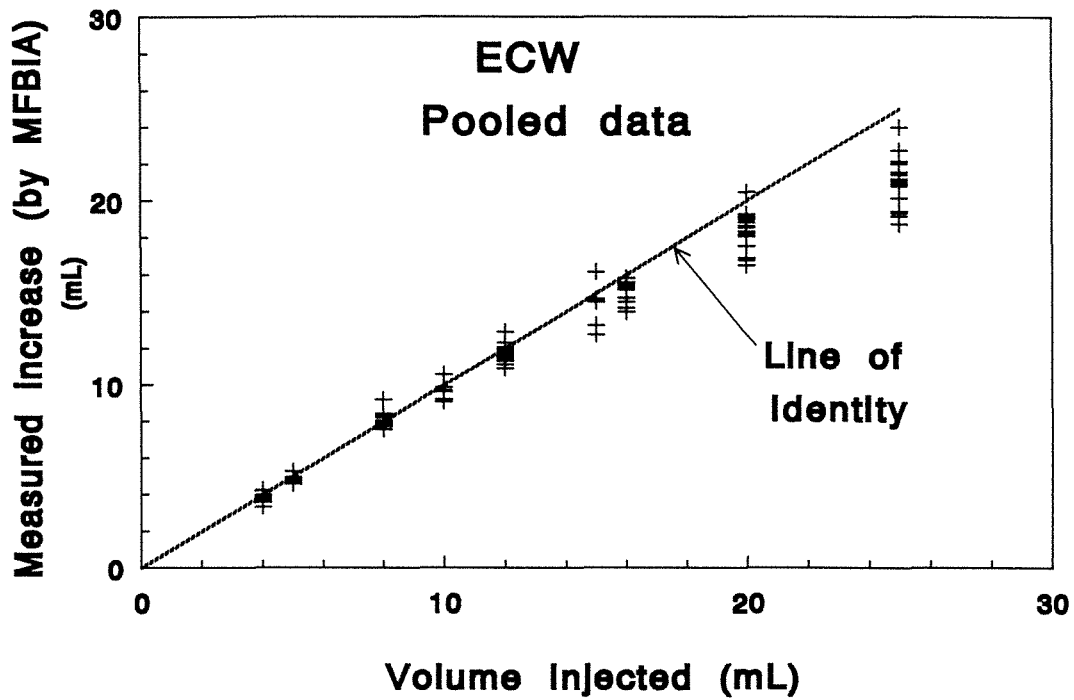
FIGURE 7.2a

Measured changes in **ECW** *vs* Volume injected (for all 20 rats).
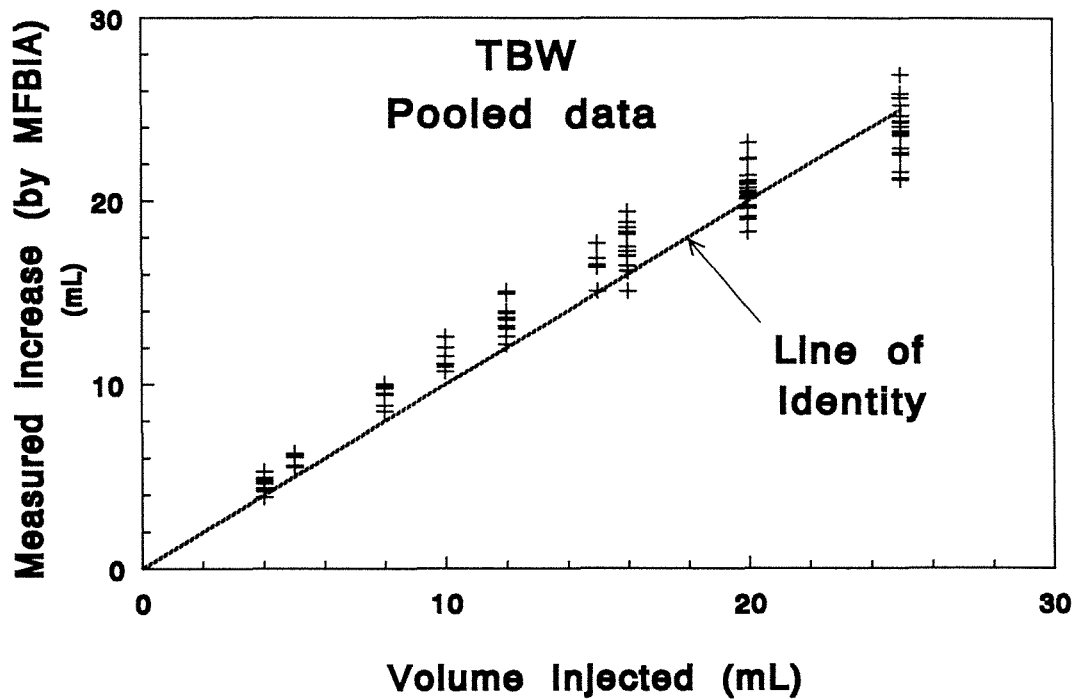
FIGURE 7.2b

Measured changes in **TBW** *vs* Volume injected (for all 20 rats).

(ii)   *Cross-validation*

The theoretical relationship between impedance and fluid volume (V), assuming a cylindrical geometry is given by equation 7.3.

$$V = \rho * \frac{L^2}{Z}$$

(equation 7.3)

Obviously if the resistivity ρ is known, the volume can be determined by measuring the length and the appropriate impedance. Equation 7.3 can be differentiated and rearranged to yield equation 7.4, and if volume changes, length and impedance are known the resistivity ρ can be determined from the gradient of the graph ΔV *vs* $\{L^2/Z_2 - L^2/Z_1\}$.

$$\Delta V = \rho * \{\frac{L^2}{Z_2} - \frac{L^2}{Z_1}\}$$

(equation 7.4)

The sample of 20 rats was randomly divided into two groups (A and B) for the purpose of double cross-validation, (as described in section §4.3). From a plot of ΔV *vs* $\{L^2/Z_2 - L^2/Z_1\}$ for each rat an estimate of ρ for ECW and TBW was obtained, table 7.4.

The mean value of the resistivity from group A (ρ_a) was then used in the prediction of volume changes in group B, and *vice versa*. The measured volume changes were then plotted against known volume changes for each rat. Typical graphs obtained are shown in figure 7.3. These plots should ideally yield a gradient of one and an intercept of zero. A summary of these regression parameters is shown in table 7.5.
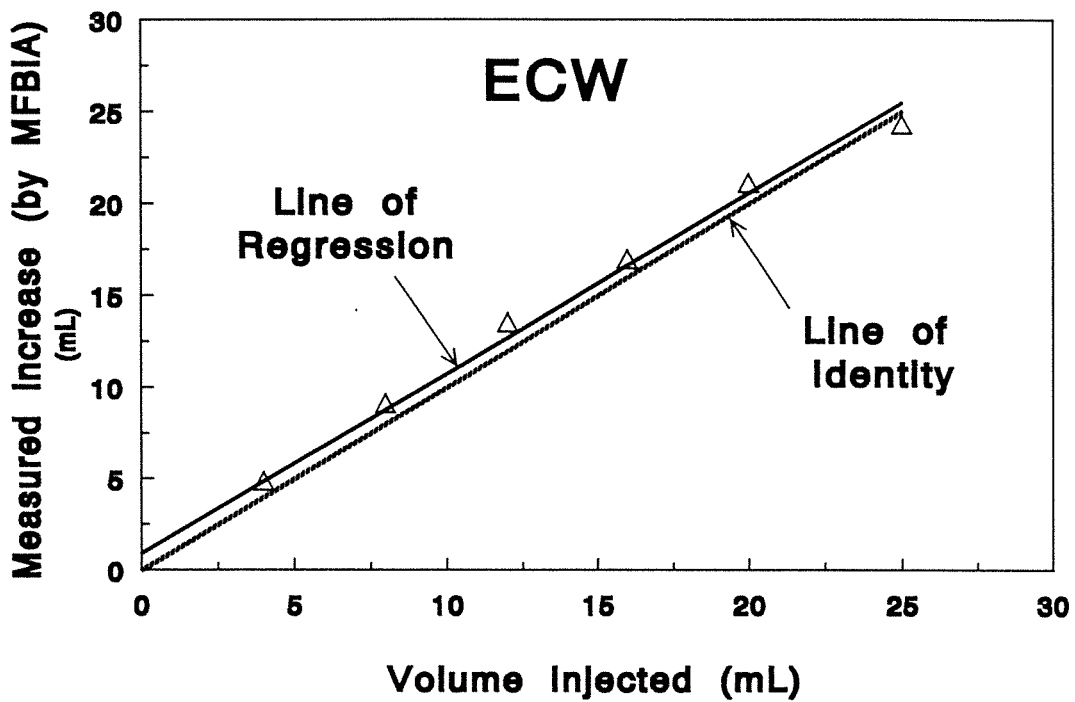
FIGURE 7.3a

Measured changes in **ECW** *vs* Volume injected for a typical rat.
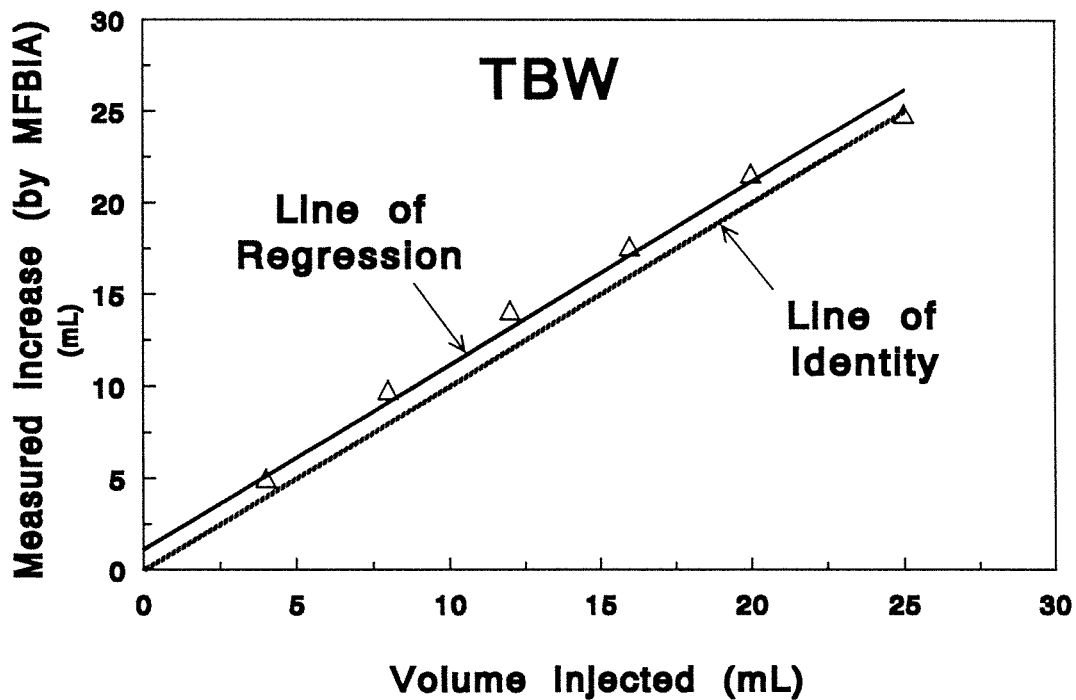
FIGURE 7.3b

Measured changes in **TBW** *vs* Volume injected for a typical rat.

TABLE 7.4

Values of resistivity, ρ, for ECW and TBW as calculated

from sub-groups A and B, and the total sample group.

		Group A (n=10)	Group B (n=10)	Total (n=20)
E C W	mean ρ (Ω cm)	124.6	126.9	125.8
	S D $_{(n-1)}$ (Ω cm)	9.0	8.5	8.6
T B W	mean ρ (Ω cm)	289.6	287.0	288.3
	S D $_{(n-1)}$ (Ω cm)	12.6	21.1	17.0

TABLE 7.5

Summary of regression parameters from the double

cross-validation and the total group.

			Group A	Group B	Total
E C W	SLOPE	Mean value	1.013	0.981	0.997
		S D $_{(n-1)}$	0.074	0.059	0.067
	INTERCEPT (mL)	Mean value	0.722	0.916	0.819
		S D $_{(n-1)}$	0.269	0.189	0.248
T B W	SLOPE	Mean value	0.982	0.987	0.985
		S D $_{(n-1)}$	0.043	0.067	0.055
	INTERCEPT (mL)	Mean value	1.002	1.322	1.162
		S D $_{(n-1)}$	0.112	0.229	0.240

While the ability of single frequency bioimpedance to predict body composition in normal rats has been established, (*eg* Hall *et al.*, 1989), no research has been published validating the technique or the prediction equations in rats where the fluid distribution has been grossly altered. In this study the ECW of animals was increased by up to 33% using isotonic saline solution resulting in extraordinarily large variations in the extra- to intra-cellular water balance.

The MFBIA impedance measurements were recorded using the same electrode placement as that used for normal healthy rats, (section §6), *viz* along the midline; one in line with the opening of the pinna, and the other in line with the iliac spines. This electrode placement was used in order to investigate the validity of previous prediction equations. Equations 6.1 and 6.2 were used to calculate the progressive changes in ECW and TBW and the relationship between these measured changes and known injected volumes is shown in figure 7.2 for the pooled data from all 20 animals. The graphs tend towards an obvious convex curve at or about 20 mL. This may be due to the gross distortion of the cylindrical geometry but the more likely explanation is that some of the injected volume was extending beyond the measurement region. It was noted during the trial that even though the saline solution was injected into the upper region of the intraperitoneal cavity, after the injection of approximately 20 mL the extra fluid was obviously extending into the lower abdomen and consequently beyond the measurement region. Correspondingly the changes in both ECW and TBW as detected by the impedance measurements at injected volumes greater than 20 mL were obviously less than the known amounts as indicated in figure 7.2. Although the extension of the injected fluid into the lower abdomen and beyond the measurement region was noted during the trial the electrode placement was not altered as the primary aim of the study was to assess the validity of the established prediction equations (equations 6.1 and 6.2).

The relationship between measured changes in body water and known changes should ideally have a gradient of 1. Table 7.3 presents a summary of the slopes of the regression lines and correlation coefficients for both ΔECW and ΔTBW *vs* known volume changes for ranges up to 20 mL and also 25 mL. Using a t-test the slopes of the regression lines, (calculated using data up to 20 mL), are not significantly different from the slope of the line of identity (P>.05). These prediction equations (equations 6.1 and 6.2) are empirical relationships established using isotope dilution techniques in healthy animals with a normal extra- to intra-cellular water balance. The very close agreement (P>.05) between measured changes and known volume changes in both ECW and TBW confirm that the MFBIA technique described and the established prediction equations are valid and accurate determinations of ECW and TBW for both normal and abnormal levels of the extra- to intra-cellular fluid balance.

The concept of the double cross-validation process divides the total group randomly into two subgroups; the measured and known data of each subgroup are used to generate the value of the resistivity which is then applied to the opposite subgroup to predict changes in body fluid volumes. This process is based on the theoretical relationship between impedance and volume as described by equations 7.3 and 7.4. The values of the resistivity determined from the two subgroups shown in table 7.4 were not significantly different (P>.05) for both ECW and TBW. The measured volume changes plotted against known volume changes (*eg* figure 7.3) for each subgroup yielded gradients equal to that of the line of identity (P>.05) but with a non-zero intercept (P<.05), (table 7.5). The reason for the non-zero value of the intercept is not known and warrants further investigation.

Using the known injected volume, the standard error of the measured volume change detected by MFBIA varied between 0.6 and 1.2 mL over the

sample of 20 animals. This would suggest that the precision of MFBIA is +/- 2 mL in a 350 g rat. The results of the cross-validation not only confirm the validity of the simple relationship between volume and impedance (equation 7.3), but also the validity, accuracy and sensitivity of the MFBIA technique irrespective of the extra- to intra-cellular fluid balance of the rat.

An analysis using single frequency BIA was conducted on the same group of 20 rats to compare the application of a single frequency technique in biologically perturbed systems. The correlation coefficient between the difference in length^2/impedance and volume injected was calculated using the total group, (n=20), at each of the 496 frequencies from 4 kHz to 1 MHz and the variation against frequency shown in figure 7.4.
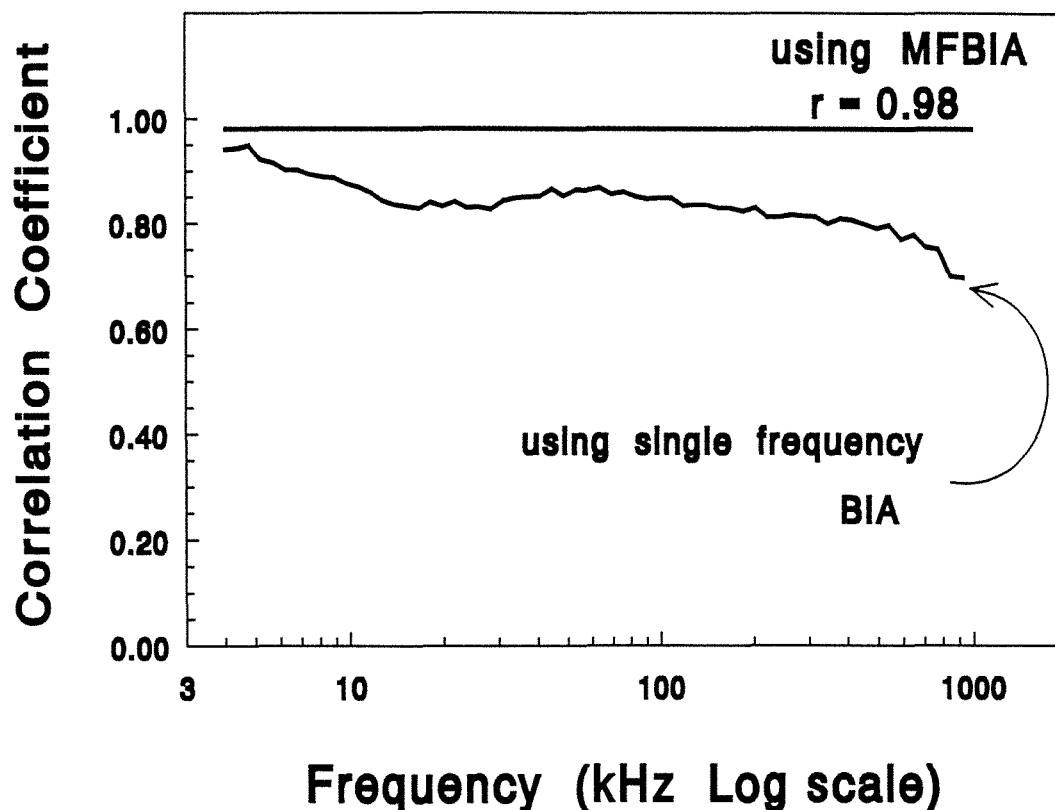
FIGURE 7.4

Variation of the correlation coefficient, (Δ (L^2/Z) vs Δ body water), with frequency.

The correlation obtained using the MFBIA predictors R_0 and Z_c were r=0.99 and r=0.98 respectively. Both of these values are considerably higher than that at any of the measured frequencies as shown by figure 7.4. However as the frequency decreases the value of correlation coefficient approaches that obtained at R_0.

These results support previous findings, (discussed in §6), that the MFBIA technique provides a more accurate and precise prediction of body water volumes. They also demonstrate that the validity, accuracy and precision of the MFBIA technique is virtually unaffected by extreme perturbations in the extra/intracellular water balance of a living animal. However the validity and accuracy of single frequency BIA estimates of body water is considerably affected by such perturbations which suggests that single frequency BIA may be inappropriate for application in individuals in various states of ill-health.

§ 7.3   SUMMARY

BIA at a single frequency has been accepted as a convenient and reliable technique of measuring body water in normal healthy subjects but its application to individuals with abnormal fluid levels has proven to be inaccurate. The MFBIA technique established in this dissertation has demonstrated a significant improvement in the prediction of body water, both ECW and TBW, in normal healthy animals, and this section of the study investigated its application to rats with abnormal fluid levels, (dehydration), and abnormal fluid balances. The results support two important aspects of the MFBIA technique:-

(i)   the validity of the simple relationship between volume and impedance *viz*

$$Volume \propto \frac{1}{Z^2}$$

(ii)   the technique and the associated prediction equations are independent of the extra- to intra-cellular fluid balance and apply to both abnormal and normal animals.

There are many methods available to estimate TBW and several methods to estimate ECW. All of the noninvasive techniques rely on a constant strong correlation between the measured quantity and actual body water; this correlation may only be valid in normal healthy subjects. The technique of MFBIA measures the impedance of the extra-cellular water and total body water which is directly determined by the quantity of ECW and TBW irrespective of the balance of extra- and intra-cellular fluids and is subsequently equally valid in rats with altered health states.

SECTION 8

APPLICATION OF MFBIA TO EVALUATE BODY WATER VOLUMES IN HUMANS.

§ 8   APPLICATION   OF   MFBIA   TO   EVALUATE BODY   WATER   VOLUMES   IN   HUMANS

The advantages of bioelectrical impedance analysis, (*viz* non-invasive, inexpensive, easily applied and reproducible), favour its application to humans in virtually any state of health or ill-health. However the accuracy of prediction of TBW in individuals with altered states of health has been less than desirable, (Battistini *et al.*, 1992; Gray *et al.*, 1989; Spence *et al.*, 1979; Jebb and Elia, 1993). The results of section §7 confirm that MFBIA does accurately predict both TBW and ECW in both normal and unhealthy animals. The ensuing detail of this section describes the investigation of MFBIA to predict body water volumes in healthy humans.

§ 8.1   APPLICATION   OF   MFBIA   IN   HEALTHY   HUMANS

In this segment of the study TBW, ECW and MFBIA measurements were performed on sixty healthy human subjects, (twenty seven males and thirty three females), aged between 18 and 45 years. None of the volunteers was on any form of medication, (apart from oral contraception). Ethical clearance for all procedures described in section §8.1 was obtained from both the Queensland University of Technology's Ethics Committee and the University of Queensland's Ethics Committee. All volunteer participants gave their written, informed consent and were free to withdraw from the study at any time they wished, (see appendix C for copies of patient consent forms).

Isotope dilution measurements

The height and weight of each subject was recorded to the nearest 0.1 cm and 0.1 kg respectively and a 10 mL sample of venous blood was obtained to determine the individual's background concentration of bromide and D_2O. All blood samples were obtained by appropriately qualified personnel. Participants then drank an accurately weighed amount of 'tracer cocktail' (which delivered a dose of 0.5 g D_2O per kg body weight, and 0.75 mmol bromide per kg body weight). The subjects drank the cocktail from a glass cup using a plastic straw. The cup plus straw were weighed before and after to determine the amount, ($\pm$.01 g), of cocktail administered. The D_2O was pyrogen free 99.9% pure (Cambridge Isotope Laboratories, Massachusetts) and the sodium bromide 99.8% pure NaBr (Ajax, Auburn, Australia). The mass of D_2O and NaBr administered was determined to the nearest 0.1 mg. After an equilibration period of 3.5 hours, (Lukaski, 1987; Blagojevic *et al.*, 1990; Kushner *et al.*, 1990), a second 10 mL blood sample was obtained to determine the concentration of the tracers. All subjects refrained from excessive oral intake and exercise during the tracer equilibration period. As far as possible the study was conducted whilst subjects continued their 'normal' daily routine.

Plasma from the heparinized venous blood samples was separated by centrifuge at 1500 x g for 6 minutes at 10°C. The plasma concentrations of D_2O and bromide for the initial background and the equilibration samples were determined by Fourier transform infrared spectroscopy and spectrophotometry respectively. These procedures are described in detail in sections §5.1 and §5.3 respectively. From the quantity of dose administered and the measured increase in tracer concentration the dilution volumes of each tracer can be calculated. Using the correction factors discussed in section §5 the corresponding values of TBW and ECW were calculated using

the previously described equations.

$$TBW \ (L) \ = \ \frac{(\ mass \ of \ D_2O \ injected\ ) \ (g)}{[\ D_2O\ ]_{plasma} \ (gL^{-1})} \ * \ 0.937$$

(§5.1 eqn 5.1)

$$ECW \ (L) \ = \ \frac{Br_{dose} \ (mmol)}{[Br]_{plasma} \ (mmol \ L^{-1})} \ * \ 0.90 \ * \ 0.95 \ * \ 0.937$$

(§5.3 eqn 5.3)

where: 0.90 is the fraction of the retained bromide dose that is assumed to remain extracellular;

0.95 is the Donnan equilibrium factor for bromide;

0.937 is the fraction of water in plasma.

MFBIA measurements

Immediately prior to the collection of the final blood sample the whole body impedance of each subject was measured. Each volunteer, clothed but without shoes or socks, was supine with limbs slightly abducted on a couch made of non-conducting materials. Adhesive electrodes (3M, Minnesota USA) were placed on the skin, previously cleaned by alcohol, at standardised sites to measure whole body impedance, (Lukaski et al., 1985; Scheltinga, 1992). Measurement electrodes were positioned on the dorsal surface of the right wrist at the level of the process of the radial and ulna bones; and on the anterior surface of the right ankle between protruding portions of the tibial and fibular bones. The source electrodes were positioned distal to the measurement electrodes; on the dorsal surface of the third metacarpal bone of the right hand; and the dorsal surface of the third metatarsal bone of the right foot, (figure 8.1). MFBIA measurements were

made using the swept frequency bioimpedance instrument described in section §3.3 and the impedance data analysed (see section §3.4) to determine the impedance at the characteristic frequency, Z_c, and the resistance at zero frequency, R_0. The resistance at frequencies of 5 and 50 kHz were also determined to enable a comparison between MFBIA and single frequency BIA predictors.
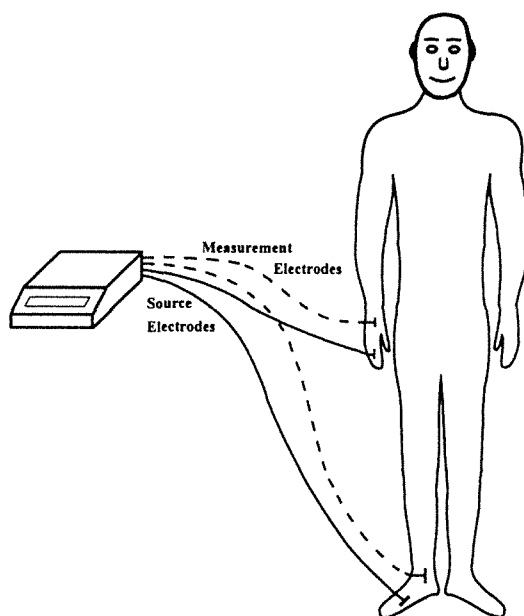
FIGURE 8.1

Electrode placement for whole body impedance measurements in humans.

As described earlier the impedance and phase were measured at frequencies ranging from 4 kHz to 1 MHz, however in many cases the measurements at the lower and upper ends of this range were subject to the effects of stray capacitance and noise introduced by the skin-electrode contact. This effect is clearly evident in the impedance locus shown in figure 8.2. Accordingly the regression analysis to determine the circular Cole-Cole plot excluded the data points at the extremities of the frequency range. The Cole-Cole plot for each subject was determined from impedance

measurements in the frequency range 10 kHz to 800 kHz and also using the range 10 kHz to 350 kHz. No significant difference was detected in the regression results derived from the two frequency ranges.
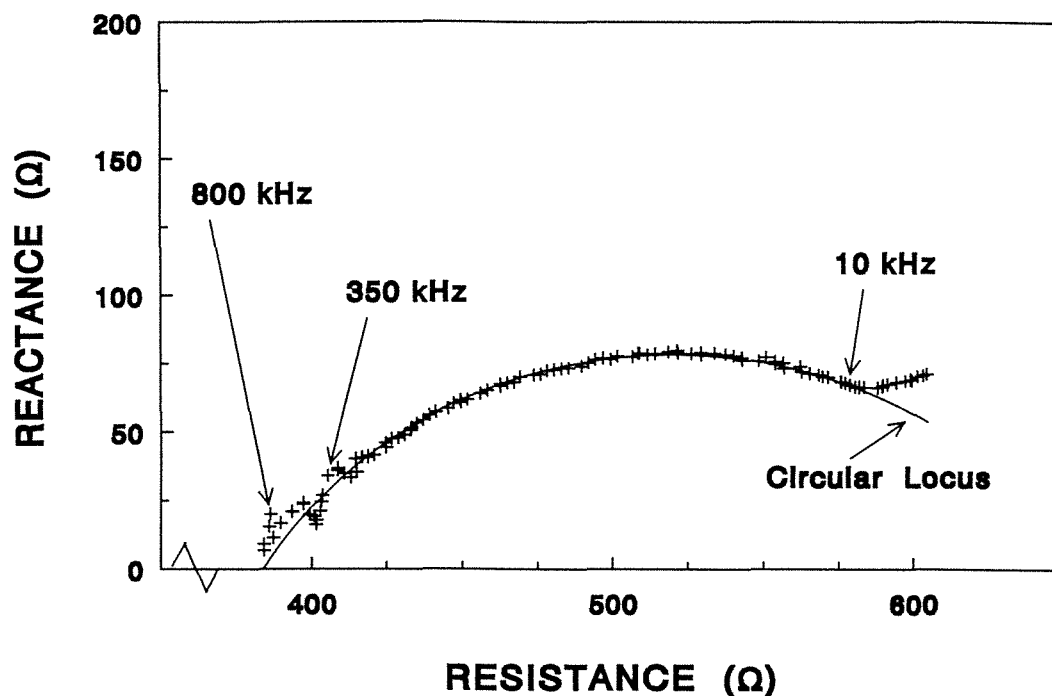
FIGURE 8.2

A typical impedance plot, obtained using skin surface electrodes,

showing the obvious deviations from the circular Cole-Cole plot

at the extremities of the frequency range, (*viz* <8 kHz & >350 kHz).

Correlation of bioimpedance with dilution measurements

Although the theoretical relationship between impedance and volume includes the total length of the conducting body, (*ie* wrist to ankle), this cannot be measured accurately and the universally accepted length for prediction of human body composition using bioimpedance is the individual's height, (Lukaski *et al.*, 1985). Table 8.1 summarises the relevant characteristics and measurements of the subjects participating in the study. The body mass index, (BMI), of all male and female subjects was well within the 5th and 95th percentiles for the Australian male and female population, (National Heart Foundation of Australia, 1990).

TABLE 8.1

Summary of impedance and isotope dilution data

for a group of healthy humans.

QUANTITY	MALES (n=27) mean ± sd range	FEMALES (n=33) mean ± sd range	TOTAL (n=60) mean ± sd range
weight (kg)	77.4 ± 10.0 60.2 - 100	62.3 ± 10.5 46.8 - 90.4	69.1 ± 12.7 46.8 - 100
height (cm)	177.5 ± 6.0 165 - 187	165.6 ± 6.8 151 - 182	170.9 ± 8.8 151 - 187
BMI (kg m^{-2}) (body mass index)	24.5 ± 2.6 18.7 - 29.3	22.7 ± 3.6 18.3 - 31.4	23.5 ± 3.3 18.3 - 31.4
age (y)	28.6 ± 7.0 19 - 45	24.4 ± 5.8 18 - 45	26.3 ± 6.7 18 - 45
R_{50} (Ω)	468 ± 44 377 - 583	607 ± 55 487 - 718	545 ± 86 378 - 718
Z_5 (Ω)	559 ± 56 451 - 714	698 ± 72 500 - 874	635 ± 94 451 - 874
Z_c (Ω)	501 ± 44 408 - 620	630 ± 52 514 - 749	572 ± 81 408 - 749
R_0 (Ω)	609 ± 53 493 - 751	745 ± 62 599 - 912	684 ± 89 493 - 912
H^2/R$_{50}$ (cm$^2\Omega^{-1}$)	68.0 ± 7.6 54.4 - 84.9	45.7 ± 6.4 35.9 - 63.1	55.7 ± 13.1 35.9 - 84.9
H^2/Z$_5$ (cm$^2\Omega^{-1}$)	56.9 ± 5.9 44.9 - 70.1	39.9 ± 6.0 29.9 - 57.1	47.6 ± 10.3 29.9 - 70.1
H^2/Z$_c$ (cm$^2\Omega^{-1}$)	63.5 ± 6.6 51.1 - 78.6	43.9 ± 5.7 34.0 - 61.8	52.7 ± 11.5 34.0 - 78.6
H^2/R$_0$ (cm$^2\Omega^{-1}$)	52.1 ± 5.4 42.1 - 65.0	37.2 ± 4.8 28.9 - 52.0	43.9 ± 9.0 28.9 - 65.0
TBW (L) (D$_2$O space)	49.0 ± 5.8 40.1 - 61.4	35.2 ± 3.9 28.2 - 43.0	41.4 ± 8.4 28.2 - 61.4
ECW (L) (bromide space)	19.8 ± 3.6 13.4 - 26.7	16.1 ± 3.0 10.3 - 22.4	17.7 ± 3.8 10.3 - 26.7

Deming's linear regression analysis, (section §4.1), was used to describe relationships between the impedance predictors, ($height^2$/impedance), and body water volumes. Table 8.2 lists the correlation coefficients and standard errors of the estimate, (see equation 4.3 §4.1), obtained using a variety of impedance quotients.

TABLE 8.2

Comparison of correlation coefficients (r) and standard errors

of the estimate (SEE) describing the relationships between

various impedance quotients and body water volumes (TBW and ECW).

TBW			
quotient	males (27)	females (33)	total (60)
H^2/R_{50}	r = 0.75 SEE = 6.1%	r = 0.75 SEE = 5.7%	r = 0.92 SEE = 5.9%
H^2/R_∞	r = 0.75 SEE = 6.1%	r = 0.72 SEE = 6.1%	r = 0.92 SEE = 6.0%
H^2/R_0	r = 0.80 SEE = 5.6%	r = 0.74 SEE = 5.8%	r = 0.93 SEE = 5.7%
H^2/Z_c	r = 0.82 SEE = 5.3%	r = 0.78 SEE = 5.4%	r = 0.94 SEE = 5.2%
ECW			
quotient	males (27)	females (33)	total (60)
H^2/Z_5	r = 0.58 SEE = 12.4%	r = 0.71 SEE = 10.3%	r = 0.72 SEE =11.4%
H^2/R_∞	r = 0.61 SEE = 11.9%	r = 0.57 SEE = 12.5%	r = 0.69 SEE = 12.0%
H^2/Z_c	r = 0.73 SEE = 9.9%	r = 0.71 SEE = 10.2%	r = 0.75 SEE = 10.8%
H^2/R_0	r = 0.75 SEE = 9.4%	r = 0.73 SEE = 10.0%	r = 0.77 SEE = 10.4%

For the prediction of TBW there is relatively little difference between the precision of the estimates using the prediction quotients listed in table 8.2. A *Fisher z transformation* was used as a test of significance for differences between the listed correlation coefficients. The optimum prediction quotient determined from the animal studies, H^2/Z_c, (section §6.3), again yielded the highest correlation coefficient, (and lowest standard error). However it was not significantly better than the other prediction quotients including the MFBIA predictor of ECW, (H^2/R_0). A similar situation existed in the prediction of ECW with the optimum prediction quotient determined from the animal studies, H^2/R_0, yielding the highest correlation coefficient, (and lowest standard error), but not significantly better than the other listed prediction quotients.

The correlation coefficient between height^2/impedance and TBW was calculated using the total group, (n=60), at each of the 496 frequencies from 4 kHz to 1 MHz and the variation against frequency shown in figure 8.3a. The same procedure was performed using ECW and the corresponding variation shown in figure 8.3b. These graphs demonstrate that there is relatively little difference in the correlation obtained between bioimpedance and body water volumes, in this group of healthy subjects, when the frequency at which the impedance is measured is varied between 4 kHz and 1 MHz. However sections §6 and §7 of this dissertation confirm that the MFBIA predictors H^2/Z_c and H^2/R_0 can accurately predict TBW and ECW respectively in both normal healthy animals as well as those in which major shifts in fluid balance have occurred. The minimal variation in the value of the correlation coefficient shown in figure 8.3 is an indication of the strict regulation of body fluids associated with homeostasis in normal healthy subjects rather than which frequency should be the optimum in predicting TBW or ECW.
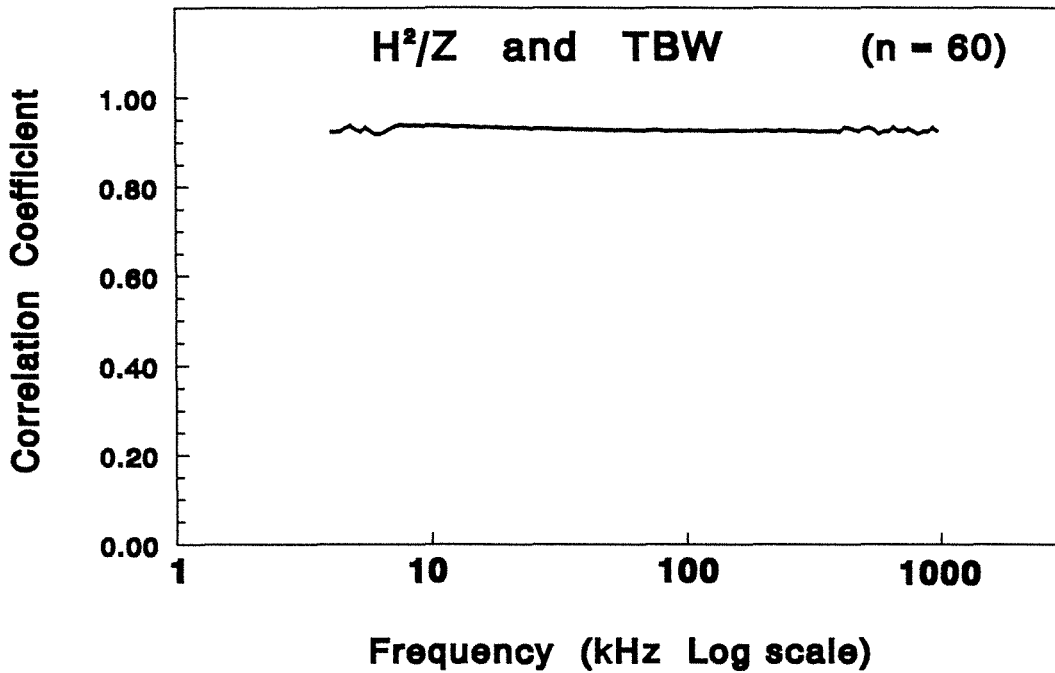
FIGURE 8.3a

Variation of the correlation coefficient (between H²/Z and TBW) with frequency.
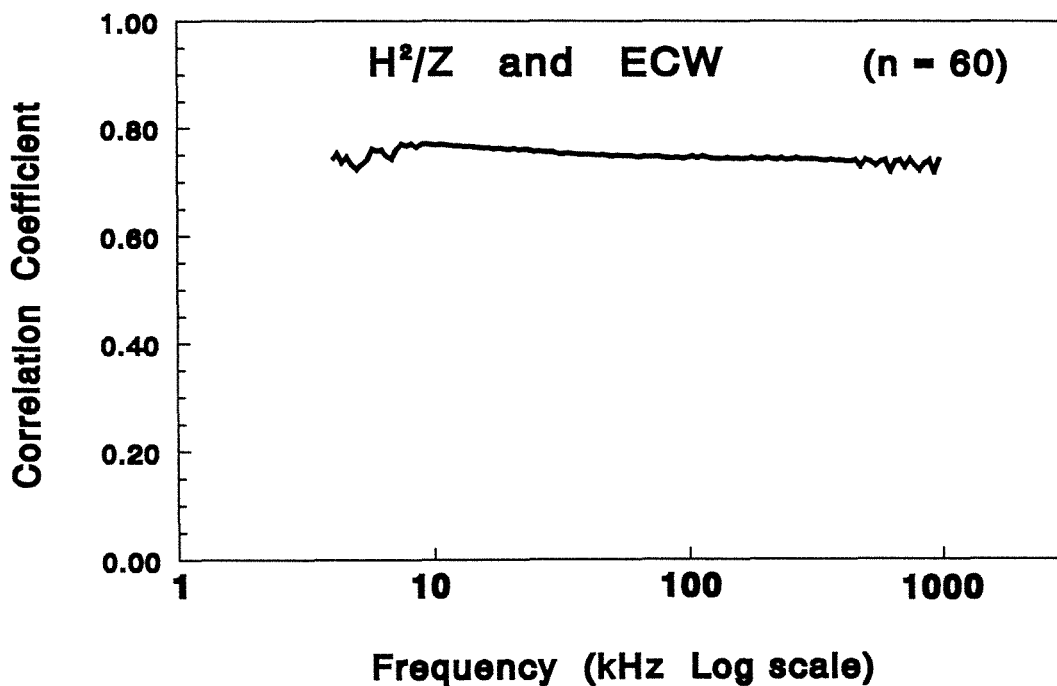
FIGURE 8.3b

Variation of the correlation coefficient (between H²/Z and ECW) with frequency.

When the correlation coefficients from the male and female sub-groups were compared with each other and with those from the total group the only significant difference found was between the single sex sub-groups and the total group in the prediction of TBW. However there is a large difference in the distributions of TBW between the male and female sample groups, (table 8.1), which could introduce an artificial increase in the correlation coefficient of the combined group. In contrast to this there is only a relatively slight difference in the distributions of ECW and little difference in the associated correlations. When the standard errors associated with the prediction of TBW are compared there is no significant difference between the various groups. This supports the notion that the increase in the observed correlation with TBW in the combined group is a result of the increased range of TBW values.

In a group of normal healthy individuals the ECW volume is expected to be closely related to the volume of TBW; in this sample the correlation between ECW and TBW was r = 0.8. Accordingly the results summarised in table 8.2 suggest that the MFBIA quotient H^2/Z_c is an equally good predictor of ECW as well as TBW in this group of normal healthy individuals. Similarly H^2/R_0 appears to be an equally good predictor of TBW as well as ECW. The correlation of TBW and ECW with body weight alone was calculated and found to be r=0.84, (SEE=8.3%), and r=0.74, (SEE=10.9%), respectively. While this is a significantly lower correlation (P<.05) with TBW, (cf. r=0.94 using H^2/Z_c), there was no significant difference in the correlation with ECW, (cf. r=0.77 using H^2/R_0). This is further evidence of the strict regulation of body fluids associated with homeostasis in normal healthy subjects.

The results of this study compare favourably with those of van Loan and Mayclin, (1992), who measured whole body resistance at 25 frequencies ranging from 1 kHz to 1.35 MHz and calculated the correlation with body water volumes at each of the 25 independent frequencies. They report

maximum correlations of BIA with TBW of r = 0.78 and 0.75 for males and females respectively, and similarly with ECW values of r = 0.85 and 0.72 for males and females respectively. Van Loan and Mayclin also found that in their sample of healthy subjects prediction quotients that were highly correlated with TBW were also highly correlated with ECW and *vice versa*.

Figure 8.4 shows the plot of TBW *vs* H^2/Z_c and ECW *vs* H^2/R_0 for this group of subjects.
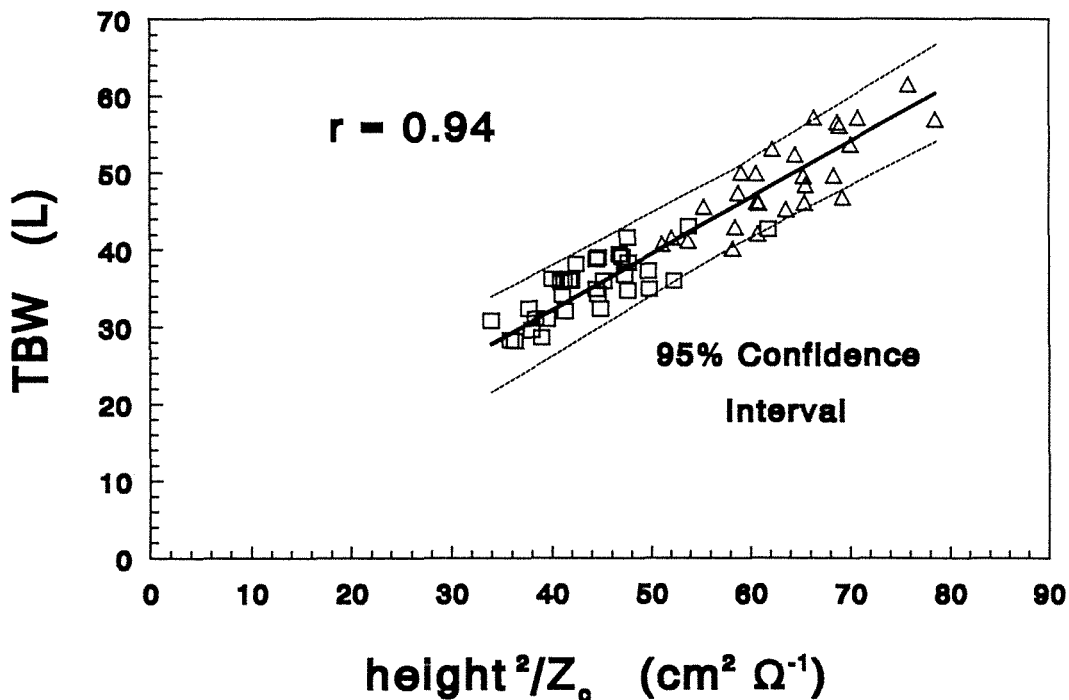
FIGURE 8.4a

Plot of TBW *vs* H^2/Z_c for the human volunteers, ($\square$ females, $\triangle$ males).
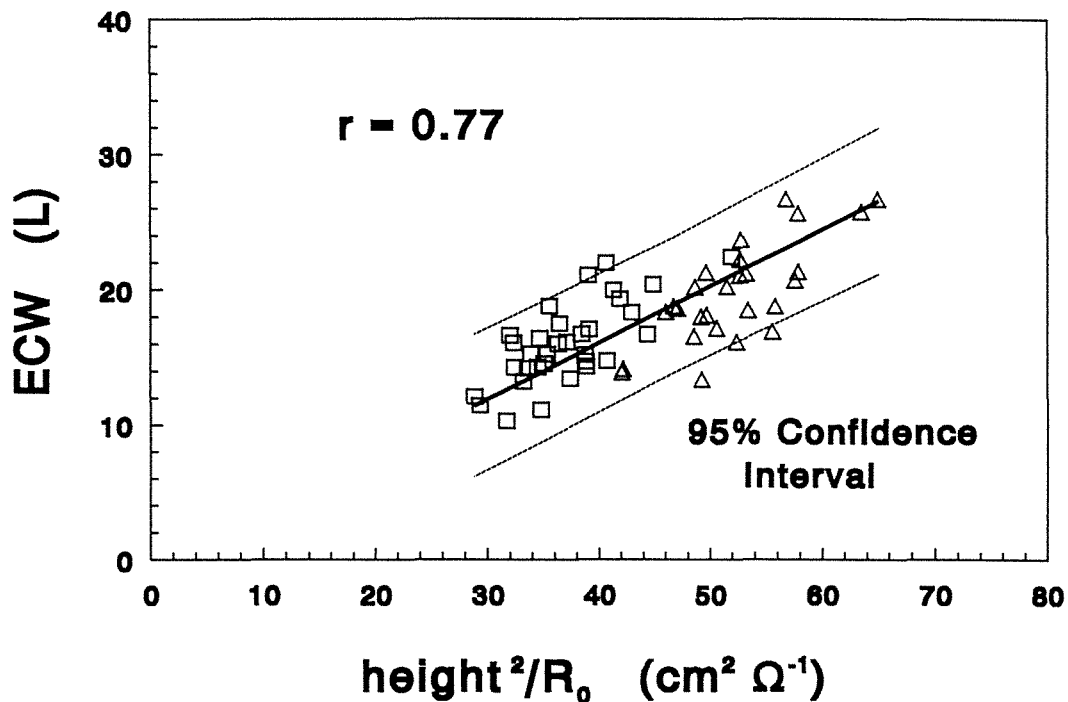
FIGURE 8.4b

Plot of ECW *vs* H^2/R_0 for the human volunteers, ($\square$ females, $\triangle$ males).

The regression lines were calculated using Deming's regression, (section §4.1), and are shown below.

$$TBW \; (L) \quad = \quad 0.733 * \frac{H^2}{Z_c} + 2.8 \qquad\qquad SEE = 2.2 \; L = 5.2\%$$

<div align="right">(eqn 8.1)</div>

$$ECW \; (L) \quad = \quad 0.417 * \frac{H^2}{R_0} - 0.59 \qquad\qquad SEE = 1.8 \; L = 10\%$$

<div align="right">(eqn 8.2)</div>

The statistical procedure described by Bland and Altman, (1986), was used to test for any difference in the prediction of body water volumes between the male and female sub-groups. Equations 8.1 and 8.2 were used

to estimate the TBW and ECW of the male subjects. These estimates were subsequently compared with the measured values determined by isotope dilution and the bias, (mean difference), and limits of agreement calculated using the procedure described in section §4.2. This process was repeated using the data of the female subjects and the results summarised in table 8.3.

TABLE 8.3

Bias and limits of agreement obtained between

the prediction equations from the total group and the

measured values of TBW and ECW (by isotope dilution).

		Males (n=27)	Females (n=33)
TBW	Bias	0.3 L (0.7%)	-0.2 L (-0.6%)
	Limits of agreement (95%)	-1.0 L to 1.6 L	-1.2 L to 0.7 L
ECW	Bias	1.4 L (7.1%)	-1.2 L (-7.2%)
	Limits of agreement (95%)	0.5 L to 2.4 L	-1.9 L to -0.4 L

A *student t* test was used to detect any difference in the bias between the male and female groups. There was no significant difference in the values of the bias for TBW, (P>0.2). However there was clearly a significant difference in the values of the bias for ECW, (P<.001). Hence equation 8.1 is equally valid in predicting TBW in male and female subjects of this group, but separate prediction equations are needed to estimate ECW in male and female subjects. Regression analysis was applied to each sub-group separately to determine these relationships, (equations 8.3 and 8.4).

$$male \qquad ECW \ (L) \quad = \quad 0.670 \ * \ \frac{H^2}{R_0} \ - \ 15.2$$

$$SEE = 1.8 \ L = 9\% \qquad\qquad (eqn \ 8.4)$$

$$\textit{female} \quad ECW \ (L) \ = \ 0.624 \ * \ \frac{H^2}{R_0} \ - \ 7.1$$

$$SEE = 1.6 \ L = 10\% \qquad\qquad (eqn \ 8.4)$$

A stepwise multiple regression was performed including weight, sex (coded 0=male, 1=female, as used by van Loan and Mayclin, 1992)) and age as well as the $height^2$/impedance term. The inclusion of weight in the prediction equations was significant at the 95% confidence level (P<0.05) for TBW and ECW, but the inclusion of age, (either before or after weight), was not significant, (at the 80% confidence interval, P>0.2). The inclusion of a sex term in the regression equation for TBW was not significant (P>0.2), however the inclusion of sex in the regression equation of ECW was significant, (P<0.05). Snedecor and Cochran, (1980), describe standardised coefficients of multiple regression, b_i^*, which can be used to compare the strengths of the association between the independent variables, (x_i), and the dependent variable, (y), and are given by:- $b_i^* = b_i \ S_{xi} \ /S_y$. The standardised coefficients from the multiple regression analyses are listed in table 8.4.

TABLE 8.4

Standardised coefficients for the stepwise multiple regression analyses.

TBW	H^2/Z_c	Weight	Sex	Age
	0.71	0.29	—	—
	0.87	—	-0.08	—
	0.98	—	—	-0.06
ECW	H^2/R_0	Weight	Sex	Age
	0.47	0.39	—	—
	1.15	—	0.46	—
	0.79	—	—	-0.04
	0.85	0.33	0.40	—

The very low relative values of the standardised regression coefficients, (table 8.4), for the parameters of age and sex in TBW and age in ECW confirm that their inclusion in the prediction equations is not significant. The resulting prediction equations including weight and sex are:

$$TBW \ (L) \ = \ 0.520 \ \frac{H^2}{Z_c} \ + \ 0.193 \ Wt \ + \ 0.6$$

$$r = 0.954 \qquad SEE = 2.5 \ L = 6.1\% \qquad eqn \ (8.5)$$

$$ECW \ (L) \ = \ 0.194 \ \frac{H^2}{R_0} \ + \ 0.115 \ Wt \ + \ 1.2$$

$$r = 0.805 \qquad SEE = 2.2 \ L = 12.7\% \qquad eqn \ (8.6)$$

$$ECW \ (L) \ = \ 0.480 \ \frac{H^2}{R_0} \ + \ 3.50 \ Sex \ - \ 5.3$$

$$r = 0.810 \qquad SEE = 2.2 \ L = 12.6\% \qquad eqn \ (8.7)$$

$$ECW \ (L) \ = \ 0.352 \ \frac{H^2}{R_0} \ + \ 0.099 \ Wt \ + \ 3.09 \ Sex \ - \ 6.3$$

$$r = 0.836 \qquad SEE = 2.1 \ L = 11.7\% \qquad eqn \ (8.8)$$

where: H = height (cm) R_0 = resistance (zero frequency) (Ω)

         Wt = weight (kg) Z_c = impedance (characteristic frequency) (Ω)

         Sex: coded as   0 = male   and   1 = female

When the standard errors of the prediction equations from the human study are compared with those of the animal investigations (section §6) an obvious difference is noted. Using MFBIA to predict TBW in animals results in a standard error of 5.9%; this is comparable to that obtained in the humans, (5 to 6% depending on the parameters included). However the precision of the prediction of ECW by MFBIA in humans, (SEE = 10 to 12%), is considerably worse than that in the animal group, (SEE = 3.2%). The reason for this is not known and warrants further investigation before prediction equations are employed in the clinical situation. The standard error of the estimate from the regression of the Cole-Cole plot was typically less than 0.5%, similar to that obtained in the animal studies. This may suggest that the loss in precision in the prediction of ECW was not a result

of the MFBIA technique but rather the independent method of determining the ECW value.

As described earlier, isotope dilution is accepted as the gold standard for the determination of body water volumes. However there are a number of methods of measuring the plasma concentration of a particular tracer and their precision is dependent upon the assay used. The precision associated with the radioactive assay of tritium by liquid scintillation spectroscopy is very high, ($\pm$<1%). However the precision associated with the spectrophotometric assay of bromide incorporates the error associated with temperature and time dependence of the reaction with sodium fluorescein, (Trapp and Bell, 1989). A further consideration is the actual space measured by the various tracers. Vaisman *et al.*, (1987), explains that the volume measured by the bromide and sulfate ion tracers is greater than that measured by the polysaccharides inulin and mannitol; Russell *et al.*, (1988 p257), State ".. *the inulin space can be regarded as the 'true' ECV* " and that the space measured by other tracers is larger than the inulin space. This difference in cell penetration and 'tracer space' may contribute to the greater variation observed in the MFBIA correlation with bromide space.

The protocol for the determination of ECW described in the literature varies; the strictest being nil by mouth for 12 hours immediately prior to and during the study (Kushner and Schoeller, 1986; Lukaski and Bolunchuk, 1988). The purpose of these strict conditions is to ensure complete and rapid absorption of the bromide tracer. The protocol used in this study did not involve fasting prior to the procedure and participants were free to eat or drink small quantities during the study. While it is unlikely that this relaxation of the protocol would interfere with the absorption of bromide it may cause fluctuations in the concentration of bromide in the body fluids thus decreasing the precision obtained from a single blood sample taken at a given time.

§ 8.2   SUMMARY

The results of this study confirm that the MFBIA predictors H^2/Z_c and H^2/R_0 can be used to estimate TBW and ECW respectively. The correlation coefficients describing the relationships between body water volumes and the MFBIA predictors alone were comparable with those reported by van Loan and Mayclin, (1992). When other parameters such as weight and sex were also included in the regression equation a significant improvement in the correlation resulted. This increase in correlation by the addition of anthropometric parameters has been reported by almost all research groups, (*eg* Lukaski and Bolunchuk, 1988; Segal *et al.*, 1991; van Loan and Mayclin, 1992).

Van Loan and Mayclin, (1992), measured whole body impedance at 25 frequencies ranging from 1 kHz to 1.35 MHz to determine which frequency yielded the best prediction of TBW and ECW. They reported correlation coefficients of the order r=0.78 for several frequencies above 100 kHz and a significantly lower correlation (r=0.60) between H^2/R_1 and ECW in females, (R_1 = resistance at 1 kHz). From this they deduced that impedance measured at low frequencies was not a good predictor of ECW, and that both TBW and ECW could be accurately predicted from the resistance measured at a single frequency of 224 kHz. Segal *et al.*, (1991), also investigated the association between body water volumes and bioimpedance measured at three independent frequencies, (*viz* 5, 50, 100 kHz). However Segal *et al.* reported that H^2/R_{100} was the best predictor of TBW and H^2/R_5 was the best predictor of ECW, (R_{100} and R_5 are the resistances at 100 and 5 kHz respectively). They state, (p28), "*Although ECW and TBW were themselves significantly intercorrelated (r=0.797, P<.001), partial correlation analyses indicated that height $^2/R_5$ and height $^2/R_{100}$ measured distinctly independent components of body water*".

Van Loan and Mayclin, (1992), have reported that impedance measured at low frequencies (< 5kHz) is not a reliable predictor of ECW and that impedance measured at a higher frequency can be used to reliably predict both TBW and ECW. The results of this study have shown that in normal healthy individuals there is a strong correlation between TBW and ECW and that prediction quotients of TBW, (using impedance measured at high frequencies >50 kHz), are also reliable predictors of ECW. Also noted in this study was the capacitive effect of the skin-electrode contact which had significant effects, (in some individuals), at frequencies below 8 kHz, (figure 8.2). Thus the impedance measured at low frequencies is not simply due to the body impedance but also affected in a non-systematic manner by the electrode-skin contact, and would explain the poorer correlation with body water volumes.

The technique established in this study enables the resistance at zero frequency to be determined by extrapolation of the Cole-Cole plot. This Cole-Cole plot can be obtained from measurements at frequencies greater than 8 kHz and without interference from the skin-electrode contact. While this study has shown that H^2/Z_c and H^2/R_0 can both predict TBW and ECW in normal healthy individuals, the results from the animal section of this study with an abnormal level or balance of body fluids, (section §7), demonstrates that H^2/Z_c is a true and reliable predictor of TBW in both normal and abnormal animals. Similarly H^2/R_0 is a true and reliable predictor of ECW in both normal and abnormal animals.

SECTION 9

CLINICAL APPLICATIONS

OF MFBIA.

§ 9   CLINICAL APPLICATIONS OF MFBIA

Lymphoedema, also called 'lymphostatic disorder', is characterised by excess protein and oedema in the tissues which leads to chronic inflammation and fibrosis, (Casley-Smith, 1985). Primary lymphoedema is rare. However, secondary lymphoedema is a common sequela of either radiotherapeutic or surgical treatment for different types of malignancy including breast, uterine, ovarian and prostatic carcinoma, (Casley-Smith *et al.*, 1989). It usually occurs in one limb and presents as an enlargement and distortion of the limb and usually accompanied by pain, recurrent infection, reduced mobility and impaired function.

Surgery or radiotherapy to the axillary or inguinal areas brings with it a substantial risk of producing lymphoedema of the arms or legs. This is brought about by coincident unavoidable and irreversible damage to the lymphatic channels. Whilst the true incidence of secondary lymphoedema is unknown the reported incidence of lymph stasis, for example after mastectomy varies from 25.5% to 38.3% depending on the type of surgery and whether or not the patient received radiotherapy, (Tobin *et al.*, 1993). Treatment of breast cancer alone therefore, given the incidence of the disease produces a large at-risk population.

§ 9.1   MONITORING THE TREATMENT OF LYMPHOEDEMA

Lymphoedema is an incurable, progressive, often disfiguring and disabling disorder, the course of which can, however, be arrested by intervention, preferably at the earliest opportunity. Complex physical therapy, a regimen of exercises, compression bandaging, massage and other physical techniques is reported to be effective in reducing limb volume, (Földi, 1985; Bunce *et al.*, 1994), and in improving the quality of life,

function and body image of patients, (Bunce *et al.*, 1991; Mirolo *et al.*, 1994).

Although lymphoedema has been thoroughly described in physiological and biochemical terms no published literature has been found describing a recognised sensitive, quantifiable and scalable measure of the severity of the condition or its response to therapy. At present, the best index appears to be an estimate of the excess size of the affected limb compared with the unaffected limb as measured either by circumferential measurements or immersion. Both methods have difficulties: circumferential measurements are time consuming (5 - 7 min) requiring five measurements to be made at precisely defined locations along the length of the limb, while immersion is messy and undignified. Both procedures measure total limb volume which may not reflect the actual hydrostasis of the limb. Indeed, in some individuals the disparity in limb size may be due simply to hand-use preference. This study investigated the application of MFBIA to the measurement of lymphoedema in the upper limb.

Patients and Methods

Patients were randomly chosen from those attending the Lymphoedema Management Program of The Wesley Clinic for Haematology and Oncology. All patients had developed at least grade two lymphoedema of the upper limb characterised by firm, non-pitting oedema, following surgery and/or radiotherapy for carcinoma of the breast (unilateral, either side). A group of volunteers from the clinic and university staff acted as the control group; all patients and controls were female. Clinical and anthropometric data are presented in table 9.1. The purpose of the study was fully explained to all participants and written consent obtained. The study was approved by the Human Ethics Committees of the Queensland University of Technology, the University of Queensland and the Wesley Hospital.

The program for the treatment of lymphoedema provided by the clinic aims at the self-management of the condition by the patient but begins with an intensive daily schedule that includes compression therapy, massage and compression bandaging for the first 4 weeks. During these 4 weeks the patient is educated in the self-management of their condition and encouraged to maintain the treatment. Quarterly clinical reviews are conducted to advise patients of their progress in the self-management of the condition.

This study involved the comparison of impedance measurements with the current technique of estimating limb lymphoedema. During this initial phase of the treatment the efficacy of the régime was monitored daily by measurement of the total limb volume and by appropriate MFBIA measurements.

TABLE 9.1

Clinical and anthropometric data of all participants.

Values expressed as median (range).

	Patients (n=20)	Controls (n=20)
Age (years)	60 (32-78)	40 (29-56)
Weight (kg)	81 (50-100)	64 (47-90)
Height (cm)	167 (153-180)	170 (156-180)
BMI[#] (kg m^{-2})	27.2 (19.5-38.1)	22.5 (18.1-29.7)
Oedematous limb (L/R)	13/7	—
Dominant limb (L/R)[*]	1/19	2/18

[#] Body Mass Index = body weight / height ^{2}
[*] As defined by the subject.

The method of determining the total limb volume was the established procedure using the measured circumference at fixed intervals along the limb. The accuracy and validity of this procedure has been reported by

Kaulesar Sukul *et al.*, (1993), as being equivalent to that of water displacement techniques. Circumferential measurements of the limb using a tape measure were recorded at 10 cm intervals from the pisiform prominence of the wrist up to a total distance of 40 cm. Volumes of each 10 cm segment of the limb were calculated using the average of two circumferential measures and assuming a simple cylindrical geometry. Limb volume was calculated as the sum of the volumes of the four individual segments.

Impedance measurements of each limb were recorded using the swept frequency bioimpedance meter (section §3.3) with the subject supine, limbs slightly abducted and palms flat on the couch. The two measurement electrodes were placed at either end of the 40 cm length over which the circumference measurements were made. The source electrodes were positioned 5 to 6 cm distal to the measurement electrodes. These electrode sites were chosen in preference to the standard shoulder to wrist sites, as described by Scheltinga, (1992), so that direct comparisons could be made between the volumes measured by the circumference method and by the MFBIA predictors.

Body water volumes of limbs or individual body segments cannot be determined by isotope dilution techniques and without any direct measure of TBW and ECW, algorithms for prediction using impedance of the limb do not exist. However by using the theoretical relationship between volume and impedance the ratios of the limb volumes are given by equations 9.1 and 9.2.

$$\frac{TBW_{affected\ limb}}{TBW_{unaffected\ limb}} = \frac{\rho \dfrac{L^2}{Z_c^*}}{\rho \dfrac{L^2}{Z_c}} = \frac{Z_c}{Z_c^*}$$

where * denotes the impedance of the affected limb
eqn (9.1)

$$\frac{ECW_{affected\ limb}}{ECW_{unaffected\ limb}} = \frac{\rho\ \dfrac{L^2}{R_0^*}}{\rho\ \dfrac{L^2}{R_0}} = \frac{R_0}{R_0^*}$$

where * denotes the impedance of the affected limb   eqn (9.2)

While the length of the limb is measured the resistivity, ρ, is unknown. Hence, absolute values of TBW and ECW of a single limb are not attainable and the increase in the affected limb volumes is expressed as a ratio of the unaffected limb. In the control group the ratio was calculated as dominant limb over non-dominant limb.

Results

As shown in table 9.1 both groups were somewhat similar in height, but the controls were younger and weighed less and subsequently had a lower body mass index (BMI). No attempt was made in this study to match controls to patients as both the circumferential and impedance measurements of increases in ECW were expressed as a ratio of the unaffected limb, *ie* each individual acted as their own control. The variation of daily impedance measurements on the same limb of the same control subject over the 4 week period was characterised by a standard deviation of 9Ω, corresponding to approximately 3% of the measured value. However when the ratio of the impedance of the limbs was calculated this variation was reduced to less than 1.5%.

The results of the impedance and volume measures of both controls and patients recorded on 'day one' of the study are represented in figure 9.1. A Mann-Whitney two-sample test for group comparisons was applied and no

significant asymmetry in circumferential estimates of volume was observed between the two limbs of individuals of the **control** group. However a small but significant asymmetry was detected in the impedance predicted values of the TBW and ECW ratios, (P<.01). A binomial test of the impedance quotients, L^2/Z_c and L^2/R_0, indicated that this asymmetry was significantly associated (P<.001) with handedness as ascribed by the subjects. Application of the Mann-Whitney test to the data of the **patient** group found the circumferential estimates of the volume of the lymphoedematous limb was significantly greater, (P<.005), than that of the contralateral, unaffected limb.
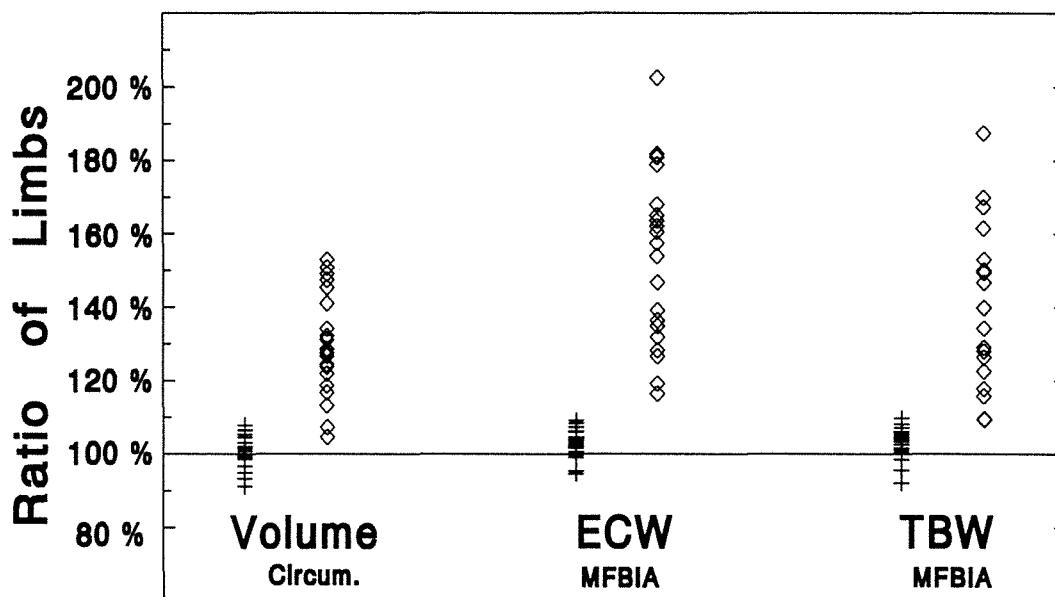
FIGURE 9.1

Comparison of MFBIA estimates and volume measurements for control

and patient groups. Values are the ratio of the two limbs,

(+ controls, {dominant / non-dominant}; ◊ patients, {affected / unaffected}).

As mentioned previously there is a small but significant association between ECW, (measured by MFBIA), and handedness which would

subsequently affect the population distribution of the ECW ratio. Using the data from the control group the 95% confidence interval, (dominant / non-dominant), was determined; -3.3% < ECW ratio < 10.5%. Applying this confidence interval to the patient group 19 out of the 20 would be classified as outside the 'normal' range of variation in the ECW ratio. Hence diagnosis of unilateral lymphoedema using MFBIA measurements should be possible with 95% confidence.

Obviously before this mode of diagnosis can be employed in a clinical situation a more extensive study, (with a far greater number of participants), needs to be undertaken to determine with greater precision the dominant limb confidence limits and also the validity of these confidence intervals to individuals with large differences in muscle mass between the limbs, (eg athletes who practise unilateral exercise; squash and tennis players, archers, etc).

The distribution of the TBW ratio is not markedly different from that of the ECW ratio, (figure 9.1), and appears to provide the same information. However, the volume of intra-cellular water (ICW), proposed as an accurate measure of fat-free mass, can be calculated by subtracting the ECW from the TBW volume, (equation 9.3). It should be noted that equation 9.3 assumes that the effective resistivity of ECW is the same as that of TBW. It is difficult to confirm this assumption, particularly in a body segment, and caution is needed in interpreting the absolute values of ICW obtained. However, the trends in the ICW ratio over the 4 week period provides valuable information about muscle mass changes during the treatment régime.

$$ICW \quad = \quad TBW - ECW \quad = \quad \frac{\rho L^2}{Z_c} - \frac{\rho L^2}{R_0}$$

$$\frac{ICW_{affected\ limb}}{ICW_{unaffected\ limb}} \quad = \quad \{ \frac{(R_0^* - Z_c^*)}{R_0^*\ Z_c^*} \quad * \quad \frac{R_0\ Z_c}{(R_0 - Z_c)} \}$$

eqn (9.3)

As described previously, impedance and circumferential measurements were recorded daily throughout the 4 week treatment régime of the patients and an equivalent period for the controls. The daily variation of the limb differences, (expressed as a ratio of the unaffected limb), in ECW, ICW and circumferential estimates of volume are shown in figure 9.2 for typical subjects from both the patient and control groups.
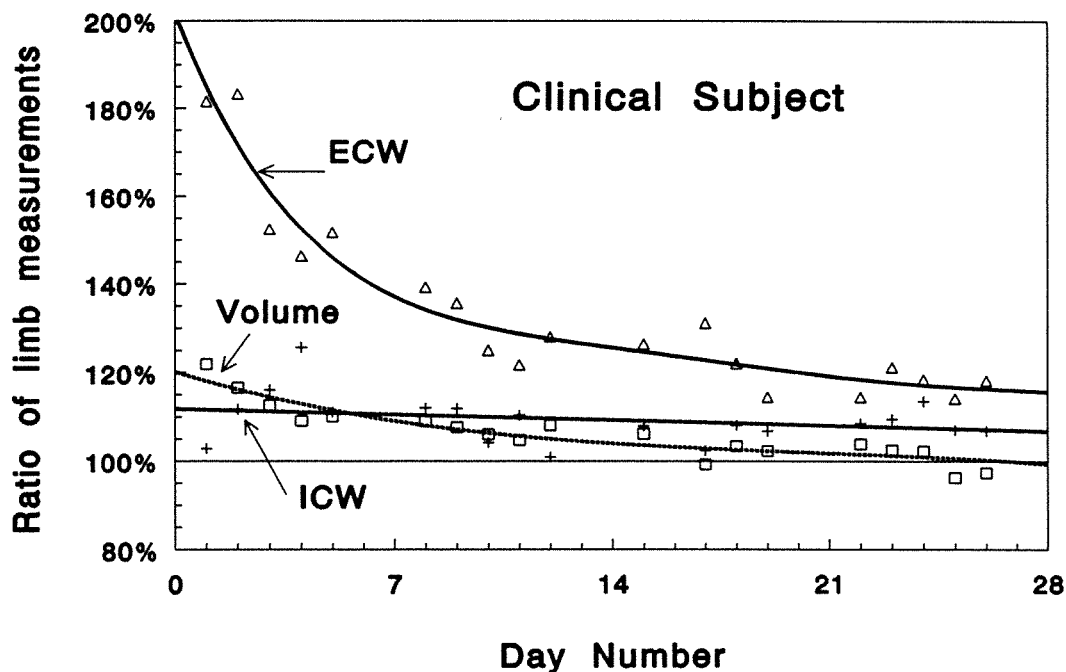
FIGURE 9.2a

Trends in the measured quantities for a typical patient during

the 4 week treatment period.   Δ = ECW ratio (by MFBIA);

+ = ICW ratio (by MFBIA);   □ = Volume ratio (by circumference).
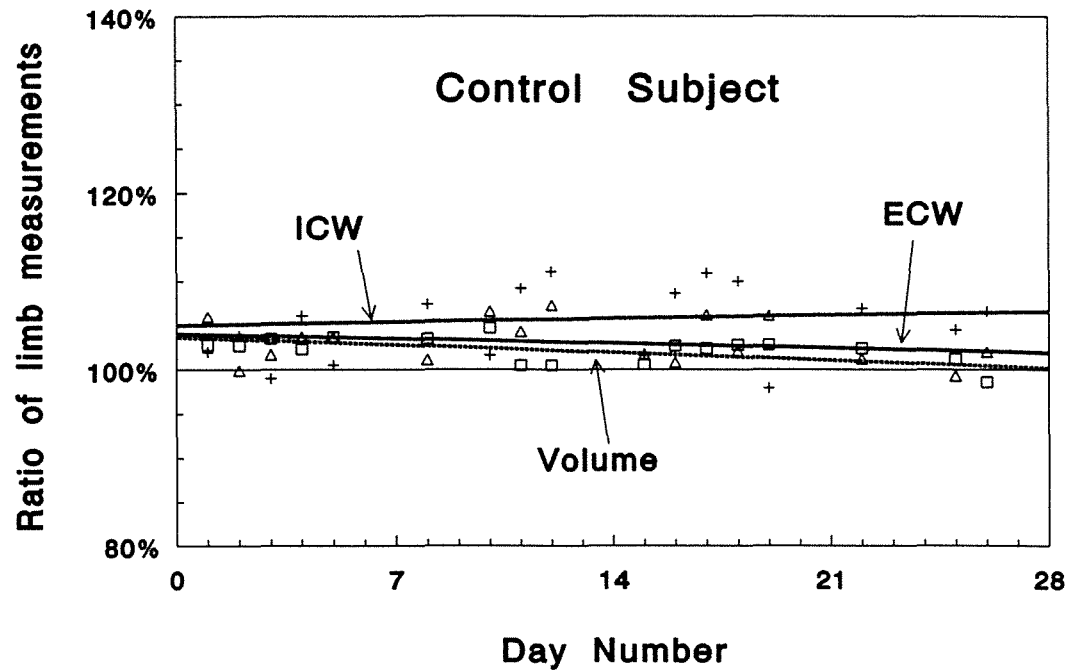
FIGURE 9.2b

Trends in the measured quantities for a typical control subject

during a 4 week period.   Δ = ECW ratio (by MFBIA);

+ = ICW ratio (by MFBIA);   □ = Volume ratio (by circumference).

The procedure of Bland and Altman, (1986), (see section §4.2) was used to analyse the agreement between the two relative measures of lymphoedema, (*viz* ECW ratio by MFBIA and volume by circumference measurements).   Table 9.2 shows the bias, (mean difference), and the standard error of the bias between the two measures at various stages throughout the 4 week program.

TABLE 9.2

Agreement between the MFBIA and circumferential measures

of lymphoedema at various stages; bias and standard error.

	Day no.	Bias	Std. Error
PATIENTS (n=20)	1	31%	± 33%
	2	31%	± 31%
	3	20%	± 23%
	5	14%	± 19%
	8	17%	± 20%
	10	17%	± 21%
	12	14%	± 16%
	15	16%	± 18%
	17	15%	± 12%
	19	16%	± 10%
	22	15%	± 14%
	24	13%	± 10%
	26	15%	± 12%
CONTROLS (n=20)		3.1%	± 4.6%

The reasonably close agreement between the two measures in the group of controls is indicated by a small bias, (3.1%), but more importantly a small standard error, (4.6%). Hence the limits of agreement, using a 95% confidence interval, in the control group are ±9%. However as shown in table 9.2 the standard error of the bias for the patient group is large at the beginning of the treatment program and decreases rapidly in the first week, and then more slowly in the following weeks, and appears to approach a steady value of approximately 10%. Comparing the trend illustrated in table

9.2 with the data represented in figures 9.2a and 9.2b it would appear that both measures of lymphoedema are in close agreement in controls and reasonable agreement in patients after several weeks of treatment. However in patients who have received little or no treatment the MFBIA estimates of ECW are quite different from the circumferential estimates of volume. Hence the differences in the two graphs shown in figure 9.2a are a result of the different techniques measuring variables representing two distinctly different quantities.

Figure 9.2a highlights several features, the first is that the amount of lymphoedema, as measured by both techniques, is substantially reduced during the 4 week treatment régime. The method of curvilinear regression analysis was applied to investigate the trends displayed by the loci shown in figure 9.2. An F-test, (described by Kerlinger and Pedhazur, 1973), was used to statistically determine the lowest order polynomial which best quantifies the trend observed. The trends displayed by the graphs in figure 9.2a are:- ECW- polynomial degree 5; Volume- polynomial degree 3; ICW-linear, (all at the P<.05 level or better). These significantly different trends demonstrate that the physiological quantities represented by the MFBIA and circumferential measurements are in fact different, and that the two measures are not simply scalar multiples of each other.

A second noticeable feature is that the ECW ratio, measured by MFBIA, closely follows the same directions as the locus of the Volume graph, but with magnitudes 2 to 3 times greater. Since both measures are a ratio of the unaffected limb this difference in magnitude cannot be to a scaling factor. The possible explanation is that MFBIA measurements of ECW have a greater sensitivity and are a more appropriate measure of lymph volume than the ratio of total volume by circumferential measurements.

A further noteworthy feature of figure 9.2a is that from day 16 through to completion the circumferential estimates of the volume ratio are very close to 100%, and in fact fluctuates above and below 100%. However the nursing staff were still able to identify the symptomatic characteristics of lymphoedema; viz:- a firm, non-pitting swelling. The MFBIA measure of the ECW ratio continued to detect the presence of lymphoedema, although decreasing in magnitude, up to day 26; hence demonstrating the greater sensitivity of MFBIA.

Figure 9.2b shows the daily variation in measured limb fluid volumes for a typical control subject. This graph displays the reasonably small variability of the circumference measurements, (mean ratio 102.2%; s.d. 1.5%) and the slightly greater variability in the ECW ratio values, (mean ratio 103.1%; s.d. 2.4%). However the daily variation in ECW incorporates not only that of the MFBIA technique but also the diurnal variation in water content, which has been shown to be significantly affected by physical activity and diet, (Kanai et al., 1987). The regression line of the ICW data has a relatively constant value, (105%). Given the data is expressed as a ratio of dominant / non-dominant limb, this result is not unexpected in an active young subject as handedness is usually associated with a greater muscle mass.

§9.2   ABSOLUTE QUANTIFICATION OF LYMPHOEDEMA VOLUME

As mentioned previously, independent absolute measures of body water volumes of an individual limb cannot be obtained by any in vivo method, (eg isotope dilution). Hence algorithms for the prediction of TBW or ECW using bioimpedance do not exist and cannot be obtained. However

research has been conducted on the resistivity of various body segments, Burger and van Milaan, (cited in Geddes and Baker, 1967), used an applied DC current with needle electrodes and a tetrapolar arrangement to measure human body resistivities. They found the average resistivity of the human arm in the longitudinal direction to be 230 Ωcm. As these measurements were conducted using DC they represent the resistivity of the extracellular fluid. Therefore the absolute value of ECW of the human arm can be calculated by equation 9.4.

$$ECW \ (mL) \quad = \quad 230 \ \frac{L^2}{R_0}$$

eqn (9.4)

Using this relationship, (with L=40 cm), the absolute value of the increased extracellular fluid was calculated using the MFBIA measurements of R_0. The variation of this absolute measure of lymphoedema during the course of treatment of a typical patient is shown in figure 9.3, (the patient whose data are represented in figure 9.3 is the same patient and measurements used to generate the graph in figure 9.2a). It is readily noticeable that the shape of the locus in figure 9.3 is identical to that of the ECW graph of figure 9.2a, the only difference is the scaling and the units of the y-axis. The reason being, the ECW ratio was a ratio of the affected to the unaffected limb, hence removing the effect of the resistivity from the ECW ratio, (equation 9.2). Therefore the only real difference between the two graphs is merely the units.
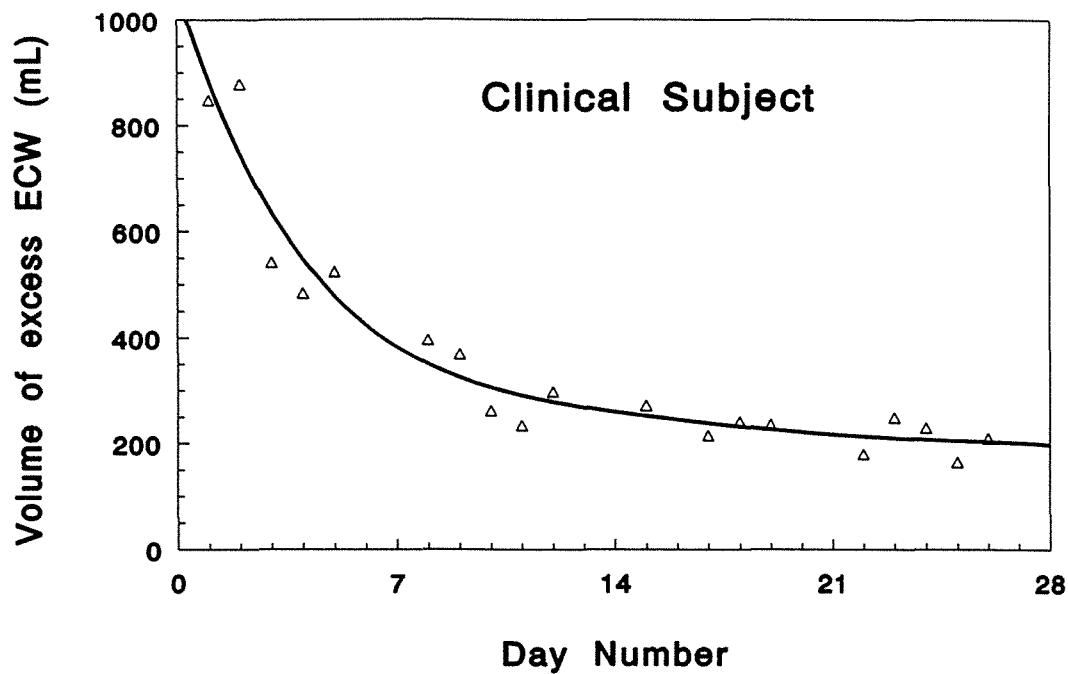
FIGURE 9.3

Daily variation in excess ECW volume, (for a typical patient),

expressed in absolute units.

While the volumes of lymphoedema calculated using a resistivity of 230 Ωcm appear reasonable there are a number of assumptions which need careful consideration. In normal healthy subjects the electrolyte concentrations of all body fluids and tissues is very well regulated and maintained within a very small range of the mean normal value. However this may not be the case in the lymph fluid of a patient with lymphoedema. Apart from the increased protein concentration little is known about the variation of composition of lymph fluid in these subjects, and very little if anything is known about the variation in lymph composition between patients. The validity of applying the value of resistivity obtained from normal healthy subjects to a group of patients with acute and/or chronic lymphoedema is therefore of some concern.

If one assumes that the circumferential measurements are an accurate and precise means of determining limb volume and that the difference in total limb volume is equal to the volume of lymphoedema, then equation 9.2 can be rearranged to enable the determination of the resistivity, (equation 9.5).

$$\rho \;=\; \frac{\Delta \; Volume}{L^2 \; \{ \dfrac{1}{R_0^*} - \dfrac{1}{R_0} \}}$$

where ΔVolume = the difference in limb volumes as   eqn (9.5)

determined by circumferential measurements.

While equation 9.5 is theoretically correct it becomes ill-conditioned when the difference in R_0's approaches zero. Hence it can only be applied to patients with a considerable amount of lymphoedema. Equation 9.5 was applied to the 'day 1' data of the patient group to estimate the resistivity of lymph fluid.

mean ρ = 244 Ωcm   s.d. = 133 Ωcm   range = 100 to 490 Ωcm

Although these results rely on the accuracy and precision of the circumferential measurements, (coefficient of variation 1.5%), they indicate that the average resistivity of lymph fluid is similar to that of other extracellular fluids. However the variation of resistivity between lymphoedema patients is extremely great and consequently no fixed value can be applied to obtain an absolute value of lymphoedema measured in litres.

§ 9.3   SUMMARY

The MFBIA procedure of determining the resistance at zero frequency, R_0, of each limb and hence the percentage increase in ECW of the affected limb has been shown to be a more sensitive measure of lymphoedema than total volume. ECW occupies approximately 25% of the total body, (section §8.1). A 40% increase in ECW of a body segment therefore would lead to only a 10% increase in the total volume. It is obvious that a technique which measures actual ECW will have greater sensitivity and precision in detecting this increase than one which measures total segment volume. Another advantage of MFBIA is that a measure of ICW which is very closely correlated with muscle mass can be obtained. While the precision of this measure is less than that of the ECW measurement, its trend over the four week period of treatment gives the clinician valuable information which may reflect changes in mobility and exercise of the limb.

To date, awareness amongst clinicians of the incidence and severity of lymphoedema has been persistently clouded by the lack of simple qualitative and quantitative measures of extra-cellular fluid accumulation. As demonstrated measures of ECW by bioimpedance were superior to estimates from total limb volumes in monitoring efficacy of the 4 week treatment program of patients with unilateral lymphoedema. MFBIA provides for the first time a quick (1 -2 min), relatively inexpensive, non-invasive, quantitative and causally-related measure of fluid accumulation and thus represents an advance in the assessment of lymphoedema.

SECTION   10

CONCLUSION.

§ 10 CONCLUSION

The concept of using impedance to examine biological systems was investigated as early as 1928 by Cole with his studies on the impedance of cell suspensions. In 1943 Nyboer *et al* demonstrated that biological volumes were inversely related to impedance. This was further investigated and confirmed by Thomasset, (1962), who used a bipolar, needle electrode arrangement to study total body water volume in human volunteers. Hoffer *et al.*, (1969), established the tetrapolar electrode arrangement which allowed body impedance to be measured using skin surface electrodes. This made bioelectrical impedance analysis, BIA, a truly noninvasive, *in vivo* method of body composition analysis, after which many research groups devoted considerable effort to its development.

Research in the latter part of the 1970's and the 1980's established BIA measurements at a frequency of 50 kHz as being an accurate and reliable predictor of total body water, (TBW). The precision with which TBW could be estimated by BIA at 50 kHz depended on what other anthropometric parameters were included in the prediction equation, (*eg* sex, weight, age, stage of menstrual cycle, *etc*). From the latter part of the 1980's to date a number of research groups have examined impedance measurements recorded at a variety of frequencies and investigated their success at predicting TBW and also extracellular water, (ECW). Similarly, the precision obtained depended on the number of anthropometric parameters included. Some researchers have recently focused on determining the optimum frequencies for predicting TBW and ECW, but in all studies the only estimates considered were those calculated from measurements at a single frequency. A variety of frequencies have been suggested in the literature as being the optimum for predicting TBW or ECW, but all have been based purely on an empirical relationship derived from a group of

subjects limited in both number and variation.

In this study a swept frequency bioimpedance meter was developed; this instrument measures and records the impedance and phase using a tetrapolar electrode arrangement at 496 frequencies ranging from 4 kHz to 1 MHz. Rather than selecting particular frequencies from which to predict body water volumes the entire spectrum of measurements was analysed to establish the impedance locus as a function of frequency. This was identified as a Cole-Cole plot and its circular shape allowed the accurate determination of the impedance at maximum reactance, Z_c (occurring at the characteristic frequency), as well as the resistance at zero frequency, R_0. The theoretical basis for investigating these frequencies was:-

(i)   at Z_c the **ratio** of the currents passing through the intra- and extra-cellular pathways is independent of the cell membrane capacitance and due solely to the resistance of the intra- and extra-cellular fluids;

(ii)   at R_0 all of the current passes through the extracellular fluid, hence the resistance is due to the ECW only.

Studies on normal healthy animals in which TBW and ECW were measured by the gold standard of isotope dilution were used to establish the relationship between body water volumes and the results of the multiple frequency bioelectrical impedance analysis, (MFBIA). The association between body water volumes and a range of individual frequency measurements, (eg the resistance at 50 kHz, R_{50}, and the impedance at 5 and 1 kHz, Z_5 Z_1), as well as several MFBIA results were tested for statistical significance. The prediction variables with the greatest precision were L^2/Z_c and L^2/R_0 for TBW and ECW respectively. These prediction quotients yielded standard errors of the estimate of 4.2% and 3.2% respectively, which were both significantly better than any reported prediction quotient derived

from a single frequency in this group of animals.

One of the greatest points of contention in the use of bioimpedance to determine body composition is whether the algorithms developed in a group of healthy subjects are applicable to subjects in altered states of health. Isotope dilution methods were used to determine body water volumes in a sample of rats which had been deprived of water for 40 hours. Their resulting TBW and ECW were significantly lower than normal and they were obviously in a state of dehydration. The bioimpedance of these rats were measured and the MFBIA quotients, L^2/Z_c and L^2/R_0, determined. The prediction equations established from the group of normal rats was found to accurately predict both TBW and ECW in this group of dehydrated rats.

A second sample of rats with abnormal fluid levels was created by the progressive injection of normal saline into the upper peritoneal cavity. Bioimpedance measurements were recorded at each stage of the injection process and the MFBIA prediction quotients calculated. Using the prediction equations established in normal healthy rats the increases in TBW and ECW were calculated. The agreement between the known volumes injected and the calculated increases in both TBW and ECW were extremely high, (SEE = 0.9 mL); the plot of calculated increases vs known volumes yielded a regression line very close to the line of identity. This again demonstrates that using the MFBIA technique and the prediction quotients L^2/Z_c and L^2/R_0, TBW and ECW can be accurately measured irrespective of the extra- to intra-cellular fluid balance.

The application of MFBIA in humans was investigated using a sample of 60 volunteers, (male and female). The volumes of TBW and ECW were determined by isotope dilution methods using non-toxic and non-radioactive tracers. Whole body impedance, (wrist to ankle), was measured using the

swept frequency bioimpedance meter and several single frequency prediction quotients, (H^2/R_{50} and H^2/Z_5), were determined as well as the MFBIA quotients, (H^2/Z_c and H^2/R_0). Results of the study showed that H^2/Z_c and H^2/R_0 were the best predictors of TBW and ECW respectively, but only at the P<0.2 level of significance. This minor difference in significance is partly due to the sample group being comprised of all normal healthy subjects with only a moderate variation in anthropometric parameters such as age, weight and height. In such a group one expects a high correlation between TBW, ECW and many other body composition components. The correlations obtained between the MFBIA predictors and body water volumes were similar to that recently reported by others.

The inclusion of other anthropometric parameters in the prediction equations were tested and it was found that the inclusion of body weight, (for both TBW and ECW), and sex, (for ECW only), resulted in a slight improvement in the correlation (P<.05). Several statistical tests were performed to determine if there was any difference in the resulting prediction equations for males and females. No sex difference was found in the equations for TBW but a slight difference, (.04<P<.05), was detected in the prediction of ECW.

The potential of using the MFBIA technique to monitor the efficacy of the treatment of lymphoedema was investigated. Twenty patients with unilateral lymphoedema of the upper limb following surgery and/or radiotherapy for carcinoma of the breast were monitored daily throughout their four week treatment program. The amount of lymphoedema was estimated by the volume difference between the limbs of a patient as calculated by circumferential measurements. The bioimpedance of each limb was measured daily and from the MFBIA predictors the excess ECW and TBW of the lymphoedematous limb was calculated as a ratio of the

unaffected limb. An identical procedure for 4 weeks was conducted on a group of 20 healthy volunteers who acted as a control group.

The MFBIA technique yielded significantly larger estimates of the percentage difference between the two limbs of any given patient, particularly during the first two weeks of treatment. The extracellular fluid of an adult occupies slightly less than 20% of the total volume, therefore a method which measures ECW directly will be more sensitive in detecting changes in the ECW volume than a method which attempts to detect these changes by measuring the total volume. Hence it was shown that the larger estimates, by MFBIA, of the amount of lymphoedema was due to its greater sensitivity in measuring ECW. This greater sensitivity suggests that MFBIA would be an effective and reliable procedure to assist in the diagnosis and early detection of lymphoedema. Early detection of the condition would be a major factor in its management and accordingly is under further investigation.

Assuming the volume estimates from the circumferential measurements to be accurate and precise, estimates of the resistivity of ECW were calculated and compared with published values of extracellular fluid. While the mean value obtained compared closely with the published value, (244 cf 230 Ωcm), the variation of the 'measured' resistivity of ECW between patients was extremely large, (coefficient of variation 55%). However this variation in electrical conductance was minimised in this study by expressing the difference between limbs as a ratio of the unaffected limb for each patient. The effect, of variations in ion concentration, on the resistivity of body fluids warrants further investigation.

A further advantage demonstrated by MFBIA was the capacity to estimate intracellular water (ICW), the difference between TBW and ECW.

Intracellular water is known to be highly correlated with fat-free mass (muscle mass). In practice the most debilitating feature of lymphoedema of the limb is the decrease in mobility and function of the limb which can cause a dramatic decrease in quality of life. The information provided by the MFBIA procedure includes trends in ICW volumes over the 4 week treatment period and the clinician is able to detect changes in the amount of muscle mass which details physiological information on mobility and function which is otherwise unobtainable.

The purpose of this study was to investigate MFBIA as a method of measuring body composition. It has been shown that MFBIA can be used as a reliable and accurate predictor of TBW and ECW in individuals in virtually any state of health. However while a strong association has been shown further research needs to be conducted using much larger sample sizes, with a greater range of subject ages, to determine the precise relationship between body water volumes and impedance quotients as accurately as possible.

One important condition assumed by all current applications of bioimpedance is the presumed constant electrolyte concentration of body fluids. While there is a considerable amount of research in the literature to confirm the minimal variation of specific ion concentrations, even in subjects of extreme ill-health, very little research has been conducted to investigate the effects of this variation on the impedance of body fluids. Variations in the major ion concentrations may have a significant effect on the resistivity of different body fluids. Inclusion of this variation in the prediction of TBW and ECW may enhance the accuracy and precision of the technique and further research in this area is recommended.

The need, usefulness and importance of accurate and precise *in vivo* body composition analysis is paramount in the minds of clinicians who

monitor and supervise the progress of critically ill neonates, burns patients, acute anorexic patients and others in which the fluid balances are critical. This need is characterised by the volume and diversity of research that has been published over the past 15 years. There are numerous methods for predicting body composition and all have their relative merits. Bioelectrical impedance was hailed in the 1970's as the method with greatest promise; it was non-invasive, inexpensive and yielded reproducible and accurate estimates of TBW. However TBW alone did not provide sufficient information in clinical situations and subsequent research, (late 1980's & 1990's), using BIA was able to estimate ECW as well as TBW, (in normal subjects). However the application of these techniques to patients in widely varying states of health were not validated.

This dissertation details the development of an entirely new approach to the measurement and analysis of bioimpedance data using impedance and phase measurements recorded at multiple frequencies between 4 kHz and 1 MHz. The concept of Multiple Frequency Bioelectrical Impedance Analysis (MFBIA) described herein is a **true** multiple frequency approach in that it recognises, uses and combines measurements, over a large range of frequencies, using standard regression procedures to arrive at the biological impedance at the appropriate frequencies. The prediction quotients used were selected using a theoretical basis: the criteria for this basis being ratified by the resulting correlations and standard errors. By analysing the frequency response of electrical circuits used to model biological systems the resistance to current flow of the two components of the body's conducting pathways, (ICW and ECW), can be determined. Using the simple relationship between the resistance and volume of a conductor, ECW and TBW volumes were calculated. The resulting estimates of ECW and TBW from MFBIA were shown to be accurate and precise in normal healthy humans and animals, and in animals with altered fluid balances.

Bioimpedance is a characteristic of all body tissues which conveys information directly determined by their hydration status. Many physiological states affect the hydration status; hence the balance of fluids in the extra- and intra-cellular compartments act as a diagnostic 'flag' for the body. The distribution of body water volumes is therefore of critical importance and needs to be evaluated with assured precision and accuracy. The technique of MFBIA has shown that this can be achieved with a high degree of accuracy and precision using a technique that is highly reproducible, non-invasive, causing little inconvenience for the subject and able to be operated by unskilled technicians. Therefore it would appear that MFBIA provides the best method of estimating ECW and TBW irrespective of the state of health of the individual.

APPENDIX A

COMPUTER CODE FOR THE ANALYSIS OF DATA FROM THE SWEPT FREQUENCY BIO-IMPEDANCE METER.

APPENDIX A

Copy of the computer code for the analysis of data from the Swept frequency bioimpedance meter (SFBIM). The program was written in *Quick Basic* and an executable (EXE) file generated for normal use. The section of code presented here is details the conversion of the impedance and phase indicies to impedance and phase values, (in ohm and degrees respectively), and the regression analysis to determine the impedance at the characteristic and zero frequencies.

```
'THIS PROGRAM CONVERTS SFBIM DATA TO IMPEDANCE, REACTANCE AND PHASE VALUES

DIM d(10, 3)
DIM C(496, 12, 2) AS INTEGER
DIM CR(2, 12)
DIM f(496, 6)
DIM fillst$(5)
DIM R50KHz(20)
DIM R50AV(5), R5AV(5), R100AV(5)


'   **** READING DATA   ****
OPEN path$ + "\" + dataxx$ FOR INPUT AS #1
'               eliminate and display the text header of the SFBIM log
LINE INPUT #1, head1$
LINE INPUT #1, head2$
DELTA% = VAL(MID$(head2$, 42, 3))
loglen% = 496 / DELTA%
cal$ = "CAL" + MID$(head2$, 31, 2) + MID$(head2$, 47, 1) + ".TXT"
'               input data file from SFBIM log
REDIM d(loglen%, 3)
FOR i = 1 TO loglen%
FOR j = 1 TO 3
        INPUT #1, d(i, j)
        IF d(i, 1) < ufl% THEN ufl1% = loglen% - i - 1
        IF d(i, j) >= 900000 THEN GOTO EX
      NEXT j
   NEXT i
EX:
CLOSE #1


'                 input the calibration matrix
where$ = "DRN "
OPEN cal$ FOR INPUT AS #2
where$ = "DRN " + path$
INPUT #2, phasang%
FOR K = 1 TO 2
FOR i = 1 TO 496
FOR j = 1 TO 12
```

```
        INPUT #2, C(i, j, K)
        NEXT j
      NEXT i
    NEXT K
  CLOSE #2
  '                    set the values of the calibration resistors
  IF MID$(head2$, 47, 1) = "5" THEN
  '                high current calibration resistors
    CR(1, 2) = 2.2
    CR(1, 3) = 3.9
    CR(1, 4) = 6.8
    CR(1, 5) = 10
    CR(1, 6) = 18
    CR(1, 7) = 33
    CR(1, 8) = 56
    CR(1, 9) = 100
    CR(1, 10) = 150
    CR(1, 11) = 250
    CR(1, 12) = 400
  ELSE
  '              low current calibration resistors
    CR(1, 2) = 10
    CR(1, 3) = 18
    CR(1, 4) = 30
    CR(1, 5) = 52
    CR(1, 6) = 91
    CR(1, 7) = 159
    CR(1, 8) = 270
    CR(1, 9) = 470
    CR(1, 10) = 740
    CR(1, 11) = 1210
    CR(1, 12) = 1940


    END IF
  '                    find the row in the calibration matrix which is closest
  '                    to 50 kHz and store the row NUMBER in C(1,1).
  FOR i = 1 TO 496
  IF C(i, 1, 1) > 50 THEN
  IF (C(i, 1, 1) - 50) > (50 - C((i - 1), 1, 1)) THEN
          CR(1, 1) = i - 1
          ELSE CR(1, 1) = i
          END IF
        GOTO PH
        END IF
    NEXT i
  '                    find the "measured R" at 50 kHz of each cal resistor
  '                    and store this in CR(2,2-12). ie rows 2-12 of CR has
  '                    (true value, measured value) of each cal resistor.
  PH:
   CR(2, 1) = C((CR(1, 1)), 1, 1)
   FOR j = 2 TO 12
     CR(2, j) = C((CR(1, 1)), j, 1)
     NEXT j
  '                    by interpolation through the calibration matrix
  '                    convert measured data into "real" data (in ohms etc).
```

```
'initialise sigma totals
SIGR = 0
SIGX = 0
SIGZ = 0
SIGRX = 0
SIGZR = 0
SIGZX = 0
SIGR2 = 0
SIGX2 = 0
SIGZ2 = 0
NR = 0
FOR i = 1 TO loglen%
    ii = (i - 1) * DELTA% + 1
FOR j = 3 TO 12
IF d(i, 2) < C(ii, j, 1) THEN
            RR = (d(i, 2) - C(ii, (j - 1), 1)) / (C(ii, j, 1) - C(ii, (j - 1), 1))
            '               RR is the interpolation ratio
            f(i, 1) = d(i, 1)
            '               F(I,1) is the frequency
f(i, 2) = EXP((LOG(CR(1, j)) - LOG(CR(1, j - 1))) * RR + LOG(CR(1, j - 1)))
            '               F(I,2) is the impedance in ohms
            ZEF = RR * (C(ii, j, 2) - C(ii, (j - 1), 2)) + C(ii, (j - 1), 2)
            '               ZEF is the phase zero at the given frequency
            f(i, 3) = 10 * (d(i, 3) - ZEF) / (phasang% - C((CR(1, 1)), 9, 2))
            '               phasang% is the measured phase for 10 degrees & Z=470 (or Z=100 Hi current)
            '               C((CR(1,1)),9,2) is the phase zero at 50 kHz for Z=470 (Z=100 Hi current)
            f(i, 4) = f(i, 2) * (COS(.0174533 * f(i, 3)))
            f(i, 5) = f(i, 2) * (SIN(.0174533 * f(i, 3)))
            '               F(I,4) & F(I,5) is the resistance and reactance
            f(i, 6) = 1


            '       calculate SIGMA values needed for regression
IF f(i, 3) > 0 AND f(i, 1) >= LFL% AND i < loglen% - ufl1% THEN
            SIGZ = SIGZ + f(i, 2) ^ 2
            SIGR = SIGR + f(i, 4)
            SIGR2 = SIGR2 + f(i, 4) ^ 2
            SIGX = SIGX + f(i, 5)
            SIGX2 = SIGX2 + f(i, 5) ^ 2
            SIGRX = SIGRX + f(i, 4) * f(i, 5)
            SIGZR = SIGZR + f(i, 2) ^ 2 * f(i, 4)
            SIGZX = SIGZX + f(i, 2) ^ 2 * f(i, 5)
            SIGZ2 = SIGZ2 + f(i, 2) ^ 4
            NR = NR + 1
            END IF
        GOTO S2
        END IF
    NEXT j
S2:
    NEXT i
loglen% = loglen% - ufl1%
'   perform regression analysis to calculate R0, etc.
cenx = (SIGR * SIGX - NR * SIGRX) * (SIGRX * SIGR - SIGX * SIGR2) - (SIGX * SIGRX - SIGX2 *
SIGR) * (NR * SIGR2 - SIGR ^ 2)
cenx = ((SIGZX * SIGR - SIGZR * SIGX) * (NR * SIGR2 - SIGR ^ 2) - (NR * SIGZR - SIGZ * SIGR) *
(SIGRX * SIGR - SIGX * SIGR2)) / cenx
```

```
cenr = (cenx * (SIGR * SIGX - NR * SIGRX) + (NR * SIGZR - SIGZ * SIGR)) / (NR * SIGR2 - SIGR ^ 2)
A0 = (SIGZ - cenr * SIGR - cenx * SIGX) / NR
cenx = cenx / 2
cenr = cenr / 2
RAD = (cenr ^ 2 + cenx ^ 2 + A0) ^ .5
ZC = ((RAD + cenx) ^ 2 + cenr ^ 2) ^ .5
FOR i = 1 TO loglen% + ufl1%
IF f(i, 1) < LFL% THEN
        fl = i
        f(i, 6) = 444
        END IF
    IF i >= loglen% THEN
    f(i, 6) = 444
    IF ufl% = 1012 THEN f(loglen%, 6) = 0
    ELSE
    END IF
    NEXT i
est:
 SIGE = 0
 SIGE2 = 0
FOR i = fl TO loglen%
        T = ((f(i, 4) - cenr) ^ 2 + (f(i, 5) - cenx) ^ 2) ^ .5
        SIGE = SIGE + (T - RAD)
        SIGE2 = SIGE2 + (T - RAD) ^ 2
    NEXT i
SEE = ((SIGE2 / NR + (SIGE / NR) ^ 2) ^ .5) * 100 / RAD
 ' RE-DO  THE  REGRESSION  IGNORING  DATA  POINTS
 ' OUTSIDE  THE  DEFINED  ACCEPTABLE  LIMITS  OF
 ' DEVIATION  FROM  THE  FIRST  APPROXIMATION  TO
 ' THE   COLE - COLE   PLOT
 ' THE  LIMIT  IS  SELECTED  BY  NOMINATING  THE  REJECTION  LEVEL
 ' WHICH  DETERMINES  THE  REJECTION  FACTOR   -   eg  0.05
 ' ( ie  only data points within 5% of the estimated radial
 '   distance from the estimated centre are used in the regression.)
 IF rl% = 0 GOTO cont:
 '********  beginning  of  iterative  cycle
FOR CY = rl% TO 1 STEP -1
SELECT CASE CY
        CASE rl%
        RF = .1
        CASE (rl% - 1)
        RF = .05
        CASE (rl% - 2)
        RF = .02
        END SELECT
        'initialise  sigma  totals
        SIGR = 0
        SIGX = 0
        SIGZ = 0
        SIGRX = 0
        SIGZR = 0
        SIGZX = 0
        SIGR2 = 0
        SIGX2 = 0
        SIGZ2 = 0
```

```
        SIGE = 0
        SIGE2 = 0
        NR = 0
FOR i = fl TO loglen%
        f(i, 6) = 999
        T = ((f(i, 4) - cenr) ^ 2 + (f(i, 5) - cenx) ^ 2) ^ .5
        TR = ABS(T - RAD) / RAD
IF f(i, 3) > 0 AND TR < RF THEN
        SIGZ = SIGZ + f(i, 2) ^ 2
        SIGR = SIGR + f(i, 4)
        SIGR2 = SIGR2 + f(i, 4) ^ 2
        SIGX = SIGX + f(i, 5)
        SIGX2 = SIGX2 + f(i, 5) ^ 2
        SIGRX = SIGRX + f(i, 4) * f(i, 5)
        SIGZR = SIGZR + f(i, 2) ^ 2 * f(i, 4)
        SIGZX = SIGZX + f(i, 2) ^ 2 * f(i, 5)
        SIGZ2 = SIGZ2 + f(i, 2) ^ 4
        SIGE = SIGE + (T - RAD)
        SIGE2 = SIGE2 + (T - RAD) ^ 2
IF CY = 1 THEN
        f(i, 6) = 1
        END IF
        NR = NR + 1
        END IF
    NEXT i
    NRR = loglen% - NR - fl + 1
    '    perform  regression  analysis to calculate  R0, etc.
    cenx = (SIGR * SIGX - NR * SIGRX) * (SIGRX * SIGR - SIGX * SIGR2) - (SIGX * SIGRX - SIGX2 *
SIGR) * (NR * SIGR2 - SIGR ^ 2)
    cenx = ((SIGZX * SIGR - SIGZR * SIGX) * (NR * SIGR2 - SIGR ^ 2) - (NR * SIGZR - SIGZ * SIGR)
* (SIGRX * SIGR - SIGX * SIGR2)) / cenx
    cenr = (cenx * (SIGR * SIGX - NR * SIGRX) + (NR * SIGZR - SIGZ * SIGR)) / (NR * SIGR2 - SIGR ^
2)
    A0 = (SIGZ - cenr * SIGR - cenx * SIGX) / NR
    cenx = cenx / 2
    cenr = cenr / 2
    RAD = (cenr ^ 2 + cenx ^ 2 + A0) ^ .5
    SEE = ((SIGE2 / NR + (SIGE / NR) ^ 2) ^ .5) * 100 / RAD
    NEXT CY
    '*********  end  of  cycle
cont:
ZC = ((RAD + cenx) ^ 2 + cenr ^ 2) ^ .5
R0 = 0
RINF = 0
fc = 0
IF RAD > cenx THEN
    R0 = cenr + (cenr ^ 2 + A0) ^ .5
    RINF = cenr - (cenr ^ 2 + A0) ^ .5
    END IF
IF cenx <= 10 THEN
    '            perform regression analysis to calculate Fc
    SIGX = 0
    SIGY = 0
    SIGX2 = 0
    SIGXY = 0
```

```
      NR = 0
      IF rl% = 0 THEN RF = 1
      FOR i = fl TO loglen%
          TR = ((f(i, 4) - cenr) ^ 2 + (f(i, 5) - cenx) ^ 2) ^ .5
          TR = ABS(TR - RAD) / RAD
IF f(i, 3) > 0 AND TR < RF THEN
              LUV = LOG((((RINF - f(i, 4)) ^ 2 + f(i, 5) ^ 2) ^ .5) / (((R0 - f(i, 4)) ^ 2 + f(i, 5) ^ 2) ^ .5))
              LF = LOG(f(i, 1))
              SIGX = SIGX + LF
              SIGY = SIGY + LUV
              SIGX2 = SIGX2 + LF ^ 2
              SIGXY = SIGXY + LUV * LF
              NR = NR + 1
          END IF
        NEXT i


      fc = (SIGX / NR) - (SIGY / NR) * (SIGX2 - NR * (SIGX / NR) ^ 2) / (SIGXY - NR * (SIGX / NR) *
(SIGY / NR))
       fc = EXP(fc)
      END IF
IF MID$(dataxx$, 1, 5) <> "CALIB" THEN
 Capc = 100000 / ((RAD + cenx) * 2 * 3.14 * fc)
 ELSE
 END IF
 stdfrq% = 50
 GOSUB frqpick
FOR i = 1 TO 4
    R50AV(i) = AV(i)
    NEXT
 stdfrq% = 5
 GOSUB frqpick
FOR i = 1 TO 4
    R5AV(i) = AV(i)
    NEXT
 stdfrq% = 100
 GOSUB frqpick
FOR i = 1 TO 4
    R100AV(i) = AV(i)
    NEXT
dataprint:
      '                    write the data file
 OPEN path$ + "\" + outnm$ FOR OUTPUT AS #3
 form$ = "#####.##    #####.##    #####.##    #####.##    #####.##    \       \"
FOR i = 1 TO loglen% + ufl1%
    PRINT #3, USING form$; f(i, 1); f(i, 2); f(i, 3); f(i, 4); f(i, 5); code$
    NEXT i
    CLOSE #3
    ELSE
    END IF
IF pq$ = "y" OR pq$ = "Y" THEN
    OPEN "lpt1:" FOR OUTPUT AS #3
    GOSUB PRINTXT
    PRINT #3,
    PRINT #3, "                       Full data set"
    HEADER$ = "Frequency      Z        Theta      Resistance    Reactance"
```

```
        PRINT #3, HEADER$
        PRINT #3,
FOR i = 1 TO loglen% + ufl1%
            PRINT #3, USING form$; f(i, 1); f(i, 2); f(i, 3); f(i, 4); f(i, 5); code$
        NEXT i
PRINT #3,
PRINT #3, "CENTRE:              "; cenr; cenx; " ohms"
PRINT #3, "RADIUS:              "; RAD; " ohms"
IF R0 <> 0 THEN
        PRINT #3, "R zero:              "; R0; " ohms"
        ELSE PRINT #3, "R zero:   "; " ohms"
        END IF
PRINT #3, "Z 50:                "; R50AV(1); " ohms"
PRINT #3, "R 50:                "; R50AV(3); " ohms"
PRINT #3, "Phase 50:            "; R50AV(2); " deg"
PRINT #3, "Xc 50:               "; R50AV(4); " ohms"
PRINT #3, "Z 5:                 "; R5AV(1); " ohms"
PRINT #3, "R 5:                 "; R5AV(3); " ohms"
PRINT #3, "Phase 5:             "; R5AV(2); " deg"
PRINT #3, "Xc 5:                "; R5AV(4); " ohms"
PRINT #3, "Z 100:               "; R100AV(1); " ohms"
PRINT #3, "R 100:               "; R100AV(3); " ohms"
PRINT #3, "Phase 100:           "; R100AV(2); " deg"
PRINT #3, "Xc 100:              "; R100AV(4); " ohms"
IF R0 <> 0 THEN
        PRINT #3, "R infinite:          "; RINF; " ohms"
        ELSE PRINT #3, "R infinite: "; " ohms"
        END IF
PRINT #3, "Z characteristic:    "; ZC; " ohms"
IF R0 <> 0 THEN
        PRINT #3, "F characteristic:    "; fc; " kHz"
        PRINT #3, "Mean cell capacitance    "; Capc; " nF"
        ELSE
        PRINT #3, "F characteristic:    "; " kHz"
        END IF
PRINT #3, "SEE  of the  RADIUS     "; SEE;
PRINT #3, "%"
PRINT #3, "Lower Frequency Limit    "; LFL%; "kHz"
PRINT #3, "Upper Frequency Limit    "; ufl%; "kHz"
PRINT #3, "data rejected: "; NRR; " out of "; loglen% - fl + 1; "       rejection factor    "; rej%; " %"
PRINT #3,                          .
PRINT #3, "Input data file name:    "; dataxx$
PRINT #3, "Output data file name:   "; outnm$
PRINT #3, "File analysis date:      "; DATE$
PRINT #3, "Phase angle calibration: "; phasang%
PRINT #3, "Calibration file used:   "; cal$
PRINT #3, "Input file headers:      "; head1$
PRINT #3, "                         "; head2$
        CLOSE #3
        ELSE
        END IF
END
```

APPENDIX B

A TYPICAL OUTPUT FILE AND ASSOCIATED GRAPHICS FROM THE MFBIA ANALYSIS PROGRAM.

APPENDIX B

A typical output file detailing frequency, impedance, phase resistance, reactance and a code indicating how the data point was treated by the analysis. As explained in section §3 lower and upper limits can be imposed on the frequency range for the purpose of regression; data points outside this range are ignored and indicated by I. Data within the selected frequency range but not within a given percentage of the radius from the centre are also excluded from the regression and are indicated by a code R. The rejection factor in this analysis was ±2%. Other data are coded as OK. Below this listing is a printout of the values of all quantitative aspects of the circular locus including the standard error of the estimate of the radius, a measure of the 'goodness of fit' of the circular locus. Also included are the resistance, reactance and impedance values at various frequencies commonly used in BIA prediction. The analysis program also displays a plot of resistance and reactance *vs* frequency and the Cole-Cole plot. The figures shown below are screen captures of these displays.

f (kHz)	R (Ω)	ϕ (°)	R (Ω)	R (Ω)	Code
4.00	326.42	4.12	325.58	23.46	I
4.04	325.34	4.45	324.36	25.27	I
4.09	325.34	4.30	324.42	24.41	I
4.14	324.26	4.18	323.40	23.65	I
4.18	324.79	4.18	323.93	23.68	I
4.23	323.18	4.15	322.33	23.40	I
4.28	324.79	4.36	323.85	24.71	I
4.33	325.87	4.45	324.88	25.31	I
4.37	323.18	4.36	322.24	24.59	I
4.42	323.18	4.27	322.28	24.08	I
4.47	324.79	4.55	323.77	25.74	I
4.52	323.71	4.45	322.73	25.14	I
4.57	321.57	4.45	320.60	24.98	I
4.63	323.18	4.30	322.27	24.24	I
4.68	322.08	4.57	321.05	25.69	I
4.73	322.08	4.52	321.08	25.36	I
4.78	321.57	4.45	320.60	24.98	I
4.84	322.66	4.61	321.62	25.92	I
4.89	321.57	4.61	320.53	25.83	I

4.95	321.57	4.55	320.56	25.48	I
5.00	322.66	4.60	321.62	25.90	I
5.06	319.96	4.73	318.88	26.37	I
5.12	321.57	4.55	320.56	25.48	I
5.17	318.37	4.49	317.39	24.93	I
5.23	317.90	4.67	316.85	25.90	I
5.29	318.85	4.64	317.80	25.77	I
5.35	319.96	4.64	318.92	25.86	I
5.41	318.37	4.64	317.33	25.73	I
5.47	317.25	4.61	316.22	25.50	I
5.53	318.37	4.57	317.36	25.38	I
5.59	319.48	4.55	318.48	25.32	I
5.66	316.33	4.73	315.26	26.07	I
5.72	318.37	4.67	317.31	25.94	I
5.78	317.90	4.69	316.84	25.99	I
5.85	317.90	5.00	316.69	27.71	I
5.92	316.33	4.70	315.27	25.93	I
5.98	318.37	4.70	317.30	26.09	I
6.05	316.78	5.03	315.57	27.75	I
6.12	315.21	5.03	314.00	27.61	I
6.19	315.21	4.84	314.08	26.61	I
6.26	317.90	4.84	316.77	26.85	I
6.33	313.64	5.00	312.44	27.34	I
6.40	314.06	4.93	312.90	27.01	I
6.47	315.21	5.03	314.00	27.61	I
6.54	316.33	4.94	315.16	27.21	I
6.62	314.77	5.03	313.56	27.57	I
6.69	316.78	4.88	315.64	26.96	I
6.76	313.64	4.84	312.52	26.48	I
6.84	313.64	4.93	312.47	26.97	I
6.92	313.64	4.93	312.47	26.97	I
7.00	314.77	5.21	313.47	28.57	I
7.07	313.64	5.21	312.34	28.46	I
7.15	313.64	5.09	312.40	27.83	I
7.23	312.49	5.27	311.16	28.72	I
7.32	313.64	5.36	312.26	29.32	I
7.40	313.64	5.31	312.29	29.05	I
7.48	311.67	5.34	310.32	29.02	I
7.57	312.07	5.32	310.73	28.94	I
7.65	313.22	5.18	311.94	28.29	I
7.74	311.67	5.43	310.27	29.50	I
7.82	310.52	5.25	309.22	28.41	I
7.91	310.52	5.57	309.05	30.13	I
8.00	312.07	5.43	310.67	29.54	I
8.09	312.07	5.36	310.71	29.17	I
8.18	312.07	5.41	310.68	29.43	I
8.27	312.07	5.50	310.64	29.92	I
8.37	308.97	5.48	307.56	29.49	I
8.46	309.35	5.45	307.95	29.41	I
8.56	310.13	5.64	308.63	30.46	I
8.65	307.80	5.41	306.43	29.00	I

8.75	308.60	5.61	307.12	30.19	I
8.85	308.60	5.64	307.11	30.31	I
8.95	308.97	5.61	307.49	30.23	I
9.05	308.97	5.73	307.43	30.83	I
9.15	308.60	5.59	307.13	30.06	I
9.25	308.97	5.80	307.39	31.20	I
9.36	307.08	5.91	305.45	31.61	I
9.46	308.97	5.82	307.38	31.32	I
9.57	307.08	5.89	305.46	31.50	I
9.67	310.13	5.91	308.48	31.93	I
9.78	307.43	5.73	305.90	30.68	I
9.89	307.08	5.77	305.52	30.87	OK
10.00	308.60	6.16	306.82	33.11	OK
10.12	304.38	6.07	302.67	32.19	OK
10.23	304.38	6.06	302.68	32.13	OK
10.35	305.90	5.88	304.29	31.34	OK
10.46	305.90	6.20	304.11	33.05	OK
10.58	304.38	6.11	302.65	32.40	OK
10.70	307.08	6.16	305.30	32.95	OK
10.82	304.71	6.11	302.98	32.44	OK
10.94	304.38	6.04	302.69	32.02	OK
11.06	304.05	6.32	302.20	33.50	OK
11.19	305.56	6.04	303.87	32.16	OK
11.31	302.86	6.27	301.05	33.09	OK
11.44	304.05	6.27	302.23	33.22	OK
11.57	302.86	6.34	301.01	33.47	OK
11.70	302.86	6.02	301.19	31.76	R
11.83	301.35	6.35	299.51	33.31	OK
11.96	304.05	6.44	302.14	34.08	OK
12.10	302.86	6.55	300.89	34.52	OK
12.23	301.35	6.55	299.39	34.35	OK
12.37	304.05	6.45	302.13	34.18	OK
12.51	301.35	6.45	299.44	33.88	OK
12.65	301.35	6.38	299.49	33.50	OK
12.79	298.63	6.55	296.68	34.04	OK
12.94	301.35	6.53	299.40	34.26	OK
13.08	301.35	6.80	299.23	35.68	OK
13.23	299.85	6.40	297.99	33.41	OK
13.38	299.85	6.65	297.83	34.74	OK
13.53	299.85	6.80	297.74	35.51	OK
13.68	299.57	6.58	297.60	34.33	OK
13.84	299.57	6.91	297.40	36.04	OK
13.99	299.57	6.64	297.56	34.62	OK
14.15	298.36	6.93	296.18	35.98	OK
14.31	298.09	6.76	296.02	35.09	OK
14.47	298.36	6.80	296.26	35.34	OK
14.63	298.36	6.73	296.30	34.95	OK
14.80	296.87	7.08	294.61	36.57	OK
14.96	296.62	6.98	294.42	36.07	OK
15.13	296.87	6.98	294.67	36.10	OK
15.30	296.87	6.82	294.77	35.24	OK

15.47	295.39	6.94	293.23	35.69	OK
15.65	295.39	7.15	293.10	36.78	OK
15.82	296.62	6.91	294.47	35.68	OK
16.00	295.39	7.01	293.18	36.07	OK
16.18	293.92	7.18	291.62	36.75	OK
16.36	295.39	7.18	293.08	36.93	OK
16.55	293.92	7.10	291.67	36.35	OK
16.73	295.39	7.12	293.12	36.62	OK
16.92	293.92	7.17	291.63	36.67	OK
17.11	292.46	7.18	290.16	36.56	OK
17.30	293.70	7.03	291.49	35.93	OK
17.50	293.92	7.36	291.50	37.67	OK
17.69	293.92	7.27	291.56	37.21	OK
17.89	292.25	7.35	289.85	37.39	OK
18.09	289.55	7.38	287.16	37.17	OK
18.30	291.20	7.55	288.68	38.24	OK
18.50	291.20	7.18	288.92	36.41	OK
18.71	290.81	7.39	288.39	37.39	OK
18.92	291.00	7.29	288.65	36.90	OK
19.13	289.74	7.53	287.23	37.99	OK
19.35	289.37	7.48	286.91	37.66	OK
19.57	289.55	7.38	287.16	37.17	OK
19.79	289.55	7.56	287.04	38.08	OK
20.01	286.83	7.65	284.28	38.16	OK
20.23	290.81	7.64	288.23	38.64	OK
20.46	289.55	7.56	287.04	38.08	OK
20.69	288.11	7.56	285.61	37.89	OK
20.92	287.94	7.47	285.50	37.41	OK
21.16	286.83	7.58	284.33	37.81	OK
21.40	286.83	7.57	284.33	37.76	OK
21.64	285.25	7.65	282.71	37.95	OK
21.88	288.11	7.73	285.49	38.74	OK
22.13	288.11	7.65	285.55	38.34	OK
22.38	285.39	7.82	282.74	38.82	OK
22.63	285.25	7.75	282.64	38.44	OK
22.88	286.52	7.73	283.92	38.53	OK
23.14	286.52	7.91	283.80	39.43	OK
23.40	285.25	7.90	282.54	39.21	OK
23.66	282.41	7.99	279.67	39.27	OK
23.93	285.11	8.00	282.33	39.68	OK
24.20	283.70	8.09	280.88	39.93	OK
24.47	283.70	8.01	280.93	39.52	OK
24.74	282.41	7.90	279.73	38.82	OK
25.02	282.41	7.92	279.72	38.93	OK
25.30	281.00	8.01	278.27	39.14	OK
25.59	282.30	8.00	279.55	39.29	OK
25.88	279.61	7.91	276.95	38.47	OK
26.17	279.61	8.01	276.88	38.94	OK
26.46	281.00	8.01	278.26	39.17	OK
26.76	281.00	8.09	278.21	39.55	OK
27.06	279.61	8.09	276.83	39.33	OK

27.36	279.69	8.00	276.97	38.93	OK
27.67	278.21	8.19	275.38	39.62	OK
27.98	279.61	8.18	276.76	39.79	OK
28.30	276.83	8.27	273.95	39.81	OK
28.61	278.21	8.01	275.50	38.77	OK
28.94	279.52	8.18	276.68	39.75	OK
29.26	276.83	8.45	273.82	40.66	OK
29.59	276.83	8.28	273.94	39.85	OK
29.92	278.14	8.36	275.18	40.43	OK
30.26	276.83	8.18	274.01	39.38	OK
30.60	275.45	8.19	272.64	39.22	OK
30.94	275.45	8.37	272.51	40.10	OK
31.29	274.08	8.18	271.29	39.01	OK
31.64	276.76	8.45	273.76	40.69	OK
32.00	276.76	8.45	273.76	40.69	OK
32.36	274.08	8.45	271.10	40.30	OK
32.72	274.04	8.27	271.19	39.43	OK
33.09	272.71	8.27	269.87	39.25	OK
33.46	272.71	8.36	269.81	39.66	OK
33.84	272.71	8.55	269.68	40.52	OK
34.22	271.35	8.45	268.40	39.90	OK
34.60	274.04	8.28	271.19	39.44	OK
34.99	271.35	8.36	268.47	39.47	OK
35.39	272.69	8.19	269.91	38.82	OK
35.78	271.35	8.36	268.47	39.47	OK
36.19	270.00	8.27	267.19	38.85	OK
36.59	270.00	8.45	267.07	39.70	OK
37.01	270.00	8.36	267.13	39.27	OK
37.42	271.34	8.55	268.33	40.32	OK
37.84	271.33	8.36	268.44	39.47	OK
38.27	268.68	8.54	265.70	39.92	OK
38.70	270.00	8.45	267.07	39.70	OK
39.13	267.39	8.45	264.48	39.31	OK
39.57	268.68	8.36	265.82	39.08	OK
40.02	267.39	8.54	264.42	39.71	OK
40.47	266.09	8.36	263.26	38.70	OK
40.92	267.39	8.63	264.36	40.14	OK
41.38	267.39	8.27	264.61	38.48	OK
41.85	264.80	8.54	261.87	39.33	OK
42.32	267.34	8.55	264.37	39.73	OK
42.79	267.37	8.45	264.46	39.29	OK
43.28	263.52	8.36	260.72	38.33	OK
43.76	264.80	8.45	261.93	38.92	OK
44.25	264.76	8.27	262.00	38.08	OK
44.75	264.76	8.45	261.88	38.91	OK
45.25	263.52	8.64	260.53	39.57	OK
45.76	264.76	8.54	261.82	39.31	OK
46.28	262.24	8.35	259.46	38.10	OK
46.80	262.17	8.63	259.21	39.32	OK
47.32	260.97	8.36	258.20	37.96	OK
47.86	260.89	8.45	258.06	38.33	OK

48.39	260.97	8.28	258.25	37.58	OK
48.94	262.10	8.46	259.25	38.56	OK
49.49	260.89	8.46	258.05	38.38	OK
50.04	259.61	8.62	256.68	38.92	OK
50.61	259.61	8.45	256.80	38.14	OK
51.18	260.89	8.63	257.94	39.15	OK
51.75	259.71	8.28	257.00	37.40	OK
52.33	259.52	8.45	256.70	38.16	OK
52.92	259.61	8.36	256.85	37.76	OK
53.52	258.45	8.54	255.59	38.37	OK
54.12	257.08	8.27	254.41	36.99	OK
54.73	257.08	8.55	254.22	38.24	OK
55.34	258.34	8.55	255.47	38.42	OK
55.96	258.34	8.19	255.71	36.80	OK
56.59	255.95	8.27	253.29	36.83	OK
57.23	256.96	8.28	254.28	37.01	OK
57.87	255.70	8.44	252.93	37.51	OK
58.52	255.82	8.36	253.10	37.21	OK
59.18	255.82	8.35	253.11	37.17	OK
59.85	254.57	8.33	251.88	36.90	OK
60.52	253.48	8.35	250.79	36.82	OK
61.20	254.71	8.45	251.94	37.45	OK
61.89	253.48	8.18	250.90	36.07	OK
62.58	254.57	8.44	251.81	37.38	OK
63.29	254.43	8.36	251.73	37.01	OK
64.00	251.19	8.45	248.46	36.93	OK
64.72	252.25	8.27	249.62	36.29	OK
65.45	252.25	8.17	249.69	35.85	OK
66.18	252.25	8.27	249.62	36.29	OK
66.93	251.93	8.25	249.32	36.15	OK
67.68	253.33	8.27	250.69	36.45	OK
68.44	253.33	8.18	250.75	36.05	OK
69.21	251.03	8.26	248.42	36.06	OK
69.99	250.86	8.35	248.20	36.43	OK
70.77	251.03	8.27	248.41	36.12	OK
71.57	250.86	8.00	248.41	34.91	OK
72.37	249.81	8.18	247.27	35.55	OK
73.19	248.60	8.26	246.02	35.71	OK
74.01	248.41	8.00	245.99	34.57	OK
74.84	249.81	8.10	247.31	35.22	OK
75.68	249.63	8.08	247.15	35.08	OK
76.54	247.39	8.17	244.88	35.14	OK
77.40	248.41	8.05	245.96	34.78	OK
78.27	247.39	7.92	245.03	34.11	OK
79.15	248.60	8.17	246.08	35.32	OK
80.04	247.19	8.09	244.73	34.79	OK
80.93	246.19	8.18	243.69	35.04	OK
81.85	248.41	8.08	245.94	34.90	OK
82.77	246.19	8.17	243.70	34.97	OK
83.70	245.98	7.89	243.65	33.78	OK
84.64	245.98	8.07	243.55	34.55	OK

85.59	243.81	7.91	241.49	33.55	OK
86.55	245.00	8.02	242.61	34.17	OK
87.52	243.58	8.04	241.19	34.06	OK
88.51	245.00	8.24	242.47	35.11	OK
89.50	243.81	7.93	241.48	33.62	OK
90.51	243.81	7.64	241.65	32.40	OK
91.53	243.81	7.62	241.66	32.33	OK
92.56	243.81	7.87	241.51	33.40	OK
93.60	243.35	7.84	241.08	33.19	OK
94.65	243.58	7.64	241.42	32.37	OK
95.71	242.39	7.86	240.12	33.13	OK
96.79	241.21	7.68	239.05	32.21	OK
97.88	241.46	7.82	239.21	32.85	OK
98.98	242.15	7.80	239.91	32.86	OK
100.09	242.39	7.64	240.24	32.21	OK
101.21	240.29	7.66	238.14	32.01	OK
102.35	240.95	7.60	238.84	31.86	OK
103.50	240.54	7.69	238.38	32.18	OK
104.66	240.03	7.64	237.90	31.90	OK
105.84	240.29	7.60	238.18	31.76	OK
107.03	239.76	7.58	237.67	31.61	OK
108.23	239.76	7.62	237.65	31.78	OK
109.45	239.76	7.58	237.67	31.61	OK
110.68	240.03	7.71	237.86	32.19	OK
111.92	238.58	7.59	236.49	31.53	OK
113.18	238.85	7.27	236.93	30.24	OK
114.46	237.68	7.41	235.70	30.66	OK
115.74	236.81	7.20	234.94	29.70	OK
117.04	237.09	7.32	235.16	30.20	OK
118.36	235.66	7.43	233.68	30.48	OK
119.69	237.68	7.18	235.82	29.71	OK
121.04	235.66	7.32	233.74	30.01	OK
122.40	235.95	7.09	234.15	29.13	OK
123.77	235.66	7.21	233.80	29.56	OK
125.16	234.52	7.18	232.68	29.32	OK
126.57	236.52	7.32	234.60	30.13	OK
127.99	233.38	7.13	231.58	28.97	OK
129.43	234.82	7.27	232.93	29.73	OK
130.89	234.21	7.07	232.44	28.81	OK
132.36	234.21	7.07	232.44	28.81	OK
133.85	233.69	7.31	231.79	29.75	OK
135.35	234.52	7.09	232.73	28.95	OK
136.88	234.52	6.98	232.78	28.48	OK
138.41	231.93	7.13	230.14	28.79	OK
139.97	234.21	6.93	232.50	28.27	OK
141.54	233.38	6.97	231.66	28.34	OK
143.14	232.25	7.12	230.46	28.77	OK
144.74	232.75	6.91	231.06	28.00	OK
146.37	232.25	6.97	230.53	28.20	OK
148.02	232.25	6.97	230.53	28.20	OK
149.68	230.79	6.95	229.10	27.91	OK

151.36	231.13	6.79	229.51	27.33	OK
153.07	230.34	6.79	228.73	27.24	OK
154.79	230.01	6.70	228.44	26.83	OK
156.53	231.13	6.79	229.51	27.33	OK
158.29	231.13	6.52	229.63	26.24	OK
160.07	230.34	6.66	228.79	26.73	OK
161.87	231.45	6.57	229.93	26.49	OK
163.69	230.34	6.70	228.77	26.87	OK
165.53	230.79	6.64	229.25	26.67	OK
167.39	228.89	6.24	227.53	24.90	OK
169.27	228.19	6.57	226.69	26.13	OK
171.17	229.67	6.55	228.17	26.18	OK
173.10	227.78	6.57	226.28	26.08	OK
175.04	228.89	6.36	227.48	25.37	OK
177.01	227.78	6.36	226.38	25.25	OK
179.00	228.54	6.43	227.11	25.58	OK
181.01	228.19	6.30	226.81	25.05	OK
183.05	226.31	6.36	224.92	25.08	OK
185.11	226.31	6.21	224.98	24.49	OK
187.19	226.68	6.30	225.31	24.89	OK
189.29	227.04	6.27	225.68	24.81	OK
191.42	227.78	6.33	226.39	25.13	OK
193.57	227.42	6.24	226.08	24.73	OK
195.75	227.06	6.30	225.69	24.93	OK
197.95	227.42	6.09	226.14	24.13	OK
200.18	225.58	6.15	224.28	24.17	OK
202.43	225.58	6.24	224.24	24.53	OK
204.70	225.58	6.03	224.33	23.70	OK
207.00	224.82	6.12	223.54	23.98	OK
209.33	225.58	5.91	224.38	23.22	OK
211.68	225.21	5.85	224.03	22.94	OK
214.06	224.49	6.09	223.22	23.82	OK
216.47	225.21	5.82	224.05	22.83	OK
218.90	224.10	5.85	222.94	22.82	OK
221.37	225.21	5.91	224.01	23.18	OK
223.85	225.21	5.82	224.05	22.83	OK
226.37	223.01	5.97	221.80	23.18	OK
228.92	223.40	5.73	222.28	22.29	OK
231.49	224.10	5.79	222.96	22.59	OK
234.09	224.10	5.70	223.00	22.24	OK
236.72	224.49	5.82	223.33	22.76	OK
239.39	222.71	5.67	221.62	22.00	OK
242.08	224.49	5.36	223.51	20.97	R
244.80	222.32	5.51	221.29	21.35	OK
247.55	221.92	5.33	220.96	20.61	OK
250.33	223.01	5.49	221.99	21.33	OK
253.15	221.92	5.42	220.92	20.96	OK
255.99	220.83	5.49	219.82	21.12	OK
258.87	221.24	5.40	220.26	20.81	OK
261.78	221.92	5.40	220.93	20.87	OK
264.73	220.42	5.25	219.49	20.17	OK

267.70	221.24	5.48	220.23	21.12	OK
270.71	220.17	5.42	219.18	20.79	OK
273.76	221.92	5.24	220.99	20.26	OK
276.83	220.83	5.27	219.90	20.29	OK
279.95	219.10	5.31	218.16	20.27	OK
283.09	218.68	5.04	217.83	19.20	OK
286.28	221.24	5.10	220.36	19.68	OK
289.49	219.75	5.18	218.85	19.85	OK
292.75	220.17	5.27	219.24	20.23	OK
296.04	220.17	5.00	219.33	19.19	OK
299.37	219.10	5.11	218.23	19.52	OK
302.73	218.04	4.96	217.22	18.86	OK
306.14	219.10	5.18	218.20	19.79	OK
309.58	218.04	5.24	217.13	19.90	OK
313.06	219.75	5.09	218.88	19.50	OK
316.58	217.41	5.04	216.57	19.09	OK
320.14	216.98	4.76	216.23	18.02	OK
323.74	216.98	4.87	216.20	18.43	OK
327.38	216.98	5.00	216.16	18.91	OK
331.06	216.98	4.87	216.20	18.43	OK
334.78	217.61	4.73	216.87	17.93	OK
338.55	217.41	4.73	216.67	17.92	OK
342.35	216.98	4.78	216.23	18.08	OK
346.20	217.41	4.73	216.67	17.92	OK
350.09	216.37	4.78	215.62	18.03	OK
354.03	217.61	4.76	216.86	18.07	OK
358.01	215.48	4.55	214.81	17.08	OK
362.03	215.48	4.64	214.78	17.42	OK
366.10	215.93	4.49	215.27	16.92	OK
370.22	215.48	4.55	214.81	17.08	OK
374.38	215.77	4.47	215.11	16.81	OK
378.59	214.88	4.51	214.22	16.88	OK
382.85	214.88	4.32	214.27	16.20	OK
387.15	214.43	4.41	213.79	16.51	OK
391.50	214.43	4.27	213.83	15.98	OK
395.91	215.48	4.27	214.89	16.05	OK
400.36	213.84	4.41	213.21	16.46	OK
404.86	215.33	4.40	214.70	16.53	OK
409.41	215.48	4.18	214.91	15.71	OK
414.01	214.88	4.19	214.31	15.72	OK
418.67	213.84	4.18	213.27	15.59	OK
423.37	214.43	4.18	213.86	15.64	OK
428.13	214.43	4.09	213.88	15.30	OK
432.95	214.43	3.92	213.93	14.66	OK
437.81	213.38	4.13	212.83	15.37	OK
442.74	212.81	3.86	212.32	14.32	OK
447.71	213.84	3.96	213.33	14.77	OK
452.75	212.81	3.95	212.30	14.66	OK
457.84	213.38	4.05	212.85	15.07	OK
462.99	212.81	3.87	212.32	14.36	OK
468.19	212.81	3.73	212.36	13.83	OK

473.45	213.84	3.69	213.40	13.75	OK
478.78	211.77	3.72	211.33	13.74	OK
484.16	212.81	3.82	212.33	14.17	OK
489.60	212.81	3.78	212.34	14.02	OK
495.11	211.77	3.55	211.37	13.10	OK
500.67	212.91	3.64	212.48	13.50	OK
506.30	211.30	3.77	210.84	13.89	OK
511.99	211.30	3.64	210.87	13.40	OK
517.75	211.30	3.64	210.87	13.40	OK
523.57	210.27	3.63	209.84	13.32	OK
529.46	211.77	3.59	211.36	13.25	OK
535.41	211.30	3.41	210.93	12.55	OK
541.43	210.75	3.59	210.33	13.21	OK
547.52	210.27	3.50	209.87	12.83	OK
553.67	209.73	3.50	209.34	12.81	OK
559.90	210.27	3.50	209.87	12.83	OK
566.19	210.27	3.37	209.90	12.36	OK
572.56	211.22	3.36	210.86	12.39	OK
578.99	211.30	3.50	210.91	12.89	OK
585.50	209.20	3.50	208.81	12.77	OK
592.09	210.27	3.32	209.91	12.16	OK
598.74	209.77	3.55	209.37	12.97	OK
605.47	210.75	3.41	210.38	12.54	OK
612.28	210.75	3.36	210.39	12.37	OK
619.17	209.24	3.41	208.87	12.44	OK
626.13	208.71	3.32	208.36	12.08	OK
633.17	210.27	3.45	209.88	12.67	OK
640.28	210.75	3.32	210.39	12.21	OK
647.48	208.71	3.32	208.36	12.08	OK
654.76	209.24	3.41	208.87	12.44	OK
662.12	208.71	3.45	208.33	12.58	OK
669.57	208.21	3.14	207.90	11.39	OK
677.10	209.20	3.23	208.87	11.77	OK
684.71	208.21	3.14	207.90	11.39	OK
692.41	208.71	3.27	208.37	11.92	OK
700.19	207.70	3.41	207.33	12.35	R
708.06	207.70	3.45	207.32	12.51	R
716.02	206.69	3.32	206.35	11.97	R
724.07	206.69	3.14	206.38	11.31	R
732.21	206.20	3.14	205.89	11.28	R
740.44	206.20	3.09	205.90	11.12	R
748.77	206.69	3.05	206.40	10.98	R
757.19	206.69	3.05	206.40	10.98	R
765.70	206.18	3.14	205.87	11.28	R
774.31	207.70	2.95	207.42	10.70	OK
783.01	206.18	3.00	205.90	10.80	R
791.82	206.18	3.00	205.90	10.79	R
800.72	205.69	3.14	205.38	11.26	R
809.72	206.69	2.91	206.43	10.49	I
818.82	205.17	3.00	204.89	10.74	I
828.03	206.20	2.91	205.93	10.46	I

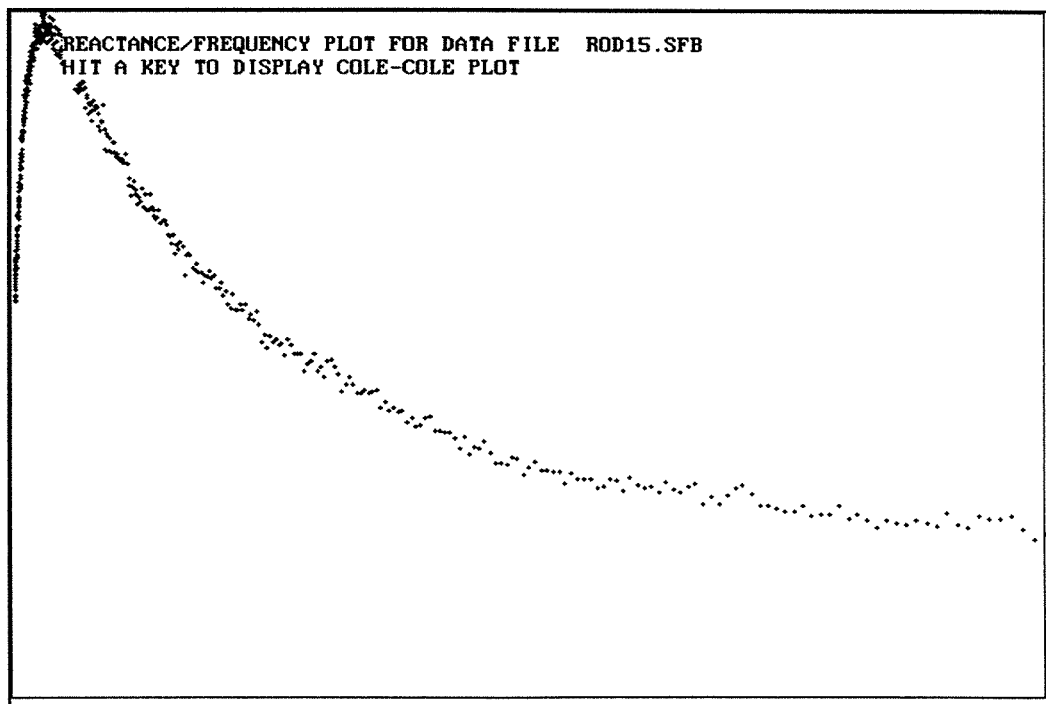|					
837.34	206.18	2.77	205.94	9.97	I
846.75	205.69	2.91	205.43	10.44	I
856.27	204.69	2.87	204.44	10.23	I
865.90	206.69	2.82	206.44	10.16	I
875.63	205.69	2.91	205.43	10.44	I
885.48	204.69	2.86	204.44	10.22	I
895.43	205.17	2.82	204.93	10.10	I
905.50	204.69	3.05	204.40	10.88	I
915.68	204.22	2.87	203.97	10.21	I
925.98	203.70	2.82	203.46	10.04	I
936.39	204.22	3.00	203.94	10.71	I
946.91	202.72	2.97	202.44	10.49	I
957.56	202.72	2.97	202.44	10.49	I
968.32	203.17	3.01	202.89	10.66	I
979.21	204.17	2.78	203.93	9.90	I
990.22	202.72	2.64	202.50	9.35	I
1001.30	202.27	2.74	202.04	9.65	I
1012.60	201.73	2.70	201.51	9.49	I

CENTRE: 271.4888 -43.01661 ohms
RADIUS: 82.28963 ohms
R zero: 341.6398 ohms
Z 50: 258.2534 ohms
R 50: 255.5831 ohms
Phase 50: 8.252953 deg
Xc 50: 37.0622 ohms
Z 5: 322.9374 ohms
R 5: 322.3113 ohms
Phase 5: 3.890232 deg
Xc 5: 22.43092 ohms
Z 100: 242.5615 ohms
R 100: 240.4112 ohms
Phase 100: 7.634755 deg
Xc 100: 32.22622 ohms
R infinite: 201.3379 ohms
Z characteristic: 274.3147 ohms
F characteristic: 32.48678 kHz
Mean cell capacitance 12.48071 nF
SEE of the RADIUS .8104125 %
Lower Frequency Limit 10 kHz
Upper Frequency Limit 800 kHz
data rejected: 14 out of 394 rejection factor 2 %

Input data file name: ROD15.SFB
Output data file name: ROD15.SFX
File analysis date: 04-24-1994
Phase angle calibration: 284
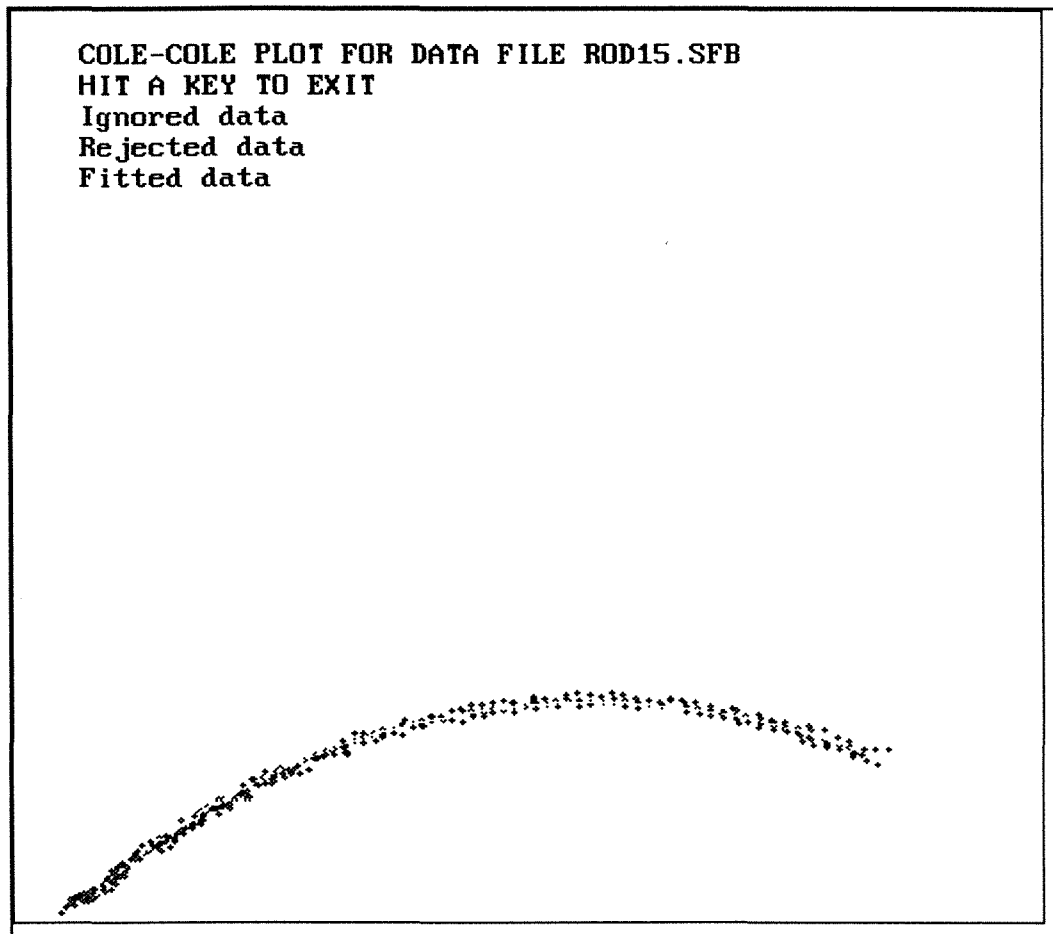Calibration file used: CAL121.TXT
Input file headers:
SEAC S-F BIM 2.3 Serial # 2312 00015 00001 01000

RESISTANCE/FREQUENCY PLOT FOR DATA FILE ROD15.SFB
HIT A KEY TO DISPLAY REACTANCE/FREQUENCY PLOT
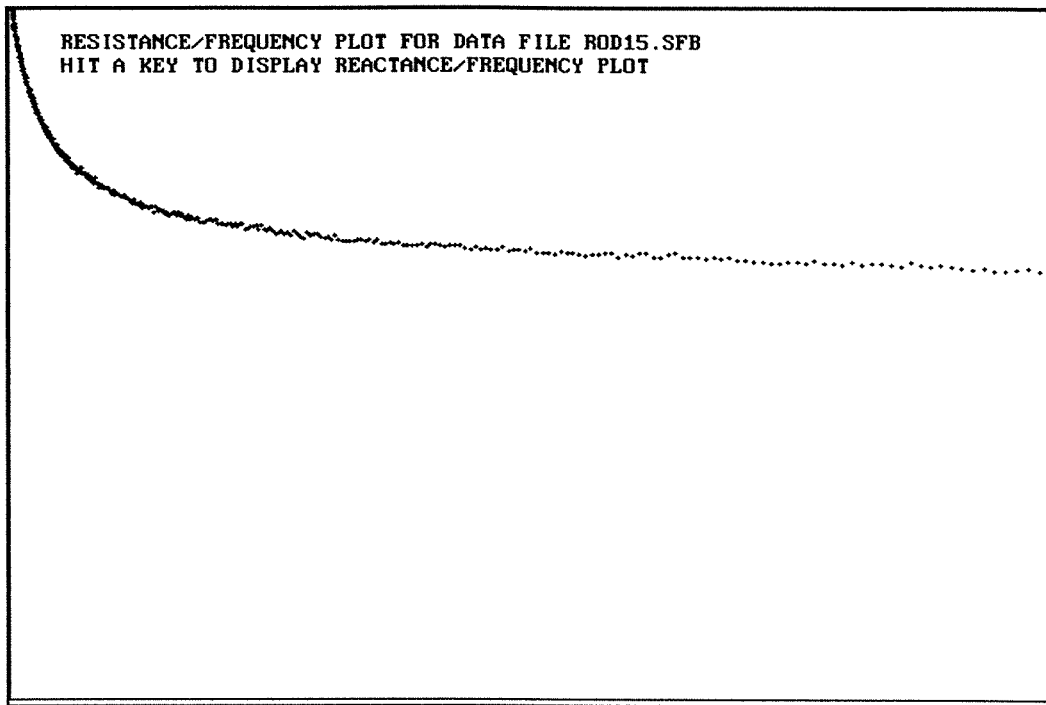
Plot of Resistance *vs* Frequency for the data listed above.

REACTANCE/FREQUENCY PLOT FOR DATA FILE   ROD15.SFB
HIT A KEY TO DISPLAY COLE-COLE PLOT

Plot of Reactance *vs* Frequency for the data listed above.

```
COLE-COLE PLOT FOR DATA FILE ROD15.SFB
HIT A KEY TO EXIT
Ignored data
Rejected data
Fitted data
```

Cole-Cole plot.
Plot of Reactance *vs* Frequency for the data listed above.

APPENDIX C

COPIES OF ALL ETHICAL CLEARANCES OBTAINED, AND VOLUNTEER CONSENT FORMS.

APPENDIX C

The following pages are copies of the all relevant ethical clearances and the volunteer consent form.

(i)   QUT Biomedical ethics committee approval for the animal studies conducted.

(ii)   University of Queensland animal experimentation ethics committee approval for the animal studies conducted.

(iii)   QUT Biomedical ethics committee approval for the studies conducted using human volunteers.

(iv)   University of Queensland medical research ethics committee approval for the studies conducted using human volunteers.

(v)   Wesley hospital ethics committee approval for the human studies conducted at the Wesley clinic for haematology and oncology.

(vi)   Human volunteer consent form.

BIOMEDICAL ETHICS COMMITTEE

Dr B J Thomas
Department of Physics
QUT Gardens Point

1 October 1990

Dear Dr Thomas

I wish to advise that the Biomedical Ethics Committee has approved the project **"Investigation of a Variable Frequency Bioelectrical Impedance Monitor for Compartmental Analysis of Body Composition"** with respect of animal experimentation (Ref No QUT BEC 202).

This approval is only valid for the period of time which you indicated in your application.

The Committee has asked that any divergence from the approved protocol indicated in the approved proposal should be reported immediately to the Committee.

During the experiments, you must ensure that adequate records are kept on the acquisition, breeding, health, care, use and disposal of animals. The Committee may wish to see these records at the conclusion of the experimentation.

Yours faithfully

RICHARD SHENTON
Secretary

Telephone Extn 2953

Queensland University of Technology

becform3.ani

Gardens Point	Kelvin Grove	Kedron Park	Carseldine	International
2 George Street	Victoria Park Road	Kedron Park Road	Beams Road	Codes
GPO Box 2434	Locked Bag No 2	PO Box 117	PO Box 284	Central Administration
Brisbane Q 4001	Red Hill Q 4059	Kedron Q 4031	Zillmere Q 4034	Phone +61 7 223 2111
Australia	Australia	Australia	Australia	Fax +61 7 229 1510
Phone: (07) 223 2111	Phone: (07) 352 8111	Phone: (07) 357 7077	Phone: (07) 263 6222	Telex 71 AA44699
Fax: (07) 229 1510	Fax: (07) 352 6382	Fax: (07) 357 7067	Fax: (07) 263 6372	

ANIMAL EXPERIMENTATION ETHICS APPROVAL NUMBER

(EXTERNALLY AND INTERNALLY FUNDED PROJECTS)

PLEASE KEEP THIS FORM. IT IS YOUR RECORD OF YOUR AEEC APPROVAL NUMBER.

From Julie Reilly, Animal Welfare Officer, c/o School of Veterinary Science
University of Queensland, ST. LUCIA. *Phone:* 377 2713

Dear Dr Ward   Date: 9 May 1991

The following project:

Title: Development of Bioelectrical impedance monitor for the estimations of
____ body composition

requesting funding from (*Grant Awarding Body*): _____
involves animal experimentation. It has been reviewed and ethical clearance obtained from the University Animal Experimentation Ethics Committee / *subject to modifications as discussed and indicated overleaf.*

AEEC APPROVAL NUMBER: BIOC/187/91/CSIRO/UQ

Ethical Approval current from: 8/5/91-8/5/92

Project commencement date/duration: ongoing

Species: Rat (Wistar)   *No.:* 2100

Species: Cattle   *No.:* 30 (done at CSIRO)

Species: _____   *No.:* _____

Please use this Approval Number:

1. **When ordering animals from the Central Animal Breeding House or from the Faculty of Medicine Animal Breeding House.**

2. **For labelling of all animal cages or holding areas, in addition please include on the label investigator's name and contact 'phone number.**

3. **When you need to communicate with this office about the project.**

IDENTICAL APPLICATIONS TO DIFFERENT GRANT AWARDING BODIES

If you intend to apply to other Grant Awarding Bodies for funding for this project, in the same year as this application, you may photocopy this certificate and sign where indicated and use it instead of filling out another *Animal Experimentation Application Form* (Form 1). Your approval number, for the particular project, will not change but a new suffix will be added to indicate the new Grant Awarding Body involved; e.g., if your original approval number was MED/234/87/NHMRC and you then apply for a Special Project Grant with the *IDENTICAL* project then the approval number for this will be MED/234/87/NHMRC/SPG.

This certificate can only be used in this way if the project is *IDENTICAL* to the one approved here. If it is not the same, a new *Animal Experimentation Application Form* (Form 1) must be filled out and returned with your application.

If this certificate is used then one copy of it and one copy of the Grant Awarding Body's form should be sent directly to the Animal Welfare Officer, for the Ethics Committee, and one copy should be sent to Research Section with the required number of Grant Awarding Body's Forms.

If a new *Animal Experimentation Application Form* is used, eight copies of the completed *Animal Experimentation Application Form* and two copies of the Grant Awarding Body's Forms should be sent to the Animal Welfare Officer. One copy of the *Animal Experimentation Application Form* should be sent to Research Section with the required number of Grant Awarding Body's Form.

— —

I certify that the project for which I am applying for funding from the:

_____ (Grant awarding Body)

is identical to the one described and approved above.

BIOMEDICAL ETHICS COMMITTEE

A/Prof B J Thomas
Centre for Medical and Health Physics
QUT Gardens Point

13 May 1993

Dear Professor Thomas

I wish to advise that the Biomedical Ethics Committee has approved the project "Bioelectrical Impedance for the Measurement of Body Fluid Volumes" with respect to human experimentation (Ref No QUT BEC 203/1).

This approval is only valid for the period of one year from the date of commencement of the project (as indicated in your proposal). If further approval for experimentation is required after this period you must submit a renewal application.

It is a strict condition of approval that any divergence from the approved protocol indicated in the approved proposal be reported immediately to the Committee. In this respect you should complete the attached form

.   when a minor change to the approved protocol is proposed, and/or

.   within six months of the duration of the approval period or when approximately 50 per cent of the experimentation is completed - whichever is the earliest.

Major changes to an approved protocol require a new application to be submitted and new approval by the Biomedical Ethics Committee to be granted. Minor changes will be assessed on merit and interim approval may be granted subject to ratification at the next full meeting of the Committee.

The Committee has requested that it be advised that where a consent form is used it should include a full explanation of the project and a statement indicating the right to withdraw from participation at any time without comment or from any consequence. The consent form must be framed in common english and a copy should be retained by the participant.

Yours faithfully

Richard Shenton
Secretary
Telephone: 864-1785

cc: Manager, Office of Research

becdisk11.mail.may ab

Queensland University of Technology

THE UNIVERSITY OF QUEENSLAND

INSTITUTIONAL APPROVAL FORM FOR EXPERIMENTS ON HUMANS
INCLUDING BEHAVIOURAL RESEARCH

:asc complete in **BLACK** type or ink only

partment:	Biochemistry
ief Investigator:	Dr Leigh Ward
rst Named in Application or Student's Name)	

her Chief Investigator(s):	Dr B J Thomas, Mrs M A Harkness & Dr I H Bunce
partment(s):	QUT, QUT & Wesley Clinic respectively
r Student's Supervisor)	

ject Title:
1. Bioelectrical impedance - a noval method for the measurement of body fluid volumes during dialysis.
2. Objective measure for diagnosis and staging of post-mastectomy lymphoedema.

anting Agency or Degree Enrolled:

hics Committee Use:	Clearance No: H/36/BIOCH/91/92/AKF/QCF

it your opinion that this project complies with the provisions contained in the Council's document atement on Human Experimentation and Supplementary Notes'?

YES   NO

it your opinion that this project complies with the regulations governing experimentation on humans within ur institution?

YES   NO

mments:

Modifications to proposal outlined in memorandum 5 March 1993 approved. Modifications involve oral administration of sodium bromide at a dose of 0.75mmol/kg body-weight and oral dose of deuterium oxide at a dosage of 0.5 to 1.0g/kg body weight.

ime of Responsible Ethics Committee:
EDICAL RESEARCH ETHICS COMMITTEE
~~EHAVIOURAL AND SOCIAL SCIENCES ETHICAL REVIEW COMMITTEE~~

ime of Ethics Committee representative (Block Letters):

of/~~Assoc Prof/Dr~~............ E. TRIGGS ....CHAIRPERSON

gnature: ....   DATE: ..2/.4./.93
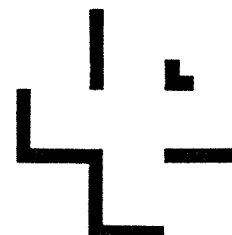
7th June, 1991.

Dr. I Bunce,
The Brisbane Haematology and Oncology Clinic,
Level 1,
The Wesley Medical Centre,
40 Chasely Street,
AUCHENFLOWER, Q.,   4066.

Dear Ian,

Thank you for your letter concerning the use of a device to measure bioelectrical impedance as a means of quantifying water and protein content of tissue.

From what you have described, I do not believe this matter has to be submitted to the Ethics Committee for approval.

New diagnostic techniques and treatments, both medical and surgical, are constantly being introduced into the Hospital.   These are not presented to the Ethics Committee.

I therefore authorize you to proceed in the way you have outlined in the letter.   I will mention your correspondence and proposal at the next meeting of the Ethics Committee, for minuting.

With best wishes,

Yours sincerely,

Douglas Killer, MBBS, FRACP,
Medical Superintendent.

Volunteer Consent Form

I, ... hereby consent to the following procedures:

Bioelectrical impedance monitoring,

Oral administration of deuterium oxide and sodium bromide,

Withdrawal of a maximum of 20 mL blood.

The nature and effect of these procedures have been explained to me by:

....

I have had the opportunity to ask any questions and all of my questions have been answered. I understand that I am free to withdraw my consent to participate in the study at any time.

Dated this .... day of .... 19....

Signed ....
          (research participant)

I, the undersigned, have fully explained the relevant details of this study to the research participant named above. I am qualified to perform this role.

Signed ....   Dated ....
        (investigator)

Witnessed ....   Dated ....

REFERENCES

REFERENCES

Allen PS. In vivo NMR spectroscopy. In: Yasumura S, Harrison JE, McNeill KG, Woodhead AD, Dilmanian FA, eds. *In vivo body composition studies: recent advances*. New York: Plenum press, 1990:419-26.

Asami K, Yakahashi Y, Takashima, S. Dielectric properties of mouse lymphocytes and erythrocytes. *Biochimica et biophysia acta*. 1989;896:203,13.

Battistini N, Brambilla P, Virgili F, Simone P, Bedogni G, Morini P, Chiumello G. The prediction of total body water from body impedance in young obese subjects. *Int J Obesity*. 1992;16:207,212.

Behnke AR. Physiologic studies pertaining to deep sea diving and aviation, especially in relation to the fat content and composition of the body. *Harvey Lect* 1941-1942;37:198-226.

Blagojevic N, Allen BJ, Gaskin KJ, Baur LA. Determination of total body water by Fourier transform infrared analysis. *Australiasian Phys Eng Sci in Med*. 1990;13:110,116.

Bland JM, Altman DG. Statistical methods for assessing agreement between two methods of clinical measurement. *The Lancet*. 1986;1:307,310.

Borkan GA, Gerzof SG, Robbins AH, Hults DE, Silbert CK, Silbert JE. Assessment of abdominal fat content by computed tomography. *Am J Clin Nutr*. 1982;36:172-7.

Borkan GA, Hults DE, Gerzof SG, Robbins AH. Comparison of body composition in middle-aged and elderly males using computed tomography. *Am J Phys Anthropol*. 1985;66:289-95.

Brozek J, Grande F, Anderson JT, Keys A. Densitometric analysis of body composition: revision of some quantitative assumptions. *Ann NY Acad Sci*. 1963;110:495-8.

Bunce IH, Mirolo B, Chapman M, Jones LC, Olsen TE, Eliadis PE. Response to intensive therapy and continuing benefit from self-management of moderate to severe lymphoedema in patients with breast cancer. *Clinical oncology society of Australia proceedings*. 1991; 18th Annual meeting.

Bunce IH, Mirolo B, Hennessey JM, Ward LC, Jones LC. Post-mastectomy lymphoedema treatment and measurement. *Med J Aust*. 1994; in press.

Casley-Smith JR. Discussion of the definition, diagnosis and treatment lf lymphoedema (lymphostatic disorder). In *Progress in Lymphology, X*. Proceedings of the International Congress on Lymphology. 1985;1,5.

Casley-Smith Judith R, Casley-Smith JR, Morgan RG. Physical therapy for lymphoedema. *Med J Aust*. 1989;150:542,543.

Cheek DB. Observations on total body chlorine in children. *J Pediatrics*. 1954;14:5,10.

Cole KS. Electric impedance of suspensions of spheres. *J. Gen. Physiol*. 1928;12:29-36.

Cole KS. *Membranes, Ions and impulses: a chapter of classical biophysics*. UCLA press, 1968, Los Angeles.

Cole KS and Cole RH. Dispersion and absorption in dielectrics. I. Alternating current characteristics. *J Chem Physics*. 1941;9:341,351.

Cornbleet PJ, Gochman N. Incorrect least-squares regression coefficients in method-comparison analysis. *Clin Chem*. 1979;25:432,438.

Culebras JM, Moore FD. Total body water and the exchangeable hydrogen. I Theoretical calculation of nonaqueous exchangeable hydrogen in man. *Am J Physiol*. 1977;232:R54-9.

Deming WE. *Statistical Adjustment of Data*. John Wiley and Sons, 1943, New York.

Diaz EO, Villar J, Immink M, Gonzales T. Bioimpedance or anthropometry. *Eur J Clin Nutr.* 1989;43:129-37.

Durnin JVGA, Womersley J. Body fat assessed from total body density and its estimation from skinfold thickness measurement on 481 men and women aged 16 to 72 years. *Br J Nutr.* 1974;32:77-97.

Dyer A. *Liquid scintillation counting practice.* Heyden and Sons, 1980, London.

Edwards DAW, Hammond WH, Healey MJR, Tanner JM, Whitehouse RH. Design and accuracy of calipers for measuring subcutaneous tissue thickness.*Br J Nutr.* 1955;9:133-50.

Espejo MGA, Neu J, Hamilton L, Eitzman B, Gimotty P, Bucciarelli RL. Determination of extracellular fluid volume using impedance measurements. *Crit Care Med.* 1989;17:360-3.

Fanelli MT, Kuczmarski RJ. Ultrasound as an approach to assessing body composition. *Am J Clin Nutr.* 1984;39:703-9.

Földi M. Complex decongestive therapy. In *Progress in Lymphology, X.* Proceedings of the International Congress on Lymphology. 1985;165,167.

Fricke H. The electric conductivity and capacity of disperse systems *Physics.* 1932;1:106,115.

Fuller NJ. Comparison of abilities of various interpretations of bio-electrical impedance to predict reference method body composition assessment. *Clinical Nutrition.* 1993;12:

Garrow JS. New approaches to body composition. *Am J Clin Nutr.* 1982;35:1152-8.

Geddes LA, Baker LE. The specific resistance of biological material - a compendium of data for the biomedical engineer and physiologist. *Med & Biol Engng.* 1967;5:271,293.

Graves JE, Pollock ML, Colvin AB, Van Loan M and Lohman TG. Comparison of different bioelectrical impedance analyzers in the prediction of body composition. *Am J Human Biology*. 1989;603-11.

Gray DS, Bray GA, Gemayel N, Kaplan K. Effect of obesity on bioelectrical impedance. *Am J Clin Nutr*. 1989;50:255,260.

Guyton AC. *Textbook of medical physiology* WB Saunders Co. 1981. Philadelphia.

Hall CB, Lukaski HC, Marchello MJ. Estimation of rat body composition using tetrapolar bioelectrical impedance analysis. *Nutr Rep Int*. 1989;39:627,633.

Hayes CE, Case TA, Ailion DC. Lung water quantitation by nuclear magnetic resonance imaging. *Science*. 1982;216:1313-5.

Heymsfield SB, McManus C, Smith J, Stevens V, Nixon DW. Anthropometric measurement of muscle mass: revised equations for calculating bone free arm muscle area. *Am J Clin Nutr*. 1982;36:680-90.

Heymsfield SB, Waki M, Lichtman S, Baumgartner R. Multicompartment chemical models of human body composition: recent advances and potential applications. In Kral JG, VanItallie TB, eds. *Recent developments in body composition analysis*. London: Smith-Gordon, 1993:75,86.

Holleman DF, Dieterich RA. Body water content and turnover in several species of rodents as evaluated by the tritiated water method. *J of Mammology*. 1973;54:456,465.

Hoffer EC, Meador CK, Simpson DC. Correlation of whole-body impedance with total body water volume. *Journal of Applied Physiol*. 1969;27(4):531,534.

International Commission on Radiological Protection. *1990 Recommendations of the International Commission on Radiological Protection, publication no. 60*. Oxford: Pergamon Press, 1991.

Jackson AS, Pollock ML, Ward A. Generalized equations for predicting body density of women. *Med Sci Sports Exerc.* 1980;12:175-82.

Jebb SA, Elia M. Assessment of changes in total body water in patients undergoing renal dialysis using bioelectrical impedance analysis. *Clinical Nutrition.* 1993;10:81,84.

Jenin P, Lenoir J, Roullet C, Thomasset AL, Ducrot H. Determination of body fluid compartments by electrical impedance measurements. *Aviat Space Environ Med.* 1975;46:152,155.

Kanai H, Haeno M, Sakamoto K. Electrical measurement of fluid distribution in legs and arms. *Medical Progress Through Technology.* 1987;12:159,170.

Kaulesar Sukul DMKS, den Hoed PT, Johannes EJ, van Dolder R, Benda E. Direct and indirect methods for the quanyification of leg volume: comparison between water displacement volumetry, the disk model method and the frustum sign model method, using the correlation coefficient and the limits of agreement. *J Biomed Eng.* 1993;15:477,480.

Kerlinger FN, Pedhazur EJ. *Multiple regression in behavioral research* Holt, Rinehart and Winston. 1973. New York.

Keys A, Brozek J. Body fat in adult men. *Physiol Rev* 1953;33:245-325.

Krishnan SS, McNeill KG, Harrison JE. Recent developments in the prompt gamma total body nitrogen measurement facility of the toronto general hospital. In: Yasumura S, Harrison JE, McNeill KG, Woodhead AD, Dilmanian FA, eds. *In vivo body composition studies: recent advances.* New York: Plenum press, 1990:303-8.

Kushner RF, Kunigk A, Alspaugh M, Andronis PT,Leitch CA, Schoeller DA. Validation of bioelectrical-impedance analysis as a measurement of change in body composition in obesity. *Am J Clin Nutr.* 1990;52:219,223.

Kushner RF, Schoeller DA. Estimation of total body water by bioelectrical impedance analysis *Am J Clin Nutr.* 1986;44:417,424.

Kvist H, Sjostrom L, Chowdhury B, Alpsten M, Arvidsson B, Larsson L, Cederblad A. Body fat and adipose tissue determinations by computed tomography and by measurements of total body potassium. In: Yasumura S, Harrison JE, McNeill KG, Woodhead AD, Dilmanian FA, eds. *In vivo body composition studies: recent advances.* New York: Plenum press, 1990:197-218.

Lesser GT, Deutsch S, Markofsky J. Fat-free mass, total body water, and intracellular water in the aged rat. *Am J Physiol.* 1980;238:R82,R90.

Lewis DS, Rollwitz WL, Bertrand HA, Masoro EJ. Use of NMR for measurement of total body water and estimation of body fat. *J Appl Physiol.* 1986;60:836-40.

Lohman TG. Skinfolds and body density and their relation to body fatness: a review. *Hum Biol.* 1981;53:181-225.

Lukaski HC. Methods for the assessment of human body composition: traditional and new. *Am J Clin Nutr* 1987;46:537-56.

Lukaski HC, Bolunchuk WW. Theory and validation of the tetrapolar bioelectrical impedance method to assess human body composition. In: Ellis KJ, Yasumura S, Morgan WD, eds. *In vivo body composition studies.* London: The institute of physical sciences in medicine, 1987:410-4.

Lukaski HC, Bolunchuk W. Estimation of body fluid volumes using tetrapolar bioelectrical impedance measurements. *Aviation Space & environmental medicine.* 1988;59:1163,1169.

Lukaski HC, Johnson PE. A simple inexpensive method of determining total body water using a tracer dose of D_2O and infrared absorption of biological fluids. *Am J Clin Nutr.* 1985;41:363-70.

Lukaski HC, Johnson PE, Bolunchuk WW, Lykken GI. Assessment of fat free mass using bioelectrical measurements of the human body. *Am J Clin Nutr.* 1985;41:810-7.

Lykken GI, Lukaski HC, Bolunchuk WW, Sandstead HH. Potential errors in body composition as estimated by whole body scintillation counting. *J Lab Clin Med.* 1983;101:651-8.

Mandel J. *The statistical analysis of experimental data.* John Wiley and sons, 1964, New York.

Mendez J, Keys A. Density and composition of mammalian muscle. *Metabolism.* 1960;9:184-8.

Mendez J, Lukaski HC. Variability of body density in ambulatory subjects measured at different days. *Am J Clin Nutr.* 1981;34:78-81.

Mirolo B, Bunce IH, Chapman M, Olsen T, Eliadis P, Hennessey JM, Ward LC, Jones LC. Psychosocial benefits of post-mastectomy lymphoedema therapy. *Cancer nursing.* 1994; in press.

Moore FD, Olesen KH, McMurrey JD, Parker HV, Ball MR, Boyden CM, eds. *The body cell mass and its supporting environment: body composition in health and disease.* Philadelphia: WB Saunders Co, 1963.

National Heart Foundation of Australia. *Risk factor prevalence study survey no 3 1989.* Australian institute of health. 1990. Canberra.

Nielsen WC, Krzywicki HJ, Johnson HL, Consolazio CF. Use and evaluation of gas chromotography for determination of deuterium in body fluids. *J Appl Physiol.* 1971;31:957-61.

Nyboer J, Bagno S, Nims LF. *The electrical impedance plethysmograph an electrical volume recorder.* Washington, DC: National Research Council, Committee on Aviation, 1943.(Report no 149.)

Oosting M, Reijnders HFR. Spestrophotometric determination of bromide in aqueous solutions. *Fresenius Z Anal Chem.* 1980;301:28,29.

Pace N, Rathburn EN. Studies on body composition III. The body water and chemically combined nitrogen content in relation to fat content. *J Biol Chem.* 1945;158:685-91.

Pethig R. *Dielectric and electronic properties of biological materials.* Chichester, 1979, John Wiley & Sons.

Pierson RN, Price DC, Wang J, Jain RK. Extracellular water measurements: organ tracer kinetics of bromide and sucrose in rats and man. *Am J Physiol.* 1978;235:F254,264.

Pinson EA. Water exchanges and barriers as studied by the use of hydrogen isotopes. *Physiol. Rev.* 1952;32:123,134.

Pritchard JE, Nowson CA, Strauss BJ, Carlson JS, Kaymakci B, Wark JD. Evaluation of dual energy X-ray absorptiometry as a method of measurement of body fat. *Eur J Clin Nutr.* 1993;47:216-228.

Pullicino E, Coward WA, Elia M. The potential use of dual frequency impedance in predicting the distribution of total body water in health and disease. *Clin Nutr.* 1992;11:69,74.

Radin MJ, Fettman MJ, Wilke WL. Single injection method for evaluation of renal function with ^{3}H-inulin and ^{14}C-tetraethylammonium bromide in conscious unrestrained Sprague-Dawley rats. *J Am Vet Med Ass.* 1986;189:1044,1046.

Rothwell NJ, Stock MJ. In vivo determination of body composition by tritium dilution in the rat. *Br J Nutr.* 1979;41:625,628.

Russell CD, Bischoff PG, Rowell KL, Lloyd LK, Dubovsky, EV. Estimation of extracellular fluid volume from plasma clearance on technetium-99m DTPA by a single-injection, two-sample method. *J Nucl Med.* 1988;29:255,258.

Ryde SJS, Morgan WD, Compston JE, Williams AJ, Evans CJ, Sivyer A, Dutton J. Determination of total body calcium by prompt gamma neutron activation analysis: absolute in vivo measurements. In: Yasumura S, Harrison JE, McNeill KG, Woodhead AD, Dilmanian FA, eds. *In vivo body composition studies: recent advances*. New York: Plenum press, 1990:353-6.

Scheltinga M. *Bioelectrical impedance analysis (BIA): A bedside method for fluid measurement.* Amsterdam, VU University press, 1992.

Schanne OF, Ceretti ERP. *Impedance measurements in biological cells*. New York, John Wiley & Sons 1978.

Schloerb PR, Friis-Hansen BJ, Edelman IS, Solomon AK, Moore FD. The measurement of total body water in the human subject by deuterium oxide dilution. *J Clin Invest.* 1950;29:1296.

Schwan HP. Electrical properties of tissue and cell suspensions. In Lawrence JH and Tobias CA (eds). *Advances in biological and medical physics*. New York, Academic press, 1957, Vol 5;147-209.

Segal K, Burastero S, Chun A, Coronel P, Pierson RN, Wang J. Estimation of extracellular and total body water by multiple-frequency bioelectrical-impedance measurement. *Am J Clin Nutr.* 1991;54:26,29.

Segal KR, Butin B, Presta E, Wang J, Van Itallie TB. Estimation of human body composition by electrical impedance methods: a comparative study. *J Appl Physiol.* 1985;58:1565-71.

Segal KR, Van Loan M, Fitzgerald PI, Hodgdon JA, Van Itallie TB. Lean body mass estimation by bioelectrical impedance analysis: a four site cross-validation study. *Am J Clin Nutr.* 1988;47:7-14.

Sharpless SK. Hypnotics and sedatives. In Goodman LS, Gilman A, eds. *The pharmacological basis of therapeutics*, 4th ed. New York, Macmillan, 1970:121,126.

Sheng HP, Huggins RA. A review of body composition studies with emphasis on total body water and fat. *Am J Clin Nutr.* 1979;32:630-47.

Siri WB, The gross composition of the body. In: Tobias CA, Lawrence JH, eds. *Advances in biological and medical physics.* Vol 4. New York: Academic press, 1956:239-80.

Snedecor GW, Cochran WG. *Statistical methods.* 7th ed. Iowa state university press, 1980, Iowa.

Sorenson JA. Relationship between patient exposure and measurement precision in dual-photon absorptiometry of the spine. *Phys Med Biol.* 1991;36:169-76.

Spence JA, Baliga R, Nyboer J, Seftick J, Fleischmann L. Changes during hemodialysis in total body water, cardiac output and chest fluid as detected by bioelectrical impedance analysis. *Trans Am Soc Artif Intern Organs.* 1979;25:51,55.

Standards Association of Australia. *Approval and test specification - medical electrical equipmentreport, Report AS 3200.1.* Standards Australia, 1990, sydney.

Streat SJ, Beddoe AH, Hill GL. Aggresive nutritional support does not prevent protein loss despite fat gain in septic intensive care patients. *Journal of Trauma.* 1987;27:262,266.

Thomas BJ, Cornish BH, Ward LC. Bioelectrical impedance analysis for measurement of body fluid volumes: A review. *Journal of Clinical Engineering.* 1992;17:505,510.

Thomasset A. Bioelectrical properties of tissue impedance measurements. *Lyon Med.* 1962;207:257,262.

Tisavipat A, Vibulsreth S, Sheng H, Huggins RA. Total body water measured by desiccation and by tritiated water in adult rats. *J App Physiol.* 1974;37:699,701.

Tobin MB, Lacey HJ, Meyer L, Mortimer PS. The psychosocial morbidityof breast cancer-related arm swelling. *Cancer*. 1993;72:3248.

Tothill P. Evaluation of methods of bone mass measurement. In: Yasumura S, Harrison JE, McNeill KG, Woodhead AD, Dilmanian FA, eds. *In vivo body composition studies: recent advances*. New York: Plenum press, 1990:107-16.

Trapp SA, Bell EF. An imporoved spectrophotometric bromide assay for the estimation of extracellular water volume *Clinica Chimica Acta*. 1989;181:207,212.

Vaisman N, Pencharz PB, Koren G, Johnson JK. Comparison of oral and intravenous administration of sodium bromide for extracellular water measurements. *Am J Clin Nutr*. 1987;46:1,4.

Van Loan M, Mayclin P. A new TOBEC instrument and procedure for the assessment of body composition: use of Fourier coefficients to predict lean body mass and total body water. *Am J Clin Nutr*. 1987;45:131-7.

Van Loan M, Mayclin P. Bioelectrical impedance analysis: is it a reliable estimator of lean body mass and total body water? *Hum Biol*. 1987;59:299-309.

Van Loan MD, Mayclin PL. Use of multi-frequency bioelectrical impedance analysis for the estimation of extracellular fluid *Eur J Clin Nutr*. 1992;46:117,124.

Wahner HW, Dunn WL, Brown ML, Morin RL, Riggs BL. Comparison of dual-energy x-ray absorptiometry and dual photon absorptiometry for bone mineral measurements of the lumbar spine. *Mayo Clin Proc*. 1988;63:1075-84.

Ward LC, Cornish BH. Use of a spreadsheet program for Deming's linear regression analysis. *Comp Biol Med* 1991;37,101.

Werdein EJ, Kyle LH. Estimation of the constancy of density of the fat free body. *J Clin Invest.* 1960;39:626-9.

Wilmore JH, Behnke AR. An anthropometric estimation of body density and lean body weight in young men. *J Appl Physiol.* 1969;27:25-31.

Wilmore JH, Behnke AR. An anthropometric estimation of body density and lean body weight in young women. *Am J Clin Nutr.* 1970;23:267-74.

Zhang M, Willison J. Electrical impedance analysis in plant tissue: a double shell model. *J Exp Bot.* 1991;42:1465,1475.